THE ROLE OF MICROBIAL SULFUR METABOLISM IN BIOGEOCHEMICAL CYCLING OF TELLURIUM AND SELENIUM

By

JENNIFER L. GOFF

A dissertation submitted to the

School of Graduate Studies

Rutgers, The State University of New Jersey

In partial fulfillment of the requirements

For the degree of

Doctor of Philosophy

Graduate Program in Microbial Biology

Written under the direction of

Nathan Yee

And approved by

_____

_____

_____

_____

New Brunswick, New Jersey

January 2020

ABSTRACT OF THE DISSERTATION

The role of microbial sulfur metabolism in biogeochemical cycling of tellurium and selenium

by JENNIFER L. GOFF

Dissertation Director:

Nathan Yee

The soluble oxyanions of tellurium and selenium are the most toxic forms of the two elements. While various stages of the biogeochemical cycles of each have been explored by other researchers, there remain large gaps in knowledge of how microorganisms interact with various tellurium and selenium compounds. What is known is that the sulfur metabolism of microorganisms is often involved in these interactions. In Chapter 2 of this thesis, explores the role of sulfate transporters in the uptake of tellurate in *Escherichia coli* K-12. Previously it was unknown how tellurate enters the cells. A mutant strain with a deletion of the *cysW* gene of the CysPUWA sulfate transporter system accumulated less cellular tellurium and exhibited higher resistance to tellurate compared to the wild type strain. Chapter 3 of this thesis begins with the observation that tellurate was significantly more toxic to *E. coli* K-12 cells grown on LB medium compared to

M9 medium. Cystine was demonstrated to be the key media component controlling this difference. The cystine must be transported intracellularly—and therefore reduced to cysteine—in order to enhance the toxicity of tellurate. Tellurate was found to be reactive with cysteine and is reduced to elemental tellurium in that reaction. Oxidation of intracellular thiols increases the resistance of *E. coli* K-12 to tellurate. These results suggest that the interaction between the two contributes to the toxicity of tellurate. In Chapter 4, a *Bacillus* species was isolated from seleniferous soils that is capable of solubilizing elemental selenium. This process occurred extracellular and was demonstrated to be mediated by the sulfur metabolites (sulfide, sulfite, and thiosulfate) secreted by the organism. Finally, in Chapter 5, expands on the study of extracellular sulfur metabolite production by microorganisms under non-sulfur-respiring conditions. The dissimilatory metal-reducing bacterium *Shewanella oneidensis* MR-1 produces a substantially larger quantity of sulfite than the *Bacillus* species isolated in Chapter 4. This sulfite production was observed under aerobic and anaerobic conditions and was suppressed by amendment with cysteine suggesting that the sulfite is generated from the assimilatory sulfate reduction pathway. The data in Chapter 4 and Chapter 5 suggest that bacteria can produce and export substantial quantities of sulfite that can impact the solubility and speciation of elements in the environment.

If I made it, it's half because I was game enough to take a lot of punishment along the way and half because there were a lot of people who cared enough to help me.

--Althea Gibson

DEDICATION

I dedicate this work to every person who has ever gone above-and-beyond to help me in both academia and outside of school…

…to every person who has ever sat there with me in person.. or on the phone.. or at the receiving end of my very long emails and texts.. and allowed me the space to vent…

…to every person who has provided me with fun and much-needed distractions…

…and to every person who has ever believed in me and, most importantly, reminded me that they believed in me.

Even seemingly small actions have made profound differences in my life. I am extremely grateful to everyone who has touched my life in a positive way during these past five and a half years.

ACKNOWLEDGEMENTS

I'd like to thank my advisor Nathan Yee for giving me the opportunity to perform my dissertation work in his lab. While I came into his lab a biologist, I learned a lot about geochemistry and analytical methods during my time here and I can say that I am leaving as a geobiologist. Thank you to the other members of my committee—Tamar Barkay, Peter Strom, and Kat Dawson—for their time and input. Other members of the Rutgers community I'd like to thank include Gerben Zylstra for his helpful suggestions regarding some of the genetics work I have done; Shun Yu in the Fawkowski lab for technical assistance with their HPLC; and Jeffra Schaeffer for tipping us off that MR-1 produces A LOT of sulfite. She also helped me get started on the HPLC back when I did not even know how to put a column on the instrument. The analytical work performed for this dissertation has been a fantastic learning experience and I am grateful for all her assistance and input in that portion of my work.

I would like to thank my former undergraduate research assistant Chioma Ekedede for her assistance in my projects; Lee Terry who did the initial work to characterize Se(0)-solubilization by JG-17; my other collaborators for that project at UC Berkeley: Joyabrata Mal, Céline Pallud, and Kathrin Schilling; and my main funding sources: the School of Environmental and Biological Sciences, the Division of Life Sciences, the Microbial Biology graduate program, the Rutgers Presidential Fellowship, the School of Graduate Studies,w and the National Science Foundation.

I have had the privilege to work as a teaching assistant and a lecturer with the Division of Life Sciences over these years. I've worked closely with and learned a lot from several instructors within that department: Alex Walczak, Doreen Glodowski, Natalia Morsci, and Susan Skelly. Each experience was different and was formative in how I see my role as an instructor. Alex Walczak taught me a lot about how to teach microbiology lab. My current supervisor, Susan Skelly, gave me the opportunity to set up our lab's electronic notebook system from the ground up. This opportunity has been very meaningful to me and deeply rewarding as it has allowed me to have an impact not only on the students that I teach but also on all future students who take the course. Finally, to all the amazing students I have been fortunate enough to work with over the years, I have probably learned the most from you.

Finally, the people who kept me—mostly—sane throughout this process. My PhD cohort and amazing and supportive friends: Michelle and Alexander. Alanna, Austin, Diala, Eliot, and George who have given me many years of good friendship and conversations. Brittany for the countless years of distracting messages while at work. My mom, stepfather, siblings, and other family members for their continued support. In particular, my sister Alex and cousin Jonathan both of whom I am lucky enough to have living close by. Finally, my partner of many years, Javier. I can't imagine having gone through this experience alone. When we first moved up here we had nothing and now we have cultivated very rich, meaningful, and vibrant lives. I could never have done that without you.

Acknowledgement of previously published work or work in preparation for submission.

Chapter 2 has been published as Jennifer Goff & Nathan Yee. 2017. Tellurate enters *Escherichia coli K*-12 cells via the SulT-type sulfate transporter CysPUWA. *FEMS Microbiology Letters*. 364(24). DOI: 10.1093/femsle/fnx241. PMID: 29126297. Jennifer Goff wrote and revised the manuscript. Jennifer Goff was directly involved in all experimental design and performed all experiments and data analysis; Figures 1,2.

Chapter 3 is being prepared for publication as Jennifer Goff & Nathan Yee. 2020. Media effects on tellurate toxicity in *Escherichia coli* K-12. Jennifer Goff wrote the entire manuscript. Jennifer Goff designed and performed all experiments and performed all data analysis.

Chapter 4 has been published as Jennifer Goff, Lee Terry, Joyabrata Mal, Kathrin Schilling, Céline Pallud & Nathan Yee. 2019. Role of extracellular reactive sulfur metabolites on microbial Se(0) dissolution. *Geobiology*. 17:320-329. DOI: 10.1111/gbi.12328; Jennifer Goff isolated and performed the initial characterization of JG-17 and also performed the experiments to measure sulfur metabolite production; Figures 1,3, S1. Jennifer Goff also performed overall data analysis and calculations that appear in the results section. Jennifer Goff wrote and revised the manuscript.

Chapter 5 is being prepared for publication as Jennifer Goff & Nathan Yee. 2020. Characterization of the extracellular sulfur metabolites produced by *Shewanella oneidensis* MR-1. Jennifer Goff was directly involved in all experimental design, experimental work and data analysis. Jennifer Goff wrote the entire manuscript.

TABLE OF CONTENTS

Abstract of the Dissertation.....ii

Dedication and Acknowledgements.....iv

List of Figures.....xii

List of Tables.....xiv

Chapter 1: Introduction.....1

The Chalcogens: Sulfur, Selenium and Tellurium.....1

Chalcogen chemistry.....1

Tellurium biogeochemistry.....3

Tellurium toxicity.....11

Selenium biogeochemistry.....14

Selenium toxicity.....19

Central Sulfur Metabolic Pathways.....22

Introduction.....22

Transport.....23

Assimilatory sulfate reduction.....24

Sulfur amino acid metabolism.....25

The Role of Sulfur Metabolism in the Biogeochemical Cycling of Tellurium and Selenium.....26

Chapter 2: Tellurate enters *Escherichia coli* K-12 cells via the SulT-type sulfate transporter CysPUWA.....44

Abstract.....44

Introduction.....45

Materials and Methods.....46

Results.....50

Discussion.....53

Chapter 3: Media effects on tellurate toxicity in *Escherichia coli* K-12.....62

Abstract.....62

Introduction.....63

Materials and Methods.....67

Results.....75

Discussion.....82

Chapter 4: Role of extracellular reactive sulfur metabolites in microbially-mediated Se(0) dissolution.....108

Abstract.....108

Introduction.....109

Materials and Methods.....112

Results.....119

Discussion.....122

Chapter 5: Characterization of the extracellular sulfur metabolites produced by *Shewanella oneidensis* MR-1.....141

Abstract.....141

Introduction.....142

Materials and Methods.....143

Results.....148

Discussion.....150

Chapter 6: Conclusions and future directions.....170

Appendices.....182

Appendix 1: Isolation and draft genome of a tellurate-resistant Enterobacter species from the Hudson river, or what is "Highly tellurate-resistant" anyways?.....183

Appendix 2: Catalase does not reduce tellurate to Te(0).....200

Appendix 3: Supplementary material for Chapter 3.....202

Appendix 4: Supplementary material for Chapter 4.....204

Appendix 5: Supplementary material for Chapter 5.....206

LIST OF FIGURES

Figure 1.1. The biogeochemical cycling of tellurium compounds.....42

Figure 1.2. The biogeochemical cycling of selenium compounds.....43

Figure 2.1. Growth of *E. coli* strains in the presence of tellurate.....59

Figure 2.2. Tellurate uptake by the *E. coli* wild-type strain, Δ*cysW* mutant and Δ*cysW*:p*cysPUWA* complimented mutant.....60

Figure 2.3. Proposed model for the transport-dependent toxicity of tellurate..61

Figure 3.1. *E. coli* cultures pre-grown with Te(VI) and spiked with cystine (CSSC).....99

Figure 3.2. Reactions of tellurate with cysteine and glutathione *in vitro*.....100

Figure 3.3. Reactions of tellurite with cysteine and glutathione *in vitro*.....102

Figure 3.4. Effect of diamide pre-treatment on cell viability following tellurate exposure.....103

Figure 3.5. Tellurate toxicity in thiol biosynthesis pathway mutants.....104

Figure 3.6. Intracellular thiol concentrations in cells grown with and without tellurate.....105

Figure 3.7. Proposed schematic for reactions of tellurate with the intracellular thiols of *E. coli* when transferred to cystine-rich media.....106

Figure 4.1. Maximum-likelihood phylogenetic tree of the 16S rRNA gene sequences showing the relationship of strain JG17 and representative *Bacillus* species.....135

Figure 4.2. Elemental selenium dissolution by cell-free filtrates.....136

Figure 4.3. Reactive sulfur metabolites in the spent medium.....138

Figure 4.4. Chemical dissolution of Se(0) by (A) sulfite (B) sulfide, and (C) thiosulfate.....139

Figure 4.5. *Bacillus* sp. JG17 colony growing on an agar plate.....140

Figure 5.1. Sample chromatogram of mBBr-derivatized sulfur metabolites in the extracellular medium of *S. oneidensis* MR-1.....163

Figure 5.2. Extracellular sulfite in *S. oneidensis* MR-1 cultures.....164

Figure 5.3. Cysteine (A),thiosulfate (B), glutathione (C), and (D) sulfide production by *S. oneidensis* MR-1 165

Figure 5.4. Sulfite (A), sulfide (C), and thiosulfate (B) production by *S. ondeidensis* MR1 on sulfate-limited medium with cysteine added as a sulfur source.....166

Figure 5.5. Oxidation of sulfite to sulfate in Milli-Q water under aerobic conditions.....167

Figure 5.6. Identification of sulfur metabolic pathways of *S. oneidensis* MR-1 cells predicted to be active during growth on sulfate (A) or cysteine (B) as the sulfur source.....168

Figure A1.1. Growth of *Enterobacter* sp. HRSW on tellurate-containing medium.....192

Figure A1.2. Maximum-likelihood phylogenetic tree of the 16S rRNA gene sequences showing the relationship of strain HRSW and closely related species.....193

Figure A1.3. Measurement of tellurate reduction to Te(0) by HRSW.....194

Figure A1.4 HRSW 16S rRNA gene sequence.....195

Figure A2.1. Reactions of catalase with tellurate and tellurite.....201

Figure A3.1. Intracellular concentration of glutathione (dotted line) and cysteine (solid line) in *E. coli* K-12 cells.....203

Figure A4.1. Gram stain of *Bacillus* sp. JG17.....205

Figure A5.1. Effect of sulfite on cell survival following H_2O_2 exposure.....207

LIST OF TABLES

Table 1.1. Standard reduction potential of tellurium, selenium, and sulfur oxyanions.....41

Table 3.1. Tellurate MICs on different types of media.....97

Table 3.2. MICs for tellurite, selenate, and selenite.....98

Table 3.3. Tellurate MICs for cystine transporter knock-out strains.....98

Table A1.1. Tellurate MICs for HRSW on different media.....193

Table A1.2. Genome characteristics of HRSW.....194

Table A1.3. Tellurate-reducing organisms reported in the literature and the MIC of tellurate for each.....196

Table A3.1. Calculated concentrations of amino acids in LB medium.....202

Table A4.1. Strain characteristics of *Bacillus* sp. JG17 and two of its close relatives: *B. aryabhatti* B8W22 (100% identity) and *B. megaterium* ATCC 14581(99% identity).....204

Chapter 1
Introduction

THE CHALCOGENS: SULFUR, SELENIUM, AND TELLURIUM

Chalcogen chemistry

Sulfur, selenium, and tellurium – along with oxygen and polonium—comprise the Group 16 elements, otherwise known as the "chalcogens". The term derives from the Greek words χαλκός ("chalkos", copper) and -γενής ("-gene", giving birth), more generally meaning "ore-forming" (Jensen, 1997). This is in reference to the fact that the vast majority of the most common minerals found on earth are oxides, sulfides, selenides, or tellurides (Jensen, 1997).

The main redox states for tellurium and selenium in the environment are 2-, 0, 4+, 6+ (Zannoni, Borsetti, Harrison, & Turner, 2007):

$$\textbf{selenide}\ (Se^{2-}) \rightarrow \textbf{elemental selenium}\ (Se^{0}) \rightarrow \textbf{selenite}\ (SeO_3^{2-}) \rightarrow \textbf{selenate}\ (SeO_4^{2-})$$

$$\textbf{telluride}\ (Te^{2-}) \rightarrow \textbf{elemental tellurium}\ (Te^{0}) \rightarrow \textbf{tellurite}\ (TeO_3^{2-}) \rightarrow \textbf{tellurate}\ (TeO_4^{2-})$$

Similarly, 2-, 0, 4+, and 6+ are the main redox state for sulfur (Edwards, 1998). Later in this review, the most common biogenic sulfur species will be discussed in the context of microbial metabolism.

It is important to note that while the oxyanion formulae are commonly used in the literature for tellurite and tellurate, it likely that these compounds exist in the environment at least partially in the form of hydroxide ions. The environmental chemistry literature recommends that for tellurite the most

accurate formulae are TeO_3^{2-}, $HTeO_3^-$, H_2TeO_3, and $Te(OH)_3^+$ and for tellurate are $TeO_2(OH)_4^{2-}$, $TeO(OH)_5^-$, and $Te(OH)_6$ (Filella, Reimann, Biver, Rodushkin, & Rodiouchkina, 2019). However, since the biological tellurium literature continues to make use of the traditional oxyanion formulae, this review will maintain the convention of [tellurite/Te(IV)/TeO_3^{2-}] and [tellurate/Te(VI)/TeO_4^{2-}] (Thomas Girard Chasteen, Fuentes, Tantaleán, & Vásquez, 2009; Zannoni et al., 2007). In contrast, selenate exists in solution mainly as the oxyanions $HSeO_4^-$ and SeO_4^- and selenite as the oxyanions H_2SeO_3, $HSeO_3^-$, and SeO_3^{2-} (Fernández-Martínez & Charlet, 2009).

While analogous in structure to sulfur compounds, selenium and tellurium compounds have different chemical properties and reactivities that result in their greater toxicity compared to their sulfur counterparts (Zannoni et al., 2007). Selenium and tellurium oxyanions are more oxidizing compared to their sulfur analogs (Bouroushian, 2010)(**Table 1.1**). This will influence the relative reactivities of the different compounds and the relative distribution of different species. For example, while sulfur species of intermediate oxidation states (e.g., sulfite [SO_3^{2-}]) are relatively unstable and will tend to be oxidized to sulfate (SO_4^{2-}), tellurite and tellurate have comparable stability – tellurite tends be stable and is not readily oxidized to tellurate due to its high reduction potential (Ba, Döring, Jamier, & Jacob, 2010).

In this chapter, the biogeochemistry of selenium and tellurium compounds will be reviewed. As will be apparent, the speciation and toxicity of these compounds in the context of the microbial system is intimately tied to microbial

sulfur metabolism. This will be followed by an overview of central sulfur metabolism in a model system and summary of the current state of knowledge of the role of sulfur metabolism in microbial interactions with tellurium and selenium.

Tellurium biogeochemistry

Tellurium in the environment

The primary forms of tellurium in the environment are telluride, elemental tellurium, tellurite, tellurate, and various organo-tellurium compounds (Zannoni et al., 2007). Tellurium has a relatively low crustal abundance of 0.002 ppm (Zannoni et al., 2007). Reliable measurements of tellurium in uncontaminated environments are often difficult to obtain due to (1) the concentrations often being below the detection limits of modern, commonly-available analytical equipment and (2) a lack of standard reference materials for various tellurium compounds (Filella et al., 2019). Nonetheless concentrations of tellurium species have been reported for seawater in the classic and often-cited study by Lee & Edmond (1985). At various oceanic sampling sites, total dissolved tellurium was at its greatest abundance in surface waters (1.3 -1.7 pmol/L) and decreased at greater depths (0.4-0.6 pmol/L at 2,500-3,000 m below sea level). While both tellurite and tellurate were detected in this study, tellurate was found to be the main dissolved tellurium species at all depths and across two different study sites (Lee & Edmond, 1985).

Dissolved tellurium species were also detected in a study of a Chinese river estuary. Tellurite and tellurate were found at similar concentrations in the surface waters (0.02 and 0.03 nmol/L, respectively). Tellurate was found to be the main dissolved species in bottom waters at a concentration of 0.11 nmol/L (Wu, Song, & Li, 2014).

Certain locations have concentrations of tellurium several orders of magnitude above the global averages. Around hydrothermal vents, tellurium has been reported at concentrations of 12-17 ppm (Knott, Fallick, Rickard, & Bäcker, 1995). In mineral deposits, tellurium is found primarily in the form of tellurides such as those of zinc, copper, tin, lead, and gold (Speirs, Gross, Candelise, & Gross, 2011). High concentrations of tellurium have been found in gold mines (14.8 ppm) as well as in silica scales of geothermal pipelines (30.6 ppt) (Reyes et al. 2003; Wray 1998). Within Japanese soils contaminated by abandoned gold and silver mine-tailings, total tellurium was measured at 15 ppm. Tellurate and tellurite accounted for, on average, 61 and 39% of all tellurium species in these soils (Qin, Takeichi, Nitani, Terada, & Takahashi, 2017). Under the acidic conditions created by the presence of pyrite in the system, the tellurium from the telluride minerals associated with the gold and silver deposits is leached as tellurate and tellurite (Qin et al., 2017).

Exact numbers for global tellurium production do not exist as most tellurium is sourced as a byproduct of the copper refining process and these numbers are proprietary information. However, it was estimated in 2011 that global tellurium production was around 500 tons per year (Speirs et al., 2014). Major tellurium

reserves are located in Peru, the United States, Canada, Australia, Belgium, China, Germany, Kazakhstan, the Philippines, and Russia (Speirs et al., 2011). The current major global producers of tellurium are the United States, Canada, Peru, and Japan (Speirs et al., 2011; Zannoni et al., 2007).

Tellurium usage falls into three major categories: metallurgical, chemical, and electronic uses. Tellurium is added to copper, lead, and iron to improve their machinability (Zannoni et al., 2007). Elemental tellurium and tellurium diethyldithiocarbamate are added to rubbers as vulcanizing agents (Zannoni et al., 2007). Additionally, tellurium has been used as a catalyst in synthetic fiber production and for giving color to ceramics, glass, and silverware (Speirs et al., 2011; Zannoni et al., 2007).

Beyond its traditional uses described above, tellurium is seeing increasing use in thin film photovoltaics. Cadmium-telluride cells are one of several types of thin film cell technologies currently in use. Thin film photovoltaics are a relatively cost-effective and efficient mode of solar electricity generation (Speirs et al., 2011). By 2030, thin film photovoltaics are estimated to make up 40% of the photovoltaic market share with the total installed capacity of photovoltaic devices also expected to increase by over 1000% from 2010 to 2030 (Speirs et al., 2011). As the demand for thin film photovoltaic technology rises, the demand for tellurium is expected to rise. Estimates of increased tellurium demand suggest that it will be 350% of 2012 levels by 2030 (Speirs et al., 2014).

It is reasonable to assume that the increase in demand, extraction, and usage of tellurium will result in increased anthropogenic inputs of tellurium

compounds into the environment. Compounding this issue is the fact that the majority of tellurium used for electronic, chemical, and metallurgical purposes is not currently collected for recycling (Peiró, Méndez, & Ayres, 2013). It is reported that less than 1% of the tellurium in these industrial products is recycled (Peiró et al., 2013). Decommissioned and disposed of tellurium electronics are likely to increase in number in landfills in the future as a result. Significant leaching of tellurium oxyanions (both tellurite and tellurate) from a cadmium telluride solar panel was observed under simulated landfill conditions (Ramos-Ruiz, Wilkening, Field, & Sierra-Alvarez, 2017). A study by the same group demonstrated that the leachate of these cadmium telluride solar panels was highly inhibitory towards acetoclastic methanogens, a group of microorganisms that provide important ecosystem services in the biodegradation of organic matter within landfills (Ramos-Ruiz, Zeng, Sierra-Alvarez, Teixeira, & Field, 2016). This suggests that tellurium-contaminated leachate within landfills has the potential to impact key biodegradation processes in the surrounding environment, influencing the biodegradation and cycling of other environmental contaminants present in the landfill. It is clear from these preliminary observations, that it will become increasingly important to develop a better understanding of the biogeochemical cycling of tellurium compounds as usage of these compounds increases.

Microbial transformations of tellurium compounds

The various forms of tellurium described above are known to be interconverted by numerous microbial processes (both prokaryotic and eukaryotic) (**Figure 1.1**). Reduction of tellurite intracellularly is a well-characterized and wide-spread

phenomenon that is apparently mediated by several non-specific cellular components within the cytoplasmic compartment. In *Escherichia coli* these include: intracellular thiols, catalase, nitrate reductase, dihydrolipoamide dehydrogenase, pyruvate dehydrogenase, glutathione reductase, alkyl hydroperoxide reductase, thioredoxin reductase, flavorubredoxine reductase, isocitrate dehydrogenase, 6-phosphogluconate dehydrogenase, and NADH-II dehydrogenase (Arenas-Salinas et al., 2016; Castro, Molina, Díaz, Pichuantes, & Vásquez, 2008; Thomas Girard Chasteen et al., 2009; Díaz-Vásquez et al., 2014; Reinoso, Appanna, & Vásquez, 2013; Sandoval et al., 2015). Tellurite reductase activity has also been observed for some of these enzymes purified from bacteria other than *E. coli* (Arenas Salinas et al., 2014; Pugin et al., 2014). Additionally, the mercuric reductase of *Staphylococcus hemolyticus* has also been reported to have tellurite reductase activity *in vitro* (Arenas-Salinas et al., 2016). The non-specific reduction of tellurite by these molecules and enzymes does not appear to be tied to energy conservation since they are performed under both aerobic and anaerobic conditions. The cytoplasmic reduction of tellurite, however, does appear to play a significant role in its mechanism of toxicity, as will be discussed in a later section. A small number of organisms have been reported to use tellurite as a terminal electron acceptor, coupling its reduction to energy generation and growth. These include *Pseudomonas* sp. CM-3, which was isolated from gold mine tailings; *Bacillus selenitireducens*; *Bacillus beveridgei;* which was isolated from Mono Lake; and *Sulfurospirillum barnesii* (Baesman et al., 2007; Baesman, Stolz, Kulp, & Oremland, 2009; Maltman, Piercey-Normore, & Yurkov, 2015). However, the mechanism of tellurite reduction coupled to

energy generation in these organisms is unknown.

Tellurate reduction, in general, has received less attention than tellurite reduction. Thus, it is unclear how ubiquitous of an activity it is. However, *E. coli* has been reported to reduce tellurate to elemental tellurium. This process, like tellurite, tellurate, and selenate reduction by *E. coli* is likely to be a co-metbolic process rather than tied to energy generation as it will occur under aerobic conditions (Theisen, Zylstra, & Yee, 2013). Maltman et. al. (2016) isolated many microorganisms that reduce tellurite and/or tellurate under anaerobic conditions. These isolates originated from tube worms living in the vicinity of hydrothermal vents (Maltman, Walter, & Yurkov, 2016). These include representatives of the genera *Vibrio, Pseudoalteromonas, Curvibacter, Shewanella, Pseudomonas, Marinobacter, Thalassospira, Aquabacterium,* and *Okibacterium* (Maltman et al., 2016). However, anaerobic reduction coupled to growth was only demonstrated for one of the isolates: a *Shewanella* species (Maltman et al., 2016). The mechanism for tellurate reduction by bacteria is largely unknown. Knock-outs of molybdopterin biosynthesis and molybdenum transport genes did decrease tellurate reduction by *E. coli* (Theisen et al., 2013). However, individual knock-outs of molybdoenzymes did not impact tellurate reduction (Theisen et al., 2013). It is unclear from these results whether multiple molybdoenzymes might be mediating tellurate reduction or if molybdopterin is involved in tellurate reduction in some other way. An enzyme with tellurate- and tellurite-reductase activity was isolated from a tellurate- and tellurite-reducing aerobic phototroph, *Erythromonas ursincola* KR99 (Maltman, Donald, &

Yurkov, 2017a). Mass spectrometry analysis did not reveal any close homolog to this protein. The closest match was the chaperone GroEL from *Blastomonas* species (Maltman et al., 2017a).

A small number of bacterial strains have also been reported to couple reduction of tellurate under anaerobic conditions to cell growth and energy generation. *B. selenitireducens* couples growth to the reduction of tellurate (Baesman et al., 2007) as does *B. beveridgei* (Baesman et al., 2009). *Pseudomonas* str. CM-3 was demonstrated to couple reduction of tellurate to both cell growth and ATP generation (Maltman et al., 2015). The enzymes responsible for tellurate respiration have not been identified in these organisms. *Shewanella* sp. ER-Te-48 is another isolate from a deep sea hydrothermal vent that has been shown to couple anaerobic tellurate reduction with cell growth and energy production (Csotonyi, Stackebrandt, & Yurkov, 2006). A periplasmic enzyme of *Shewanella* sp. ER-Te-48 was found to have both tellurite- and tellurate-reductase actvitity *in vitro*. Mass spectrometry identified it as a homolog to the alkaline phosphatase enzyme of a *Pseudomonas* species (Maltman, Donald, & Yurkov, 2017b).

While reduction of tellurium oxyanions to the elemental form perhaps receives the most attention by modern researchers, the earliest reports of biological transformations of tellurium involved methylated tellurides produced from the biomethylation of tellurium oxyanions. In 1824, Gmelin noted the presence of a garlic odor in a rabbit that had been poisoned by telluric acid (Thomas G. Chasteen & Bentley, 2003). Challenger and North (1934) pinpointed

the cause of the odor as a volatile compound formed by the fungus *Scolpulariopsis brevicaulis*, dimethyltelluride (Challenger & North, 1934). Several species of fungi and bacteria have been identified that can produce dimethyltelluride from either tellurate or tellurite. Interestingly, three photosynthetic bacteria have been identified that can methylate solid elemental tellurium to form dimethyltelluride: *Rhodocyclus tenuis, Rhodospirillum rubrum* S1*,* and *Rhodospirillum rubrum* G9 (Fleet-Stalder & Chasteen, 1998). There are also a few reported instances in the literature of the production of dimethyl ditelluride by microorganisms (T. G. Chasteen, Silver, Birks, & Fall, 1990).

Telluroamino acids are another form of biogenic organotellurium compounds. Several fungal species have been shown to uptake and incorporate tellurite into telluroamino acids under certain conditions. When the fungi *Aspergillus fumigatus, Aspergillus terreus,* and *Penicillium chrysogenum* are grown in sulfur-free media in the presence of tellurite, these organisms assimilated the tellurite in the form of telluroamino acids and incorporated these amino acid derivatives into proteins. Tellurocysteine, tellurocystine, and telluromethione were all detected in proteins isolated from these organisms (Ramadan, Razak, Ragab, & el-Meleigy, 1989). The yeast *Saccharomyces cerevisiae* was shown to assimilate tellurite in the form of telluromethionine and Te-methyltellurocysteine (Yu, He, Chai, Yang, & Zheng, 1993). While no *in vivo* function for telluroamino acids has yet been identified, synthetic telluroamino acid derivatives have been shown to have glutathione peroxidase activity *in vitro*

(Braga et al., 2009). In contrast to selenocysteine, the 21st proteinogenic amino acid, these telluroamino acids have also never been reported to occur in nature. C-Te bonds are more unstable than C-Se bonds due to the greater polarizability of tellurium compared to selenium, therefore telluroamino acids are unlikely to be stable enough to persist for long periods of time in the environment (Cunha, Gouvea, & Juliano, 2009). **Figure 1.1** summarizes the biogeochemical cycle of tellurium.

Tellurium toxicity

The toxicity of tellurium in living organisms is highly dependent upon its redox state. Tellurite is more toxic than tellurate and both are more toxic than elemental tellurium (Ba et al., 2010). Thus the microbial redox transformations of tellurium compounds described above will influence the toxicity of tellurium within the environment. Tellurium likely exerts its toxic effects through several mechanisms. In mammals, tellurium compounds interact with and alter the function of cysteine-containing enzymes. In rats, tellurite ingestion has been shown to inhibit the enzyme squalene monooxygenase resulting in peripheral neuropathy (Laden & Porter, 2001). Tellurite and methylated telluride species are both capable of binding to cysteine residues in the enzyme's active site, inhibiting its activity (Laden & Porter, 2001). Tellurium compounds also have a high affinity for selenium and can bind to the selenocysteine residues of selenoproteins. Tellurite binds to the selenocysteine residue in the active site of the oxidative stress protein glutathionine peroxidase of rat hepatocytes,

inhibiting its activity (Garberg et al., 1999). Direct interactions between tellurium compounds and microbial enzymes have not yet been studied. However, they are likely to be similar to the ones described above in eukaryotic systems as the chemical interactions between cysteine or selenocysteine residues and tellurium compounds are likely to be the same across all domains of life.

Tellurium compounds will also induce reactive oxygen species (ROS) stress in cells. Tellurite exposure generates ROS in the cytoplasm of *E. coli* (Pérez et al., 2007). ROS production was associated with protein damage via carbonylation, membrane lipid peroxidation, and inactivation of [Fe-S]-containing enzymes (Pérez et al., 2007). Similar results were observed in *Pseudomonas pseudoalcaligenes* where ROS production occurred concurrent to the depletion of cellular thiols (Tremaroli, Fedi, & Zannoni, 2007). The exact mechanism for the formation of the observed ROS is still being clarified but it has been suggested that, similar to selenite (discussed in a later section), superoxide radicals may be produced during the reduction of tellurite by cellular enzymes and/or cellular thiols (Thomas Girard Chasteen et al., 2009). Tellurite reduction by catalase *in vitro* results in generation of the superoxide radical (Pérez et al., 2007). The NADH-dehydrogenase II enzyme of *E. coli* also has tellurite-reductase activity that is coupled to superoxide radical production *in vitro* (Díaz-Vásquez et al., 2014). However, tellurite exposure also triggers the accumulation of heme biosynthetic intermediates which could potentially contribute to the formation of ROS within tellurite-exposed cells (Morales et al., 2017). The introduction to **Chapter 3** provides a more detailed description on the current state of

knowledge of the toxicity of tellurite in *E. coli.*

Interestingly, selenite exposure elicits higher ROS production in *E. coli* compared to tellurite exposure. However, tellurite is considerably more toxic towards the cells compared to selenite. Thus, while generation of ROS may certainly be a major player in the toxicity of tellurite, it is clearly not the sole agent mediating its toxicity inside the cells (Vrionis, Wang, Haslam, & Turner, 2015). Furthermore, tellurite remains toxic to cells even under anaerobic conditions (Morales et al., 2017). While there have been great strides in furthering our understanding of tellurite toxicity, much remains to be learned. Finally, the toxicity of tellurate towards microorganisms remains largely uncharacterized.

In recent years, there has been renewed interest in understanding the underlying mechanisms of tellurium compound toxicity in microorganisms for potential pharmacological purposes. The heme biosynthetic precursor 5-aminolevulinic acid (ALA) is used as a prodrug in photodynamic therapy to control the growth of infectious microorganisms (Harris & Pierpoint, 2012). However, higher (millimolar) doses of ALA are often required for it to be effective. Micromolar doses of tellurite and ALA were demonstrated by Morales et. al. to effectively inhibit the growth of *E. coli, Salmonella* Typhi, *Salmonella* Typhimurium, and *Klebsiella pneumoniae* (Morales et al., 2017). Various organotellurium compounds have also been studied for their pharmacological potential. Ammonium trichlori(dioxyethelene)tellurate is a relatively non-toxic tellurium compound with antitumor activity that is likely related to its

interactions with cysteine residues of cellular proteins (Frei et al., 2008). Other compounds have shown activity against the parasites *Plasmodium falciparum* and *Leishmania amazonensis* (Tiekink, 2012). If these tellurium compounds are to be seriously considered for their antimicrobial activity, it will be essential to first develop a better understanding of their modes of action.

Selenium biogeochemistry

Selenium in the environment

The crustal abundance of selenium is greater than that of tellurium at 0.05 ppm (Lakin, 1973). However, like tellurium, global distribution of selenium is heterogenous with substantially higher concentrations present in certain geographic locations (Fernández-Martínez & Charlet, 2009). Seleniferous soils can contain selenium concentrations ranging from 1-1,200 ppm (Fernández-Martínez & Charlet, 2009) The selenium content of coal and petroleum is higher than its crustal abundance at averages of 3 and 0.2 ppm, respectively (Lakin, 1973).

The main source of selenium in the terrestrial environment are rocks – mainly sandstone, quartzite, and limestone. Selenium release and transport from these natural sources is controlled by weathering, water interactions, and biological processes (Fernández-Martínez & Charlet, 2009). The parent material of soils is the main determinant of their selenium content (Fernández-Martínez & Charlet, 2009). Seleniferous soils are derived from selenium-rich rocks such as

black shale, carbonaceous limestone, carbonaceous chert, mudstones, and coal (Winkel et al., 2012). In addition to natural sources, a large portion of the selenium released in the environment today comes from anthropogenic sources, namely, coal combustion, petroleum combustion, and the extraction and processing of copper, zinc, uranium, phosphorus, and lead (Fernández-Martínez & Charlet, 2009). Selenium concentrations and bioavailability within soils are of major interest for both human and environmental health. Low selenium availability (whether due to low bioavailability or low overall concentration) leads to selenium-deficiency disease in the people in those regions (Wang & Gao, 2001). In contrast, high selenium concentrations and/or high selenium bioavailability in soils has the potential to induce selenosis in humans and animals (Fordyce, 2007).

The primary forms of selenium in the environment are selenate, selenite, elemental selenium, selenide, and various organoselenium compounds (Fernández-Martínez & Charlet, 2009). Within oxidizing environments, selenate and selenite predominate with selenate being more thermodynamically favored in highly-oxidizing environments while selenite is favored in more moderately-oxidizing environments (Winkel et al., 2012). Selenate tends to be more bioavailable than selenite as selenite is more prone to sorption to iron oxides, clays, and organic matter (Winkel et al., 2012). Elemental selenium and selenides are formed in anoxic sediments, mainly through the biological reduction processes described in the next section (Masscheleyn & Patrick Jr, 1993).

Microbial transformations of selenium compounds

The role of microorganisms in the biogeochemical cycling of selenium compounds is well characterized. Many microorganisms can reduce selenate and selenite to elemental selenium in both energy-generating and non-energy-generating processes (Kessi & Hanselmann, 2004; Nancharaiah & Lens, 2015). Selenate supports the anaerobic growth of a diverse group of dissimilatory selenate-reducing microorganisms (Nancharaiah & Lens, 2015). These organisms will reduce selenate to selenite, coupled to energy production and growth. This process typically results in the formation of red elemental selenium due to the further reduction of the selenite. The molecular mechanisms of selenate respiration have been clarified in *Thauera selenatis*. The SerABC selenate reductase complex of *T. selenatis* reduces selenate to selenite in the periplasmic space (Lowe et al., 2010). From there, it is assumed that selenite is transported into the cytoplasm by the sulfate transporter CysPUWA and further reduced to elemental selenium by intracellular thiols (Nancharaiah & Lens, 2015).

As described in greater detail in the following section of this review, selenite reduction in the cytoplasm of microorganisms is believed to be a glutathione-mediated process that does not generate energy but instead is (at least partially) responsible for the toxicity of selenite (Kessi & Hanselmann, 2004). While the reduction of selenite to elemental selenium coupled to the oxidation of acetate or lactate is an energetically favorable reduction, few organisms that respire selenite have been described. *Geobacter sulfurreducens, Shewanella oneidensis* MR-1, and *Veillonella atypica* reduce selenite to elemental selenium when grown with selenite and an electron donor under

anaerobic conditions (Pearce et al., 2009). Selenite reduction in *S. oneidensis* MR-1 occurs in the periplasm and is mediated by respiratory enzymes, thus avoiding its reduction within the cytoplasm by intracellular thiols (Li et al., 2014). Certain selenate-respiring isolates also appear to be capable of using selenite as a terminal electron acceptor (Nancharaiah & Lens, 2015). There has been a single report of an organism that reduces elemental selenium to selenide. The selenite-respiring organism *B. selenitireducens* forms selenide when grown on elemental selenium as an electron acceptor (Herbel, Blum, Oremland, & Borglin, 2003). This organism also produces selenide when grown on selenite as an electron acceptor, differing from most selenite- and selenate-respiring organisms, which typically end at elemental selenium (Herbel et al., 2003; Nancharaiah & Lens, 2015).

On the oxidative side of the selenium biogeochemical cycle, there have been a couple of reports of elemental selenium oxidation. These are detailed further in the introduction to **Chapter 4**. Briefly, a *Bacillus megaterium* strain was reported to oxidize elemental selenium to selenite and trace amounts of selenate (Sarathchandra & Watkinson, 1981). The chemoheterotrophic bacteria *Thiobacillus* sp. ASN-1 and *Leptothrix* sp. MnB1 also oxidize elemental selenium to a mixture of selenate and selenite (Dowdle & Oremland, 1998). The oxidation of elemental selenium is an important, yet understudied, process. The toxicity of selenium is heavily dependent upon its speciation with selenium oxyanions being substantially more toxic than elemental selenium (Painter, 1941). Additionally, the selenium oxyanions are more mobile and bioavailable than elemental

selenium (Mayland, Gough, & Stewart, 1991; Singh & Singh, 1979; Young, Nahapetian, & Janghorbani, 1982). Oxidation of elemental selenium holds great significance from an ecotoxicological perspective as the process will mobilize selenium to its more soluble and toxic forms and thus warrants further investigation.

As with tellurium, inorganic selenium species will also be reductively assimilated as organoselenium compounds. Phylogenetically diverse bacteria and fungi reduce selenite, selenate, and elemental selenium to different volatile methylated selenium species, primarily, dimethylselenide, dimethyldiselenide, and dimethylseleneyl sulfide (Thomas G. Chasteen & Bentley, 2003). Selenium can also take the place of sulfur within amino acids resulting in the formation of selenoamino acids including selenocysteine and selenomethione. The amino acid selenocysteine is found in and plays an important functional role in different prokaryotic and eukaryotic enzymes including glutathione peroxidase, thioredoxin reductase, hydrogenases, glutaredoxin and formate dehydrogenase (Gladyshev, 2011; Zwolak & Zaporowska, 2012). When grown in selenium-containing media, *S. cerevisiae, Candida albicans,* and *E. coli* will assimilate the selenium to produce selenomethionine (Schrauzer, 2000). Selenomethionine is non-specifically incorporated into proteins in the place of methionine residues (Boles et al., 1991). This substitution is often well-tolerated structurally and tends to have minimal impact on enzyme activity (Kitajima & Chiba, 2013; Schrauzer, 2000). **Figure 1.2** summarizes the biogeochemical cycle of selenium.

Selenium toxicity

Selenium is simultaneously an essential trace element for living organisms and a toxicant when present at higher concentrations. Comparatively more literature exists on the toxicity of selenium compounds in living organism and may provide insight into the mechanisms of toxicity of tellurium compounds due to the structural similarity between the two elements. Interestingly, co-exposure with selenite has been shown to decrease the susceptibility of *E. coli* to tellurite suggesting some overlap in the cellular systems impacted by the two (Vrionis et al., 2015).

It is generally held that the relative toxicity of different selenium compounds is as follows: selenite > selenate > selenide > elemental selenium (Painter, 1941). This is comparable to the relative toxicities of their tellurium counterparts (Zannoni et al., 2007). It has been suggested by some that the toxicity of selenium may be due to its non-specific incorporation into proteins in the place of sulfur amino acids, specifically selenomethionine incorporation (Staicu & Barton, 2017). However, selenomethionine incorporation in place of methionine is well-tolerated structurally and often does not substantially alter enzymatic activity (Kitajima & Chiba, 2013; Schrauzer, 2000). Interestingly, selenomethionine substitution has actually been demonstrated to enhance the activity and stability of certain enzymes (Gassner, Baase, Hausrath, & Matthews, 1999; Schrauzer, 2000).

The toxicity of selenium appears to be mainly attributed to its reactivity with intracellular thiols (Spallholz, 1994). Reduction of selenite with glutathione

results in the formation of superoxide radicals (Kessi & Hanselmann, 2004). Reactions of selenite and selenocysteine with glutathione have both been shown to generate superoxide radicals. Reaction of selenite with cysteine will also generate superoxide radicals (Spallholz, 1994). In a parallel mentioned in the prior section, *in vitro* enzymatic reduction of tellurite has also been shown to generate superoxide radical (Pérez et al., 2007).

In contrast to reactions with selenite, reactions of glutathione with selenomethionine or selenate do not produce superoxide radicals (Spallholz & Hoffman, 2002). In fact, selenate is seemingly not reduced at all by glutathione as no elemental selenium is observed to precipitate from the reaction (Spallholz, 1994). This observation has been interpreted by some to suggest that toxicity of selenate is solely due to its reduction by other enzymes/molecules to the ROS-generating selenite (Spallholz, 1994). However, as will be discussed below, the toxicity of selenite even does not appear to be entirely attributable to the glutathione-dependent generation of superoxide radical (Tarze et al., 2007).

Conflicting data exists as to whether selenite reduction to more reduced species by glutathione is protective or damaging to organisms. Glutathione-deficient strains of *E. coli* and *Salmonella* Typhimurium are more resistant to selenite than the wild-type strains (Bébien, Lagniel, et al., 2002; Kramer & Ames, 1988). In contrast, a glutathione-deficient strain of *S. cerevisiae* was found to have increased sensitivity to selenite over the wild-type strain (Gharieb & Gadd, 2004). In that study, glutathione appeared to influence the rate of uptake of selenite. The glutathione-deficient strain accumulated higher levels of selenite

than the wild-type strain (Gharieb & Gadd, 2004). Tarze et. al. (2007) observed that the presence of thiols (both glutathione and cysteine) in the growth media increased the toxicity of selenite towards *S. cerevisiae*. This was attributed to the extracellular formation of hydrogen selenide during the reaction between selenite and the exogenous glutathione rather than the generation of superoxide radical within the media (Tarze et al., 2007). Formation of selenide in the media from this reaction resulted in increased selenium accumulation within the cells. This was proposed to be the mechanism by which exogenous glutathione enhanced selenite toxicity (Tarze et al., 2007). Once inside the cells, selenide may inflict damage through its reaction with molecular oxygen to form ROS. It will also oxidize the intracellular glutathione pool (Tarze et al., 2007). Selenide toxicity may also be attributable to its ability to inhibit the activity of proteins with heme and other iron cofactors (Björnstedt, Odlander, Kuprin, Claesson, & Holmgren, 1996; Shen, Yang, Ding, Liu, & Ong, 2001).

Using selenium chemistry as a basis for comparison, one could speculate that telluride (or other reactive, reduced tellurium intermediates) might be formed from reduction of tellurite and/or tellurate with cellular thiols. It would be interesting to explore: (1) the intermediates of tellurite and tellurate reduction with various thiols to the level of detail that the reaction of selenite with glutathione has been described; and then (2) if these intermediates contribute to the oxygen-independent toxicity of tellurium oxyanions.

CENTRAL SULFUR METABOLIC PATHWAYS

Introduction

Microbial sulfur metabolism is a major player in the biogeochemical cycles of tellurium and selenium. The central sulfur metabolic pathways play a key role in the transport, toxicity, and speciation of tellurium and selenium compounds and this trend will likely be reinforced by further studies of cellular tellurium and selenium interactions. Several examples have already been described above where sulfur metabolites have influenced the toxicity and speciation of tellurium and selenium compounds.

The central sulfur metabolism of microorganisms consists of numerous complex biochemical pathways that can vary from organism to organism. However, this review will focus on the sulfur metabolic pathways of *E. coli* not only because these systems are extremely well-characterized in the literature but also because this organism is the focus of the studies performed in **Chapter 2** and **Chapter 3**. The sulfur metabolic pathways of *Shewanella oneidensis* MR-1 are the focus of **Chapter 5** and are discussed in further detail there. However, *S. oneidensis* MR-1 and *E. coli* appear to share many common pathways (**Figure 5.6)** and so a review of the well-characterized *E. coli* pathways is nonetheless informative when considering sulfur metabolism in *S. oneidensis* MR-1.

Transport

E. coli has two characterized sulfate transporters. CysPUWA is a member of the SulT-type sulfate/tungstate uptake transporter family (Aguilar-Barajas, Díaz-Pérez, Ramírez-Díaz, Riveros-Rosas, & Cervantes, 2011). SulT-type transporters are members of the ABC superfamily of transporters (Aguilar-Barajas et al., 2011). Homologs to this transporter are widely dispersed among bacteria (Aguilar-Barajas et al., 2011). CysPUWA transports both sulfate and thiosulfate into the cell in an energy-dependent process (Sirko, Hryniewicz, Hulanicka, & Böck, 1990). However, CysPUWA is a non-specific transporter and will also transport structurally similar anions into the cell. CysPUWA has been implicated in the transport of chromate, molybdate, selenate, and selenite (Lindblow-Kull, Kull, & Shrift, 1985; Mansilla & de Mendoza, 2000; Rosentel, Healy, Maupin-Furlow, Lee, & Shanmugam, 1995). These structurally similar anions will compete with sulfate for transport into the cell (Lindblow-Kull et al., 1985).

E. coli's second known sulfate transporter is CysZ (Parra, Britton, Castle, Jones-Mortimer, & Kornberg, 1983). CysZ is a proton-gradient-driven, high-affinity sulfate transporter (Zhang, Jiang, Nan, Almqvist, & Huang, 2014). The ModABC molybdate permease of *E. coli* will also non-specifically transport sulfate (Aguilar-Barajas et al., 2011).

Assimilatory sulfate reduction

Once inside the cell, the sulfate must be reduced to sulfide prior to its assimilation into organic compounds. Sulfate first reacts with ATP in a reaction catalyzed by ATP sulfurylase (CysDN) to form adenosine phosphosulfate (APS) (Sekowska, Kung, & Danchin, 2000). APS is then phosphorylated utilizing a second molecule of ATP to form 3'phosphoadinosine phosphosulfate (PAPS) in a reaction catalyzed by APS kinase (CysC) (Sekowska et al., 2000). PAPS is then reduced to sulfite by PAPS reductase (CysH), releasing adenosine 3'-5' diphosphate (PAP) as a byproduct (Sekowska et al., 2000). Sulfite is then reduced to sulfide in an NADPH-dependent step by the enzyme NADPH-sulfite reductase (CysJIH) (Sekowska et al., 2000). Sulfide then reacts with O-acetyl-L-serine (OAS) to form cysteine in a reaction catalyzed by one of two OAS sulhydrylases (CysK and CysM) (Sekowska et al., 2000).

E. coli can also assimilate other inorganic sulfur sources such as sulfite and thiosulfate. Sulfite is presumably assimilated via the same pathway as sulfate. CysM can also use thiosulfate as a substrate in the reaction with OAS, forming S-sulfocysteine (SSC) (Nakatani et al., 2012). SSC is converted to cysteine by NrdH and Grx1, releasing a molecule of sulfite in the process (Nakatani et al., 2012). However, thiosulfate assimilation also appears to occur through a process independent of CysM. In this secondary pathway, thiosulfate is first converted to sulfite by thiosulfate sulfurtransferase (GlpE). The resulting sulfite is then assimilated via the canonical sulfate assimilation pathway (Kawano et al., 2017). A second periplasmic thiosulfate sulfurtransferase, PspE, may also

play a role in this alternative pathway of thiosulfate assimilation (Kawano et al., 2017).

Sulfur amino acid metabolism

Cysteine, in addition to its role as an essential proteinogenic amino acid, is the precursor for other sulfur-containing amino acids. Cysteine is condensed with O-succinylhomoserine to produce cystathionine in a reaction catalyzed by cystathionine γ-synthase (MetB). Cystathionine is then converted by cystathionine β-lyase (MetC) to homocysteine, which is then methylated by one of two methionine synthase enzymes (MetH or MetE) to form methionine (Sekowska et al., 2000).

Glutathione is the main intracellular thiol in many Gram negative bacteria; however, it is observed less commonly in Gram positive bacteria (Fahey, Brown, Adams, & Worsham, 1978). In *E. coli,* intracellular glutathione concentrations are often an order of magnitude larger than intracellular cysteine concentrations (Chonoles Imlay, Korshunov, & Imlay, 2015; Fahey et al., 1978). Glutathione plays a role in mitigating disulfide and general oxidative stress in *E. coli* and other organisms (Carmel-Harel & Storz, 2000). Glutathione is a tripeptide (L-γ-glutamyl-L-csyteinylglycine) synthesized in a two-step reaction from cysteine by the enzymes γ-glutamylcysteine synthetase (GshA) and glutathione synthetase (GshB) (Carmel-Harel & Storz, 2000).

Several different enzymes are also involved in the breakdown of cysteine, coupled with the release of sulfide. The enzyme cysteine aminotransferase (AspC) converts cysteine and α-ketoglutarate to glutamate and 3-metcaptopyruvate (3-MP). 3-MP sulfurtransferase (SseA) breaks down 3-MP to pyruvate, releasing sulfide in the process (Shatalin, Shatalina, Mironov, & Nudler, 2011). Other enzymes in *E. coli* are known to have cysteine desulfhydrase activity (cysteine degradation with the release of pyruvate, ammonia, and sulfide). These include CysK, CysM, MetC, MalY, and TnaA. However, all of these enzymes have other activities and cysteine does not appear to be their primary substrate (Barton, Ritz, Fauque, & Lin, 2017). In mammals, it is well-established that sulfide is an important regulatory molecule (Kimura, 2009). However, its role in bacteria is just beginning to be elaborated, despite the fact that sulfide production is a relatively ubiquitous trait (Shatalin et al., 2011). Recent work has suggested that sulfide production decreases sensitivity of *E. coli* and other bacteria to antibiotics and oxidative stress by suppressing Fenton chemistry by sequestering intracellular ferrous iron and by enhancing the activity of catalase and superoxide dismutase (Shatalin et al., 2011)

THE ROLE OF MICROBIAL SULFUR METABOLISM IN BIOGEOCHEMICAL CYCLING OF TELLURIUM AND SELENIUM

A role for microbial central sulfur metabolism has been well-described in respect to microbial selenium metabolism and emerging evidence suggests that it is equally as important in microbial tellurium metabolism. The sulfate transporter

CysPUWA is also implicated in the uptake of both selenate and selenite (Lindblow-Kull et al., 1985). The relative K_m for each substrate is selenite>selenate>sulfate. The V_{max}/K_m ratio is highest for sulfate indicating that it is the preferred ligand of the enzyme with selenate and selenite having similar lower values (Lindblow-Kull et al., 1985). An *E. coli* strain with a mutation in the *cysA* gene is unable to reduce selenate due to its inability to transport selenate into the cytoplasm (Bébien, Kirsch, Méjean, & Verméglio, 2002). In contrast, tellurite is transported into the cytoplasm via phosphate transporters of the PiT family and acetate permeases (Borghese & Zannoni, 2010; Borsetti, Toninello, & Zannoni, 2003; A. Elías et al., 2015; A. O. Elías et al., 2012). However, a transporter for tellurate has yet to be described. We performed a preliminary screen of the Keio collection of *E.* coli K-12 single gene knock-out mutants for strains that lost the ability to form Te(0) when grown on tellurate. The results of this screen suggested that strains carrying deletions of the subunits of the CysPUWA transporter were unable to reduce tellurate. **Chapter 2 explores the role of the *E. coli* K-12's sulfate transporters in the transport and toxicity of tellurate.**

As described in earlier sections, the interactions between selenium, tellurium, and cellular thiols play an important role in their toxicity in microorganisms (Kessi & Hanselmann, 2004; Pérez et al., 2007). These redox reactions drive the transformation of more soluble and toxic selenium and tellurium oxyanions to their less soluble and toxic elemental forms (Zannoni et al., 2007). Selenite is reduced by both glutathione and cysteine (Spallholz, 1994).

Reduction of selenite by glutathione is a complex but well-characterized process with multiple reduced selenium compound intermediates prior to the formation of elemental selenium. Selenite first reacts with glutathione to form selenodiglutathione (GS-Se-SG). If excess glutathione is present, further reduction by the glutathione will occur yielding glutathioselenol (GS-SeH). Glutathioselenol will either dismutate into Se(0) and glutathione or, if glutathione is present in excess, it will be reduced by glutathione to form selenide. In the presence of oxygen, selenide will be oxidized to Se(0) (Tarze et al., 2007). This series of reactions is accompanied by production of harmful superoxide radical as described in a prior section (Kessi & Hanselmann, 2004). Tellurite exposure is known to deplete intracellular pools of glutathione and acetyl-CoA in *E. coli* (Turner, Aharonowitz, Weiner, & Taylor, 2001). However, the reaction mechanism for tellurite reduction by these thiol compounds is not known. Additionally, it is unknown whether tellurate will also react with these intracellular thiols. **Chapter 3 explores the role of exogenously supplied and endogenous thiol and disulfide compounds in the reduction and toxicity of tellurate in *E. coli* K-12.**

Biogenic sulfur can influence the solubility and speciation of chalcophilic elements. Baas Becking and Moore (1961) reacted biogenic sulfide derived from the sulfate-respiring bacteria *Desulfovibrio desulfuricans* with various metals to produce iron sulfide, sphalerite, argentite, covellite, digenite, and galena (Baas Becking & Moore, 1961). Bacteria grown under non-sulfur-respiring conditions are also capable of releasing endogenous sulfur metabolites such as sulfide,

glutathione, and cysteine into their external environment (Chonoles Imlay et al., 2015; Owens & Hartman, 1986; Shatalin et al., 2011). Classically, triple-sugar iron media has been used to detect the evolution of hydrogen sulfide by enteric microorganisms through the formation of the insoluble iron sulfide (Hajna, 1945). Interestingly, abiotic reactions with Se(0) to form a variety of soluble selenosulfur species have been reported for sulfite, sulfide, and thiosulfate suggesting the potential for solubilization by biogenic sulfur species (Ball & Milne, 1995; Rahim & Milne, 1996; Weres, Jaouni, & Tsao, 1989). However, this is an area of study that has not received much attention from researchers and warrants further investigation. **Chapter 4 describes the isolation of a Se(0)-solubilizing *Bacillus* species from seleniferous soils and explores the role of secreted endogenous sulfur metabolites in Se(0)-dissolution.** Finally, I sought to extend the results from **Chapter 4** to other organisms to determine the ubiquity of the production of reactive extracellular sulfur metabolites. **Chapter 5 explores the production of external sulfur metabolites by *S. oneidensis* MR-1 and considers both the functional and geochemical implications of these observations.**

REFERENCES:

Aguilar-Barajas, E., Díaz-Pérez, C., Ramírez-Díaz, M. I., Riveros-Rosas, H., & Cervantes, C. (2011). Bacterial transport of sulfate, molybdate, and related oxyanions. *BioMetals, 24*(4), 687-707. doi:10.1007/s10534-011-9421-x

Arenas-Salinas, M., Vargas-Pérez, J., Morales, W., Pinto, C., Muñoz, P., Cornejo, F., . . . Arenas Salinas, F. (2016). Flavoprotein-Mediated Tellurite Reduction: Structural Basis and Applications to the Synthesis of

Tellurium-Containing Nanostructures. *Frontiers in microbiology, 7*. doi:10.3389/fmicb.2016.01160

Arenas Salinas, F., Leal, C. A., Pinto, C. A., Arenas-Salinas, M., Morales, W. A., Cornejo, F., . . . Vásquez, C. (2014). On the mechanism underlying tellurite reduction by Aeromonas caviae ST dihydrolipoamide dehydrogenase. *Biochimie, 102*. doi:10.1016/j.biochi.2014.03.008

Ba, L. A., Döring, M., Jamier, V., & Jacob, C. (2010). Tellurium: an element with great biological potency and potential. *Organic & Biomolecular Chemistry, 8*(19), 4203-4216. doi:10.1039/C0OB00086H

Baas Becking, L. G. M., & Moore, D. (1961). Biogenic sulfides. *Economic Geology, 56*(2), 259-272. doi:10.2113/gsecongeo.56.2.259

Baesman, S. M., Bullen, T. D., Dewald, J., Zhang, D., Curran, S., Islam, F. S., . . . Oremland, R. S. (2007). Formation of Tellurium Nanocrystals during Anaerobic Growth of Bacteria That Use Te Oxyanions as Respiratory Electron Acceptors. *Applied and Environmental Microbiology, 73*(7), 2135-2143. doi:10.1128/aem.02558-06

Baesman, S. M., Stolz, J. F., Kulp, T. R., & Oremland, R. S. (2009). Enrichment and isolation of Bacillus beveridgei sp. nov., a facultative anaerobic haloalkaliphile from Mono Lake, California, that respires oxyanions of tellurium, selenium, and arsenic. *Extremophiles, 13*(4), 695-705. doi:10.1007/s00792-009-0257-z

Ball, S., & Milne, J. (1995). Studies on the interaction of selenite and selenium with sulfur donors. Part 3. Sulfite. *Canadian Journal of Chemistry, 73*(5), 716-724. doi:10.1139/v95-091

Barton, L. L., Ritz, N. L., Fauque, G. D., & Lin, H. C. (2017). Sulfur Cycling and the Intestinal Microbiome. *Digestive Diseases and Sciences, 62*(9), 2241-2257. doi:10.1007/s10620-017-4689-5

Bébien, M., Kirsch, J., Méjean, V., & Verméglio, A. (2002). Involvement of a putative molybdenum enzyme in the reduction of selenate by Escherichia coli. *Microbiology, 148*(12), 3865-3872. doi:doi:10.1099/00221287-148-12-3865

Bébien, M., Lagniel, G., Garin, J., Touati, D., Verméglio, A., & Labarre, J. (2002). Involvement of Superoxide Dismutases in the Response of Escherichia coli to Selenium Oxides. *Journal of Bacteriology, 184*(6), 1556. doi:10.1128/JB.184.6.1556-1564.2002

Björnstedt, M., Odlander, B., Kuprin, S., Claesson, H.-E., & Holmgren, A. (1996). Selenite Incubated with NADPH and Mammalian Thioredoxin Reductase Yields Selenide, Which Inhibits Lipoxygenase and Changes the Electron

Spin Resonance Spectrum of the Active Site Iron. *Biochemistry, 35*(26), 8511-8516. doi:10.1021/bi9528762

Boles, J. O., Cisneros, R. J., Weir, M. S., Odom, J. D., Villafranca, J. E., & Dunlap, R. B. (1991). Purification and characterization of selenomethionyl thymidylate synthase from Escherichia coli: comparison with the wild-type enzyme. *Biochemistry, 30*(46), 11073-11080. doi:10.1021/bi00110a009

Borghese, R., & Zannoni, D. (2010). Acetate Permease (ActP) Is Responsible for Tellurite (TeO_3^{2-}) Uptake and Resistance in Cells of the Facultative Phototroph Rhodobacter capsulatus. *Applied and Environmental Microbiology, 76*(3), 942. doi:10.1128/AEM.02765-09

Borsetti, F., Toninello, A., & Zannoni, D. (2003). Tellurite uptake by cells of the facultative phototroph Rhodobacter capsulatus is a ΔpH-dependent process. *FEBS Letters, 554*(3), 315-318. doi:https://doi.org/10.1016/S0014-5793(03)01180-3

Bouroushian, M. (2010). Electrochemistry of the Chalcogens. In M. Bouroushian (Ed.), *Electrochemistry of Metal Chalcogenides* (pp. 57-75). Berlin, Heidelberg: Springer Berlin Heidelberg.

Braga, A. L., Alberto, E. E., Soares, L. C., Rocha, J. B. T., Sudati, J. H., & Roos, D. H. (2009). Synthesis of telluroamino acid derivatives with remarkable GPx like activity. *Organic & Biomolecular Chemistry, 7*(1), 43-45. doi:10.1039/B814990A

Carmel-Harel, O., & Storz, G. (2000). Roles of the Glutathione- and Thioredoxin-Dependent Reduction Systems in the Escherichia Coli and Saccharomyces Cerevisiae Responses to Oxidative Stress. *Annual Review of Microbiology, 54*(1), 439-461. doi:10.1146/annurev.micro.54.1.439

Castro, M. E., Molina, R., Díaz, W., Pichuantes, S. E., & Vásquez, C. C. (2008). The dihydrolipoamide dehydrogenase of Aeromonas caviae ST exhibits NADH-dependent tellurite reductase activity. *Biochemical and Biophysical Research Communications, 375*(1), 91-94. doi:https://doi.org/10.1016/j.bbrc.2008.07.119

Challenger, F., & North, H. E. (1934). 20. The production of organo-metalloidal compounds by micro-organisms. Part II. Dimethyl selenide. *Journal of the Chemical Society (Resumed)*(0), 68-71. doi:10.1039/JR9340000068

Chasteen, T. G., & Bentley, R. (2003). Biomethylation of Selenium and Tellurium: Microorganisms and Plants. *Chemical Reviews, 103*(1), 1-26. doi:10.1021/cr010210+

Chasteen, T. G., Fuentes, D. E., Tantaleán, J. C., & Vásquez, C. C. (2009). Tellurite: history, oxidative stress, and molecular mechanisms of

resistance. *FEMS Microbiology Reviews, 33*(4), 820-832. doi:10.1111/j.1574-6976.2009.00177.x

Chasteen, T. G., Silver, G. M., Birks, J. W., & Fall, R. (1990). Fluorine-induced chemiluminescence detection of biologically methylated tellurium, selenium, and sulfur compounds. *Chromatographia, 30*(3), 181-185. doi:10.1007/BF02274543

Chonoles Imlay, K. R., Korshunov, S., & Imlay, J. A. (2015). Physiological Roles and Adverse Effects of the Two Cystine Importers of Escherichia coli. *Journal of Bacteriology, 197*(23), 3629. doi:10.1128/JB.00277-15

Csotonyi, J. T., Stackebrandt, E., & Yurkov, V. (2006). Anaerobic respiration on tellurate and other metalloids in bacteria from hydrothermal vent fields in the eastern Pacific Ocean. *Appl Environ Microbiol, 72*(7), 4950-4956. doi:10.1128/AEM.00223-06

Cunha, R. L. O. R., Gouvea, I. E., & Juliano, L. (2009). A glimpse on biological activities of tellurium compounds. *Anais da Academia Brasileira de Ciências, 81*, 393-407. Retrieved from http://www.scielo.br/scielo.php?script=sci_arttext&pid=S0001-37652009000300006&nrm=iso

Díaz-Vásquez, W. A., Abarca-Lagunas, M. J., Arenas, F. A., Pinto, C. A., Cornejo, F. A., Wansapura, P. T., . . . Vásquez, C. C. (2014). Tellurite reduction by Escherichia coli NDH-II dehydrogenase results in superoxide production in membranes of toxicant-exposed cells. *BioMetals, 27*(2), 237-246. doi:10.1007/s10534-013-9701-8

Dowdle, P. R., & Oremland, R. S. (1998). Microbial Oxidation of Elemental Selenium in Soil Slurries and Bacterial Cultures. *Environmental Science & Technology, 32*(23), 3749-3755. doi:10.1021/es970940s

Edwards, P. J. (1998). Sulfur cycling, retention, and mobility in soils: a review. *Gen. Tech. Rep. NE-250. Radnor, PA: US Department of Agriculture, Forest Service, Northeastern Research Station. 18 p., 250.*

Elías, A., Díaz-Vásquez, W., Abarca-Lagunas, M. J., Chasteen, T. G., Arenas, F., & Vásquez, C. C. (2015). The ActP acetate transporter acts prior to the PitA phosphate carrier in tellurite uptake by Escherichia coli. *Microbiological Research, 177*, 15-21. doi:http://dx.doi.org/10.1016/j.micres.2015.04.010

Elías, A. O., Abarca, M. J., Montes, R. A., Chasteen, T. G., Pérez-Donoso, J. M., & Vásquez, C. C. (2012). Tellurite enters Escherichia coli mainly through the PitA phosphate transporter. *MicrobiologyOpen, 1*(3), 259-267. doi:10.1002/mbo3.26

Fahey, R. C., Brown, W. C., Adams, W. B., & Worsham, M. B. (1978). Occurrence of glutathione in bacteria. *Journal of Bacteriology, 133*(3), 1126-1129. Retrieved from https://jb.asm.org/content/jb/133/3/1126.full.pdf

Fernández-Martínez, A., & Charlet, L. (2009). Selenium environmental cycling and bioavailability: a structural chemist point of view. *Reviews in Environmental Science and Bio/Technology, 8*(1), 81-110. doi:10.1007/s11157-009-9145-3

Filella, M., Reimann, C., Biver, M., Rodushkin, I., & Rodiouchkina, K. (2019). Tellurium in the environment: Current knowledge and identification of gaps. *Environmental Chemistry*. doi:10.1071/EN18229

Fleet-Stalder, V. V., & Chasteen, T. G. (1998). Using fluorine-induced chemiluminescence to detect organo-metalloids the headspace of phototrophic bacterial cultures amended with selenium and tellurium. *Journal of Photochemistry and Photobiology B: Biology, 43*(3), 193-203. doi:https://doi.org/10.1016/S1011-1344(98)00108-0

Fordyce, F. (2007). Selenium Geochemistry and Health. *AMBIO: A Journal of the Human Environment, 36*(1), 94-97, 94. Retrieved from https://doi.org/10.1579/0044-7447(2007)36[94:SGAH]2.0.CO;2

Frei, G. M., Kremer, M., Hanschmann, K. M., Krause, S., Albeck, M., Sredni, B., & Schnierle, B. S. (2008). Antitumour effects in mycosis fungoides of the immunomodulatory, tellurium-based compound, AS101. *British Journal of Dermatology, 158*(3), 578-586. doi:10.1111/j.1365-2133.2007.08414.x

Garberg, P., Engman, L., Tolmachev, V., Lundqvist, H., Gerdes, R. G., & Cotgreave, I. A. (1999). Binding of tellurium to hepatocellular selenoproteins during incubation with inorganic tellurite: consequences for the activity of selenium-dependent glutathione peroxidase. *The International Journal of Biochemistry & Cell Biology, 31*(2), 291-301. doi:https://doi.org/10.1016/S1357-2725(98)00113-7

Gassner, N. C., Baase, W. A., Hausrath, A. C., & Matthews, B. W. (1999). Substitution with selenomethionine can enhance the stability of methionine-rich proteins11Edited by B. Honig. *Journal of Molecular Biology, 294*(1), 17-20. doi:https://doi.org/10.1006/jmbi.1999.3220

Gharieb, M. M., & Gadd, G. M. (2004). Role of glutathione in detoxification of metal(loid)s by Saccharomyces cerevisiae. *BioMetals, 17*(2), 183-188. doi:10.1023/B:BIOM.0000018402.22057.62

Gladyshev, V. N. (2011). Selenoproteins and selenoproteomes. In *Selenium* (pp. 109-123): Springer.

Hajna, A. A. (1945). Triple-Sugar Iron Agar Medium for the Identification of the Intestinal Group of Bacteria. *Journal of Bacteriology, 49*(5), 516-517. Retrieved from https://www.ncbi.nlm.nih.gov/pubmed/16560950

https://www.ncbi.nlm.nih.gov/pmc/articles/PMC374079/

Harris, F., & Pierpoint, L. (2012). Photodynamic therapy based on 5-aminolevulinic acid and its use as an antimicrobial Agent. *Medicinal Research Reviews, 32*(6), 1292-1327. doi:10.1002/med.20251

Herbel, M. J., Blum, J. S., Oremland, R. S., & Borglin, S. E. (2003). Reduction of Elemental Selenium to Selenide: Experiments with Anoxic Sediments and Bacteria that Respire Se-Oxyanions. *Geomicrobiology Journal, 20*(6), 587-602. doi:10.1080/713851163

Jensen, W. B. (1997). A Note on the Term "Chalcogen". *Journal of Chemical Education, 74*(9), 1063. doi:10.1021/ed074p1063

Kawano, Y., Onishi, F., Shiroyama, M., Miura, M., Tanaka, N., Oshiro, S., . . . Ohtsu, I. (2017). Improved fermentative l-cysteine overproduction by enhancing a newly identified thiosulfate assimilation pathway in Escherichia coli. *Applied Microbiology and Biotechnology, 101*(18), 6879-6889. doi:10.1007/s00253-017-8420-4

Kessi, J., & Hanselmann, K. W. (2004). Similarities between the Abiotic Reduction of Selenite with Glutathione and the Dissimilatory Reaction Mediated by Rhodospirillum rubrum and Escherichia coli. *Journal of Biological Chemistry, 279*(49), 50662-50669. doi:10.1074/jbc.M405887200

Kimura, H. (2009). Hydrogen Sulfide: From Brain to Gut. *Antioxidants & Redox Signaling, 12*(9), 1111-1123. doi:10.1089/ars.2009.2919

Kitajima, T., & Chiba, Y. (2013). Selenomethionine metabolism and its toxicity in yeast. *Biomol Concepts, 4*(6), 611-616. doi:10.1515/bmc-2013-0033

Knott, R., Fallick, A. E., Rickard, D., & Bäcker, H. (1995). Mineralogy and sulphur isotope characteristics of a massive sulphide boulder, Galapagos Rift, 85 55′ W. *Geological Society, London, Special Publications, 87*(1), 207-222.

Kramer, G. F., & Ames, B. N. (1988). Mechanims of mutagenicity and toxicity of sodium selenite (Na2SeO3) in in Salmonella typhimurium. *Mutation Research/Fundamental and Molecular Mechanisms of Mutagenesis, 201*(1), 169-180. doi:https://doi.org/10.1016/0027-5107(88)90123-6

Laden, B. P., & Porter, T. D. (2001). Inhibition of human squalene monooxygenase by tellurium compounds: evidence of interaction with vicinal sulfhydryls. *Journal of Lipid Research, 42*(2), 235-240. Retrieved from http://www.jlr.org/content/42/2/235.abstract

Lakin, H. W. (1973). Selenium in Our Enviroment. In *Trace Elements in the Environment* (Vol. 123, pp. 96-111): AMERICAN CHEMICAL SOCIETY.

Lee, D. S., & Edmond, J. M. (1985). Tellurium species in seawater. *Nature, 313*(6005), 782-785. doi:10.1038/313782a0

Li, D.-B., Cheng, Y.-Y., Wu, C., Li, W.-W., Li, N., Yang, Z.-C., . . . Yu, H.-Q. (2014). Selenite reduction by Shewanella oneidensis MR-1 is mediated by fumarate reductase in periplasm. *Scientific Reports, 4*, 3735. doi:10.1038/srep03735

https://www.nature.com/articles/srep03735#supplementary-information

Lindblow-Kull, C., Kull, F. J., & Shrift, A. (1985). Single transporter for sulfate, selenate, and selenite in Escherichia coli K-12. *J Bacteriol, 163*(3), 1267-1269. Retrieved from https://www.ncbi.nlm.nih.gov/pubmed/3897189

Lowe, E. C., Bydder, S., Hartshorne, R. S., Tape, H. L. U., Dridge, E. J., Debieux, C. M., . . . Butler, C. S. (2010). Quinol-cytochrome c Oxidoreductase and Cytochrome c4 Mediate Electron Transfer during Selenate Respiration in Thauera selenatis. *Journal of Biological Chemistry, 285*(24), 18433-18442.

Maltman, C., Donald, L. J., & Yurkov, V. (2017a). Tellurite and Tellurate Reduction by the Aerobic Anoxygenic Phototroph Erythromonas ursincola, Strain KR99 Is Carried out by a Novel Membrane Associated Enzyme. *Microorganisms, 5*(2), 20. doi:10.3390/microorganisms5020020

Maltman, C., Donald, L. J., & Yurkov, V. (2017b). Two distinct periplasmic enzymes are responsible for tellurite/tellurate and selenite reduction by strain ER-Te-48 associated with the deep sea hydrothermal vent tube worms at the Juan de Fuca Ridge black smokers. *Archives of Microbiology, 199*(8), 1113-1120. doi:10.1007/s00203-017-1382-1

Maltman, C., Piercey-Normore, M. D., & Yurkov, V. (2015). Tellurite-, tellurate-, and selenite-based anaerobic respiration by strain CM-3 isolated from gold mine tailings. *Extremophiles, 19*(5), 1013-1019. doi:10.1007/s00792-015-0776-8

Maltman, C., Walter, G., & Yurkov, V. (2016). A Diverse Community of Metal(loid) Oxide Respiring Bacteria Is Associated with Tube Worms in the Vicinity of the Juan de Fuca Ridge Black Smoker Field. *PLOS ONE, 11*(2), e0149812. doi:10.1371/journal.pone.0149812

Mansilla, M. C., & de Mendoza, D. (2000). The Bacillus subtilis cysP gene encodes a novel sulphate permease related to the inorganic phosphate transporter (Pit) family. *Microbiology, 146*(4), 815-821. doi:doi:10.1099/00221287-146-4-815

Masscheleyn, P. H., & Patrick Jr, W. H. (1993). Biogeochemical processes affecting selenium cycling in wetlands. *Environmental Toxicology and Chemistry, 12*(12), 2235-2243. doi:10.1002/etc.5620121207

Mayland, H. F., Gough, L. P., & Stewart, K. C. (1991). *Selenium mobility in soils and its absorption, translocation, and metabolism in plants*. USGS Circular

Morales, E. H., Pinto, C. A., Luraschi, R., Muñoz-Villagrán, C. M., Cornejo, F. A., Simpkins, S. W., . . . Vásquez, C. C. (2017). Accumulation of heme biosynthetic intermediates contributes to the antibacterial action of the metalloid tellurite. *Nature Communications, 8*(1), 15320. doi:10.1038/ncomms15320

Nakatani, T., Ohtsu, I., Nonaka, G., Wiriyathanawudhiwong, N., Morigasaki, S., & Takagi, H. (2012). Enhancement of thioredoxin/glutaredoxin-mediated L-cysteine synthesis from S-sulfocysteine increases L-cysteine production in Escherichia coli. *Microbial Cell Factories, 11*(1), 62. doi:10.1186/1475-2859-11-62

Nancharaiah, Y. V., & Lens, P. N. L. (2015). Ecology and Biotechnology of Selenium-Respiring Bacteria. *Microbiology and Molecular Biology Reviews, 79*(1), 61-80. doi:10.1128/mmbr.00037-14

Owens, R. A., & Hartman, P. E. (1986). Export of glutathione by some widely used Salmonella typhimurium and Escherichia coli strains. *Journal of Bacteriology, 168*(1), 109-114. doi:10.1128/jb.168.1.109-114.1986

Painter, E. P. (1941). The Chemistry and Toxicity of Selenium Compounds, with Special Reference to the Selenium Problem. *Chemical Reviews, 28*(2), 179-213. doi:10.1021/cr60090a001

Parra, F., Britton, P., Castle, C., Jones-Mortimer, M., & Kornberg, H. (1983). Two Separate Genes Involved In Sulphate Transport In Escherichia coli K12. *Journal of general microbiology, 129*, 357-358. doi:10.1099/00221287-129-2-357

Pearce, C. I., Pattrick, R. A. D., Law, N., Charnock, J. M., Coker, V. S., Fellowes, J. W., . . . Lloyd, J. R. (2009). Investigating different mechanisms for biogenic selenite transformations: Geobacter sulfurreducens, Shewanella oneidensis and Veillonella atypica. *Environmental Technology, 30*(12), 1313-1326. doi:10.1080/09593330902984751

Peiró, L. T., Méndez, G. V., & Ayres, R. U. (2013). Material Flow Analysis of Scarce Metals: Sources, Functions, End-Uses and Aspects for Future Supply. *Environmental Science & Technology, 47*(6), 2939-2947. doi:10.1021/es301519c

Pérez, J. M., Calderón, I. L., Arenas, F. A., Fuentes, D. E., Pradenas, G. A., Fuentes, E. L., . . . Vásquez, C. C. (2007). Bacterial Toxicity of Potassium Tellurite: Unveiling an Ancient Enigma. *PLOS ONE, 2*(2), e211. doi:10.1371/journal.pone.0000211

Pugin, B., Cornejo, F. A., Muñoz-Díaz, P., Muñoz-Villagrán, C. M., Vargas-Pérez, J. I., Arenas, F. A., & Vásquez, C. C. (2014). Glutathione Reductase-Mediated Synthesis of Tellurium-Containing Nanostructures Exhibiting Antibacterial Properties. *Applied and Environmental Microbiology, 80*(22), 7061. doi:10.1128/AEM.02207-14

Qin, H.-B., Takeichi, Y., Nitani, H., Terada, Y., & Takahashi, Y. (2017). Tellurium Distribution and Speciation in Contaminated Soils from Abandoned Mine Tailings: Comparison with Selenium. *Environmental Science & Technology, 51*(11), 6027-6035. doi:10.1021/acs.est.7b00955

Rahim, S., & Milne, J. (1996). Studies on the interaction of selenite and selenium with sulphur donors. Part 4. Thiosulfate. *Canadian Journal of Chemistry, 74*(5), 753-759. doi:10.1139/v96-082

Ramadan, S. E., Razak, A. A., Ragab, A. M., & el-Meleigy, M. (1989). Incorporation of tellurium into amino acids and proteins in a tellurium-tolerant fungi. *Biol Trace Elem Res, 20*(3), 225-232. Retrieved from https://www.ncbi.nlm.nih.gov/pubmed/2484755

Ramos-Ruiz, A., Wilkening, J. V., Field, J. A., & Sierra-Alvarez, R. (2017). Leaching of cadmium and tellurium from cadmium telluride (CdTe) thin-film solar panels under simulated landfill conditions. *Journal of Hazardous Materials, 336*, 57-64. doi:http://dx.doi.org/10.1016/j.jhazmat.2017.04.052

Ramos-Ruiz, A., Zeng, C., Sierra-Alvarez, R., Teixeira, L. H., & Field, J. A. (2016). Microbial toxicity of ionic species leached from the II-VI semiconductor materials, cadmium telluride (CdTe) and cadmium selenide (CdSe). *Chemosphere, 162*, 131-138. doi:http://dx.doi.org/10.1016/j.chemosphere.2016.07.081

Reinoso, C. A., Appanna, V. D., & Vásquez, C. C. (2013). α -Ketoglutarate accumulation is not dependent on isocitrate dehydrogenase activity during tellurite detoxification in Escherichia coli. *BioMed research international, 2013*, 784190-784190. doi:10.1155/2013/784190

Rosentel, J. K., Healy, F., Maupin-Furlow, J. A., Lee, J. H., & Shanmugam, K. T. (1995). Molybdate and regulation of mod (molybdate transport), fdhF, and hyc (formate hydrogenlyase) operons in Escherichia coli. *Journal of Bacteriology, 177*(17), 4857-4864. doi:10.1128/jb.177.17.4857-4864.1995

Sandoval, J. M., Arenas, F. A., García, J. A., Díaz-Vásquez, W. A., Valdivia-González, M., Sabotier, M., & Vásquez, C. C. (2015). Escherichia coli 6-phosphogluconate dehydrogenase aids in tellurite resistance by reducing the toxicant in a NADPH-dependent manner. *Microbiological Research, 177*, 22-27. doi:https://doi.org/10.1016/j.micres.2015.05.002

Sarathchandra, S. U., & Watkinson, J. H. (1981). Oxidation of elemental selenium to selenite by Bacillus megaterium. *Science, 211*(4482), 600. Retrieved from http://science.sciencemag.org/content/211/4482/600.abstract

Schrauzer, G. N. (2000). Selenomethionine: A Review of Its Nutritional Significance, Metabolism and Toxicity. *The Journal of Nutrition, 130*(7), 1653-1656. doi:10.1093/jn/130.7.1653

Sekowska, A., Kung, H. F., & Danchin, A. (2000). Sulfur metabolism in Escherichia coli and related bacteria: facts and fiction. *J Mol Microbiol Biotechnol, 2*(2), 145-177. Retrieved from https://www.ncbi.nlm.nih.gov/pubmed/10939241

Shatalin, K., Shatalina, E., Mironov, A., & Nudler, E. (2011). H_2S: A Universal Defense Against Antibiotics in Bacteria. *Science, 334*(6058), 986-990. doi:10.1126/science.1209855

Shen, H.-M., Yang, C.-F., Ding, W.-X., Liu, J., & Ong, C.-N. (2001). Superoxide radical–initiated apoptotic signalling pathway in selenite-treated HepG2 cells: mitochondria serve as the main target. *Free Radical Biology and Medicine, 30*(1), 9-21. doi:https://doi.org/10.1016/S0891-5849(00)00421-4

Singh, M., & Singh, N. (1979). The effect of forms of selenium on the accumulation of selenium, sulfur, and forms of nitrogen and phosphorus in forage cowpea (Vigna sinensis). *Soil Science, 127*(5), 264-269. Retrieved from https://journals.lww.com/soilsci/Fulltext/1979/05000/THE_EFFECT_OF_FORMS_OF_SELENIUM_ON_THE.2.aspx

Sirko, A., Hryniewicz, M., Hulanicka, D., & Böck, A. (1990). Sulfate and thiosulfate transport in Escherichia coli K-12: nucleotide sequence and expression of the cysTWAM gene cluster. *Journal of Bacteriology, 172*(6), 3351-3357. Retrieved from http://www.ncbi.nlm.nih.gov/pmc/articles/PMC209146/

Spallholz, J. E. (1994). On the nature of selenium toxicity and carcinostatic activity. *Free Radical Biology and Medicine, 17*(1), 45-64. doi:https://doi.org/10.1016/0891-5849(94)90007-8

Spallholz, J. E., & Hoffman, D. J. (2002). Selenium toxicity: cause and effects in aquatic birds. *Aquatic Toxicology, 57*(1), 27-37. doi:https://doi.org/10.1016/S0166-445X(01)00268-5

Speirs, J., Gross, R., Candelise, C., & Gross, B. (2011). *Working Paper I: Thin Film photovoltaics*. Retrieved from http://www.ukerc.ac.uk/publications/materials-availability-potential-constraints-to-the-future-lowcarbon-economy-working-paper-i-thin-film-photovoltaics.html

Speirs, J., Gross, R., Contestabile, M., Candelise, C., Houari, Y., & Gross, B. (2014). *An assessment of the evidence*. Retrieved from http://www.ukerc.ac.uk/programmes/technology-and-policy-assessment/materials-availability-for-low-carbon-technologies.html

Staicu, L. C., & Barton, L. L. (2017). Bacterial Metabolism of Selenium—For Survival or Profit. In E. D. van Hullebusch (Ed.), *Bioremediation of Selenium Contaminated Wastewater* (pp. 1-31). Cham: Springer International Publishing.

Tarze, A., Dauplais, M., Grigoras, I., Lazard, M., Ha-Duong, N. T., Barbier, F., . . . Plateau, P. (2007). Extracellular production of hydrogen selenide accounts for thiol-assisted toxicity of selenite against Saccharomyces cerevisiae. *J Biol Chem, 282*(12), 8759-8767. doi:10.1074/jbc.M610078200

Theisen, J., Zylstra, G. J., & Yee, N. (2013). Genetic Evidence for a Molybdopterin-Containing Tellurate Reductase. *Applied and Environmental Microbiology, 79*(10), 3171-3175. doi:10.1128/aem.03996-12

Tiekink, E. R. T. (2012). Therapeutic potential of selenium and tellurium compounds: Opportunities yet unrealised. *Dalton Transactions, 41*(21), 6390-6395. doi:10.1039/C2DT12225A

Tremaroli, V., Fedi, S., & Zannoni, D. (2007). Evidence for a tellurite-dependent generation of reactive oxygen species and absence of a tellurite-mediated adaptive response to oxidative stress in cells of Pseudomonas pseudoalcaligenes KF707. *Archives of Microbiology, 187*(2), 127-135. doi:10.1007/s00203-006-0179-4

Turner, R. J., Aharonowitz, Y., Weiner, J. H., & Taylor, D. E. (2001). Glutathione is a target in tellurite toxicity and is protected by tellurite resistance determinants in Escherichia coli. *Canadian Journal of Microbiology, 47*(1), 33-40.

Vrionis, H. A., Wang, S., Haslam, B., & Turner, R. J. (2015). Selenite Protection of Tellurite Toxicity Toward Escherichia coli. *Frontiers in Molecular Biosciences, 2*, 69. doi:10.3389/fmolb.2015.00069

Wang, Z., & Gao, Y. (2001). Biogeochemical cycling of selenium in Chinese environments. *Applied Geochemistry, 16*(11), 1345-1351. doi:https://doi.org/10.1016/S0883-2927(01)00046-4

Weres, O., Jaouni, A.-R., & Tsao, L. (1989). The distribution, speciation and geochemical cycling of selenium in a sedimentary environment, Kesterson Reservoir, California, U.S.A. *Applied Geochemistry, 4*(6), 543-563. doi:https://doi.org/10.1016/0883-2927(89)90066-8

Winkel, L. H. E., Johnson, C. A., Lenz, M., Grundl, T., Leupin, O. X., Amini, M., & Charlet, L. (2012). Environmental Selenium Research: From Microscopic Processes to Global Understanding. *Environmental Science & Technology, 46*(2), 571-579. doi:10.1021/es203434d

Wu, X., Song, J., & Li, X. (2014). Occurrence and distribution of dissolved tellurium in Changjiang River estuary. *Chinese Journal of Oceanology and Limnology, 32*(2), 444-454. doi:10.1007/s00343-014-3161-z

Young, V. R., Nahapetian, A., & Janghorbani, M. (1982). Selenium bioavailability with reference to human nutrition. *Am J Clin Nutr, 35*(5), 1076-1088. doi:10.1093/ajcn/35.5.1076

Yu, L. Y., He, K. M., Chai, D. R., Yang, C. M., & Zheng, O. Y. (1993). Evidence for Telluroamino Acid in Biological Materials and Some Rules of Assimilation of Inorganic Tellurium by Yeast. *Analytical Biochemistry, 209*(2), 318-322. doi:https://doi.org/10.1006/abio.1993.1126

Zannoni, D., Borsetti, F., Harrison, J. J., & Turner, R. J. (2007). The Bacterial Response to the Chalcogen Metalloids Se and Te. In R. K. Poole (Ed.), *Advances in Microbial Physiology* (Vol. 53, pp. 1-312): Academic Press.

Zhang, L., Jiang, W., Nan, J., Almqvist, J., & Huang, Y. (2014). The Escherichia coli CysZ is a pH dependent sulfate transporter that can be inhibited by sulfite. *Biochimica et Biophysica Acta (BBA) - Biomembranes, 1838*(7), 1809-1816. doi:https://doi.org/10.1016/j.bbamem.2014.03.003

Zwolak, I., & Zaporowska, H. (2012). Selenium interactions and toxicity: a review. *Cell Biology and Toxicology, 28*(1), 31-46. doi:10.1007/s10565-011-9203-9

FIGURES:

Table 1.1. Standard reduction potential of tellurium, selenium, and sulfur oxyanions (Bouroushian, 2010)

Redox couple	Standard reduction potential (mV)
TeO_4^{2-}/TeO_3^{2-}	892
SeO_4^{2-}/SeO_3^{2-}	880
$SeO_3^{2-}/Se(0)$	875
$TeO_3^{2-}/Te(0)$	827
SO_4^{2-}/SO_3^{2-}	-930

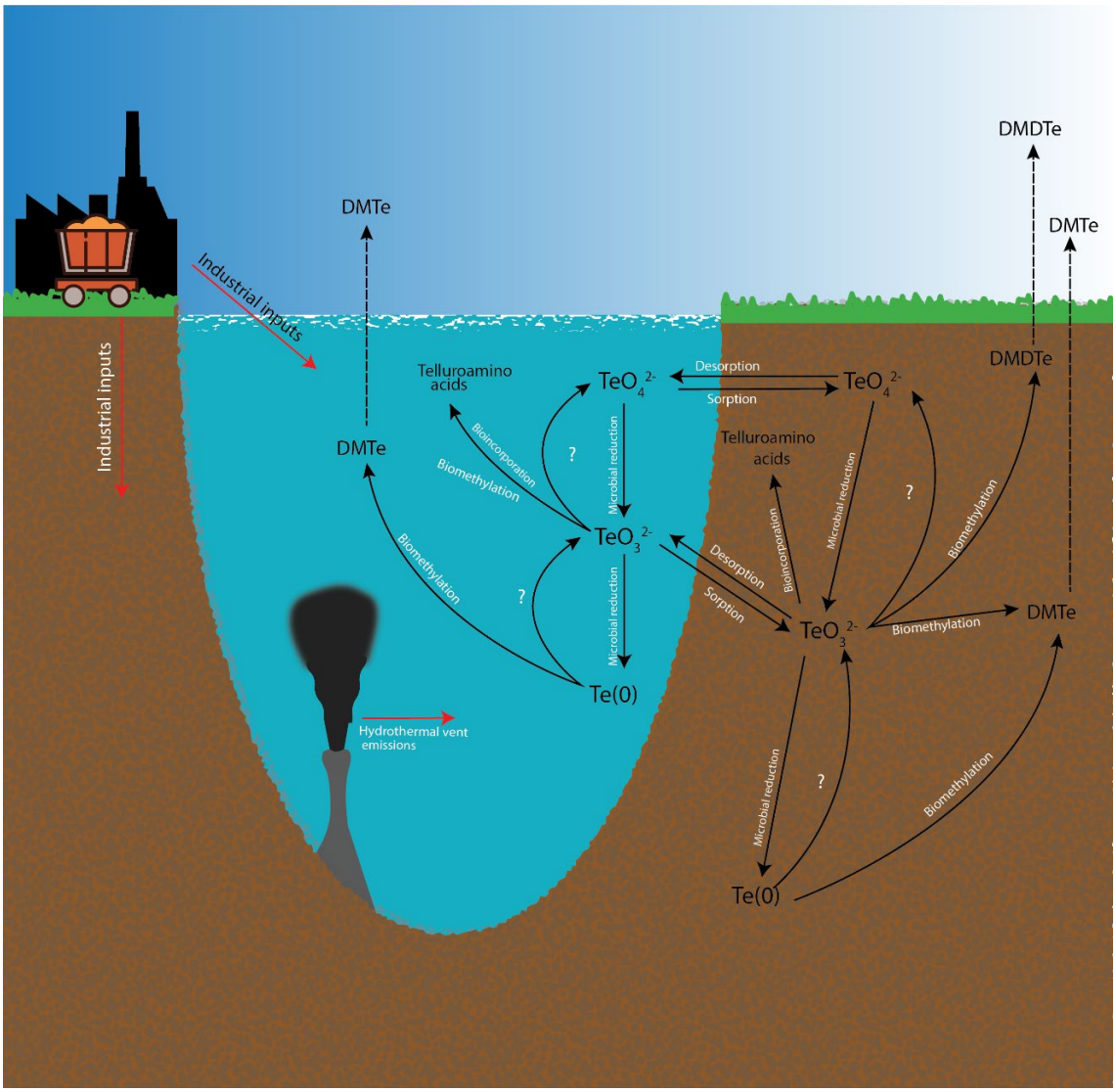

Figure 1.1. The biogeochemical cycling of tellurium compounds. Major inputs of tellurium into the environment include hydrothermal vent emissions and anthropogenic inputs including mine tailings and mineral refining waste. Microorganisms that can reduce tellurate (TeO_4^{2-}) to tellurite (TeO_3^{2-}) and then tellurite to elemental tellurium (Te(0)) have been reported in the literature. Organisms can also convert inorganic tellurium to organic forms including dimethyltelluride (DMTe), dimethylditelluride (DMDTe), and various telluroamino acids.

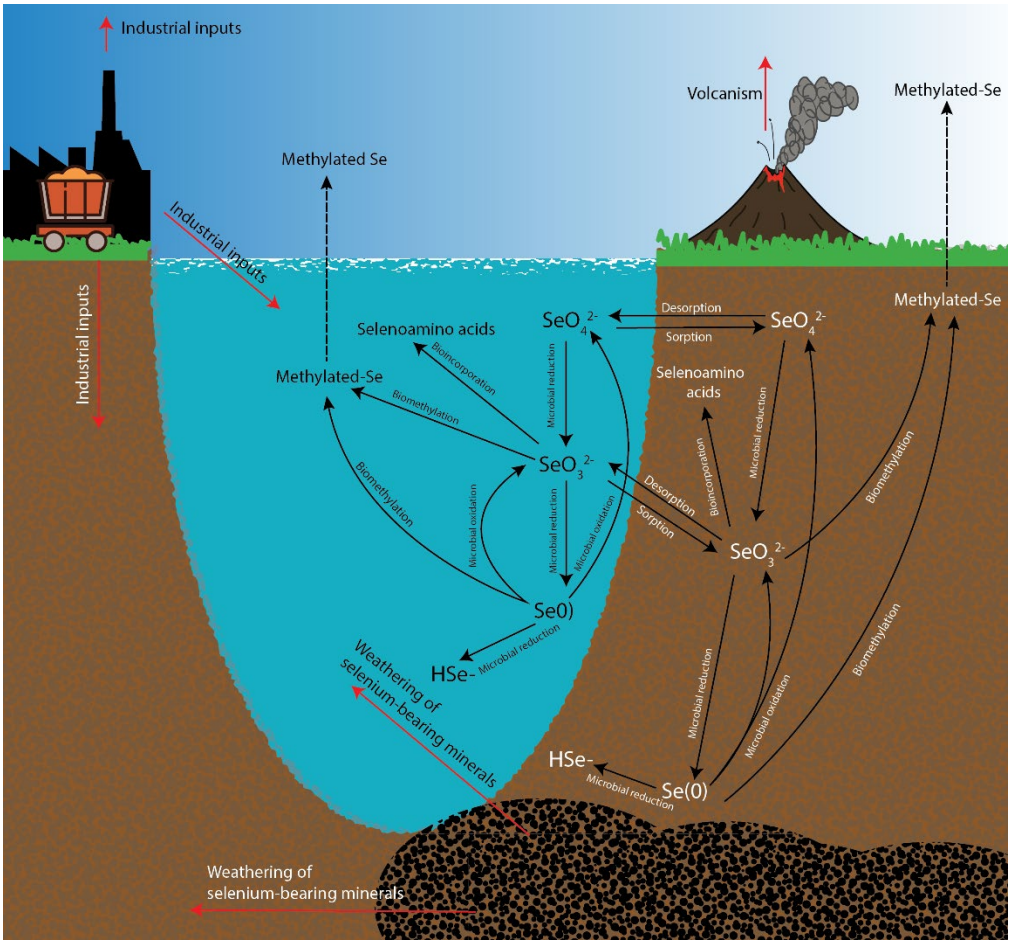

Figure 1.2. The biogeochemical cycling of selenium compounds. Major inputs of selenium into the environment include industrial inputs, weathering of selenium-bearing minerals, and volcanism. Microorganisms can carry out the reduction of selenate (SeO_4^{2-}) and selenite (SeO_3^{2-}) to elemental selenium (Se(0)). Reduction of elemental selenium to selenide (HSe^-) has also been reported. Microorganisms can also methylate selenite and elemental selenium to various methylated selenides. Selenoamino acids such as selenocysteine and selenomethione also represent other major organoseleno species in the environment. Selenocysteine is an essential proteinogenic amino acid. Finally, elemental selenium can be oxidized by some organisms to selenite and selenate.

CHAPTER 2

TELLURATE ENTERS *ESCHERICHIA COLI* K-12 CELLS VIA THE SulT-TYPE SULFATE TRANSPORTER CysPUWA

Published in FEMS Microbiology Letters as "Tellurate enters *Escherichia coli* K-12 cells via the SulT-type sulfate transporter CysPUWA" (FEMS Micro. Lett., 2017, 364(24))

ABSTRACT:

Soluble forms of tellurium are environmental contaminants that are toxic to microorganisms. While tellurite [Te(IV)] is a well-characterized antimicrobial agent, little is known about the interactions of tellurate [Te(VI)] with bacterial cells. In this study, we investigated the role of sulfate transporters in the uptake of tellurate in *Escherichia coli* K-12. Mutant strains carrying a deletion of the *cysW* gene in the CysPUWA sulfate transporter system accumulated less cellular tellurium and exhibited higher resistance to tellurate compared to the wild type strain. Complementation of the mutation restored tellurate sensitivity and uptake. These results indicate that tellurate enters *E. coli* cells to cause toxic effects via the CysPUWA sulfate transporter.

INTRODUCTION:

Tellurium (Te) is an emerging contaminant that poses a threat to environmental health due to its toxic effects on microorganisms (Ramos-Ruiz, Wilkening, Field, & Sierra-Alvarez, 2017; Ramos-Ruiz, Zeng, Sierra-Alvarez, Teixeira, & Field, 2016; Zeng, Ramos-Ruiz, Field, & Sierra-Alvarez, 2015). In addition to historic Te-contamination produced by gold-mining and metal refining operations (Perkins, 2011; Wray, 1998), increasing usage of CdTe in thin-film solar panel technologies and electronic devices has introduced new anthropogenic sources of Te in the environment (Kranz, Buecheler, & Tiwari, 2013). Recent studies have suggested that soluble forms of tellurium can leach from these devices upon decommission and disposal (Ramos-Ruiz et al., 2017; Zeng et al., 2015), with tellurate [Te(VI), TeO_4^{2-}] and tellurite [Te(IV), TeO_3^{2-}] as the main chemical species of tellurium in the leachate. While the toxicity of tellurite is well established in bacteria, comparatively very little is known about the toxic effects of tellurate (Pérez et al., 2007). To date, the molecular basis of tellurate uptake and toxicity in bacteria have not been studied in detail.

Sulfate [S(VI), SO_4^{2-}] transporters have been previously demonstrated to be gateways for toxic oxyanion entry into the cytoplasm of cells (Bébien, Kirsch, Méjean, & Verméglio, 2002; Mansilla & de Mendoza, 2000). The CysP sulfate transporter of *Bacillus subtilis*, which belongs to the Pit family of ion transporters, mediates the transport of chromate oxyanions [Cr(VI), CrO_4^{2-}] into the cell as does the SulT-type sulfate transporter of *Escherichia coli* (CysPUWA) (Mansilla & de Mendoza, 2000). Additionally, the SulT-type sulfate transporter of *E. coli* has been shown to be involved in selenate [Se(VI), SeO_4^{2-}] uptake

(Bébien et al., 2002). Given the structural and chemical similarities between sulfate, chromate, selenate and tellurate, it is possible that tellurate may also be transported into bacterial cells by a sulfate transporter. However, experimental studies on tellurate uptake are currently lacking and the transporters involved in tellurate entry into the cell have not been identified.

In this study, we examined tellurate uptake and toxicity in *E. coli* K-12. The objective of this study was to determine if the two known sulfate transporters in *E. coli* are involved in tellurate uptake and whether inactivation of specific sulfate transport systems increases tolerance to tellurate toxicity. Experiments were conducted with mutant strains carrying deletions of the SulT-type ABC transporter CysPUWA and a second unrelated pH-dependent high affinity sulfate transporter CysZ. The results of this study provide mechanistic insights into tellurate transport into bacterial cells and elucidates the first step in acute tellurate toxicity.

MATERIALS AND METHODS:

Bacterial Strains, Plasmids and Growth Procedures

Experiments were conducted with the wild-type *E. coli* K-12, and the mutant strains JW2412 (Δ*cysW*::kan), JW2417 (Δ*cysU*::kan), JW2415 (Δ*cysA*::kan) and JW2406 (Δ*cysZ*::kan) obtained from the Keio Collection of the National Institute of Genetics, Japan (Baba et al., 2006). Chemically competent *E. coli* TOP10F' cells (F´[*lac*I^{q} Tn*10* (TetR)] *mcrA* Δ(*mrr-hsdRMS-mcrBC*) Φ80*lacZ*ΔM15 *ΔlacX74 recA1 araD139* Δ(*ara-leu*)7697 *galU galK rpsL endA1 nupG*) were used for the cloning of the *cysPUWA* genetic region (Invitrogen), and pCR-XL-TOPO

(Kan^R, Zeo^R, P_{lac}) was used as the vector backbone for the cloning of *cysPUWA* to generate the p*cysPUWA* plasmid (Invitrogen).

Unless otherwise stated, cells were pre-grown overnight in LB at 37°C in a shaking incubator at 200 rpm. Prior to the start of all experiments, overnight seed cultures were washed and transferred to fresh M9 media with the following components: 10 g/L beef extract, 12.8 g/L $Na_2HPO_4 \cdot 7H_2O$, 3 g/L KH_2PO_4, 0.5 g/L NaCl, 1 g/L NH_4Cl, 2 mM $MgSO_4$, 0.1 mM, $CaCl_2$, and 0.4% glucose. JW2412:p*cysPUWA* was grown with the addition of 50 µg/mL zeocin to maintain the p*cysPUWA* vector.

Genetic Complementation

The wild type *cysPUWA* transporter was cloned from the genome of *E. coli* K-12 for complementation. Genomic DNA was extracted using the DNeasy PowerSoil Kit (MO BIO). To clone the *cysPUWA* genetic region for complementation the SPO-F (ACCGTTACTCCTTTCACGTCC) and SPO-R (GCGTCTTATCAGGTCTACAGG) primer set was designed. SPO-F is positioned 72 bp upstream of the *cysP* start codon. SPO-R is positioned 100 bp downstream of the *cysA* stop codon resulting in a product that is 3,976 bp in length. *cysPUWA* was PCR amplified using Phusion High-Fidelity Polymerase (NEB) following the manufacturer's protocol. The entire PCR amplification was run on a 1% agarose gel with 1.6 µg/mL crystal violet added. The gel was visualized under normal room lighting and the band corresponding with the correct amplicon length was excised. The PCR product was then purified using the S.N.A.P. Gel Purification Kit (Invitrogen).

A-overhangs were then added to the ends of the blunt-end *cysPUWA* PCR product by incubating the purified PCR product for 10 minutes at 72 °C in the presence of 0.2 mM dNTPs and Taq polymerase. Ligation was performed immediately after the A-tailing reaction using the TOPO-XL cloning kit (Invitrogen) following the manufacturer's protocol. The ligation mixture was then transformed into chemically competent TOP10F' cells (Invitrogen) following the manufacturer's protocol. The transformation mixture was then plated onto LB plates containing 50 μg/mL kanamycin and incubated overnight to select for successful transformants. Plasmids were extracted from kanamycin-resistant colonies using the Zyppy Plasmid Miniprep Kit (Zymo) and screened for inserts by performing a single digestion with HindIII restriction enzyme to linearize the plasmid and check for the correct size. Plasmids of the correct size were then sequenced (Genewiz,, NJ) using the M13 Reverse primer (CAGGAAACAGCTATGAC) to confirm correct orientation. Plasmids containing the correctly oriented *cysPUWA* inserts were then transformed into chemically competent JW2412 cells. Chemically competent JW2412 cells were prepared by treating exponential-phase cells with a calcium glycerol solution (10% glycerol, 50 mM calcium cholride). Competent cells were transformed with the *cysPUWA*-containing plasmid using a heat shock method and incubated overnight on low-salt LB plates with 50 μg/mL zeocin. Zeocin-resistant colonies were selected and grown in low salt LB broth with 50 μg/mL zeocin overnight. Plasmids were extracted from these cells using the Zyppy Plasmid Miniprep Kit (Zymo). Plasmids of the correct size were confirmed by performing a single digestion with the HindIII restriction enzyme. Zeocin-resistant colonies were selected and

plasmids were extracted as described above. The presence of the correct plasmid was confirmed by digesting the extracted plasmid with HindIII restriction enzyme and visualizing on an agarose gel.

Cell Growth

Experiments were carried to determine if the CysPUWA or CysZ sulfate transport systems are involved in tellurate uptake. The wild type strain, *ΔcysZ* mutant, *ΔcysW* mutant, and *ΔcysA* mutant were grown at varying concentrations of tellurate to determine the effect of inactivation of sulfate transporter genes on tellurate resistance. Cells were grown in a shaking incubator 37 °C for 10 hours and then optical densities were determined using a BioSpec-Mini UV-Vis spectrophotometer (Shimadzu) at a wavelength of 600 nm (Myers, Curtis, & Curtis, 2013). Cell densities at the difference tellurate concentrations were normalized against the control for each strain that was grown with 0 mM tellurate to determine the relative growth values. The minimum inhibitory concentration (MIC) was determined with an initial cell density of 5×10^5 cells/mL at tellurate concentrations of 0 to 800 μM.

The effect of increasing sulfate concentrations on tellurate resistance was also examined in M9 media. The wild type strain was grown overnight in LB broth at 37 °C, washed with phosphate-buffered saline (PBS), and then transferred to M9 media. Cultures containing either 2, 20 or 40 mM sulfate were spiked with 100 μM tellurate. Cells were then incubated at 37 °C in a shaking incubator for 6 hours and cell concentrations were determined at OD_{600}. Cell densities at different tellurate concentrations were normalized against the control

for each strain that was grown with no tellurate to obtain the relative growth values. For all experiments, growth data were analyzed using a Student's t-test to determine if differences were statistically significant.

Tellurate Uptake and Reduction Measurements

Tellurate uptake by the cells was analyzed using inductively-coupled plasma optical emission spectrometry (ICP-OES). All strains were initially grown overnight on LB broth. Overnight cells were washed twice with PBS and transferred to fresh M9 media at a starting OD of 0.05. After 10 hours of growth at 37 °C, late-exponential phase cultures were spiked with 100 μM of tellurate. Aliquots for tellurium analysis and cell counts were immediately taken after spiking cultures with tellurate and then again after an additional 24 hours of incubation. Samples for tellurium analysis were filtered (0.2 μm filters), acidified (2% nitric acid), and then analyzed using an iCAP 7400 ICP-OES analyzer (Thermo Fisher) at a wavelength of 214.282 nm. The loss of dissolved tellurium from the aqueous medium was attributed to cellular accumulation. Tellurium accumulation was normalized against the cell numbers to determine tellurate uptake per cell for each strain and analyzed using a Student's t-test to determine if differences were statistically significant.

RESULTS:

E. coli K-12 grown at increasing concentrations of tellurate exhibited marked decrease in growth (**Figure 2.1A**). At 100 μM tellurate, the relative growth of K-12 compared to its growth in the absence of tellurate was only 16% ±7.3%. At the

two higher concentrations (200 and 300 μM), relative growth was only 3% ± 0.2%. The growth experiments indicated that tellurate is toxic to the cells at a MIC of 200 μM.

To test if sulfate and tellurate share a common transporter, we performed a sulfate competition experiment and examined whether high levels of sulfate out-compete the low levels of tellurate for entry into the cells. *E. coli* K-12 grown with 100 μM tellurate and increasing levels of sulfate (2, 20, and 40 mM) showed increasing tolerance to tellurate. At 2 mM sulfate (the amount in basal M9 media), tellurate severely inhibited growth and the cells grew to only 14% ± 4% compared to controls grown without tellurate (**Figure 2.1B**). At 20 mM and 40 mM sulfate, the percent growth of cells in the presence of tellurate increased to 42 ± 7% and 67 ± 24% respectively (**Figure 2.1B**). The increasing tolerance to tellurate with increasing sulfate concentrations were statistically significant ($p < 0.05$), indicating that tellurate uptake is dependent on the concentration of sulfate in the media.

Inactivation of the CysPUWA sulfate transporter in *E. coli* increased tellurate resistance when grown with tellurate **(Figure 2.1C).** The Δ*cysW* mutant strain, which lacked an integral membrane protein in the sulfate transport system, showed increased relative growth on tellurate at all concentrations tested compared to the wild type strain. When analyzed for statistical significance, *p* values of 0.02, 0.002 and 0.007 were obtained for the 50, 100 and 200 μM datasets. The growth experiments indicated that the MIC for the Δ*cysW* mutant increased to 500 μM. Complementation was performed to eliminate the possibility of polar effects on downstream genes in the operon.

Complementation of this mutant strain with a plasmid carrying the entire CysPUWA transporter resulted in lower relative growth levels compared to the Δ*cysW* mutant strain, indicating that complementation of the *cysW* mutation restored sensitivity towards tellurate. These results indicate that complementation of the *cysW* mutation restored sensitivity towards tellurate. The Δ*cysA* mutant strain, which lacked the ATPase subunit of the sulfate transport system, also showed increased relative growth on tellurate with MIC of 500 μM (data not shown). This suggest that impairment of either the membrane or ATPase subunits of the CysPUWA transporter prevents tellurate entry into the cell, thereby conferring higher resistance to tellurate. Conversely, inactivation of the high affinity CysZ sulfate transporter system had no effect on tellurate tolerance **(Figure 2.1D).** The Δ*cysZ* mutant strain did not show statistically significant differences in growth compared to the wild type strain ($p > 0.05$), suggesting that the CysZ transporter is not involved in tellurate uptake. Taken together, these results suggest that CysPUWA and not CysZ is the tellurate transporter in *E. coli*.

Measurements of tellurate uptake showed that Δ*cysW* mutant accumulated less cellular tellurium compared to the wild-type strain **(Figure 2.2).** After 24 hours of incubation in media containing 100 μM of tellurate, the wild type strain accumulated 5.73 ± 0.20 pmol of Te per cell compared to 0.79 ±0.23 pmol of Te per cell in the Δ*cysW* mutant. This represents a decrease of more than 86% in tellurium accumulation in the cells ($p < 0.01$). Complementation of the Δ*cysW* knock-out mutant increased tellurium accumulation to 2.18 ± 0.23 pmol/cell indicating partial restoration of tellurate

uptake activity. These results indicate that inactivation of the CysPUWA transporter impaired tellurate uptake and decreased cellular tellurium accumulation.

DISCUSSION:

Inactivation of the SulT-type CysPUWA sulfate transporter increased tellurate resistance in *E. coli* (**Figure 2.1C**). The CysPUWA transporter is known to mediate sulfate transport into the cell in an ATP-dependent manner (Aguilar-Barajas, Díaz-Pérez, Ramírez-Díaz, Riveros-Rosas, & Cervantes, 2011)**.** CysU and CysW are the transmembrane subunits of this transporter complex and CysA and CysP are the ATPase and sulfate binding subunits, respectively (Sirko, Hryniewicz, Hulanicka, & Böck, 1990). Sulfate enters the cell by first binding to either CysP or a functionally redundant subunit Sbp encoded at a separate genetic location from the other four Cys subunits. While there are several conserved residues in both Sbp and CysP that have been implicated in sulfate binding (Hryniewicz, Sirko, Pałucha, Böck, & Hulanicka, 1990), it is unclear whether these same residues are involved in the non-specific binding of tellurate. The membrane proteins CysW and CysU form the transmembrane channel through which sulfate oxyanions pass through the inner membrane (Sirko et al., 1990). It has been shown that *cysW* mutants are defective in sulfate transport (Aguilar-Barajas et al., 2011; Farmer & Thomas, 2004). Similarly, our experiments showed that the loss of the transmembrane subunit CysW inhibited transport of tellurate and tellurium accumulation in the cell (**Figure 2.2**). The

Δ*cysA* mutant also exhibited higher tellurate resistance, indicating that the ATP hydrolysis subunit is necessary to drive tellurate transport across the membrane.

Tellurium exerts its toxic effects mainly within the cytoplasm after entry into the cells (Chasteen, Fuentes, Tantaleán, & Vásquez, 2009). Our experiments showed that the exclusion of tellurate from the cytoplasm by inactivation of its transporter enabled mutant cells to survive at higher concentrations of tellurate compared to the wild type strain (**Figure 2.3**). This effect is similar to previous observations of increased chromate resistance from disruption of CysPUWA (Aguilar-Barajas et al., 2011), as well as increased tellurite resistance from inactivation of the transporters PitA and ActP (Elías et al., 2015). The mechanism of toxicity of tellurate after entry into the cell has not been determined. Tellurite exerts toxicity through the oxidation of intracellular thiols and the cysteine residues of proteins. (Turner, Aharonowitz, Weiner, & Taylor, 2001; Turner, Weiner, & Taylor, 1999; Vrionis, Wang, Haslam, & Turner, 2015). Likewise, we would expect tellurate to interact strongly with sulfur-containing functional groups, possibly oxidizing free thiols and diminishing redox buffering system or binding to cysteine residues and inhibiting protein function. Also similar to tellurite, tellurate may generate reactive oxygen species (ROS) inside cells (Pérez et al., 2007), resulting in cellular damage to proteins, lipids and essential cofactors (e.g. Fe-S clusters).

Darkening of the cultures was observed with both the wild type strain and the complemented Δ*cysW* mutant indicating the precipitation of elemental tellurium. Thus, *E. coli* cells with a functional CysPUWA sulfate transporter reduced tellurate [Te(VI)] to its elemental form [Te(0)], presumably by an

intracellular process that is dependent on uptake of tellurate from the media. Te-resistant strains of *E. coli* are known to produce black elemental tellurium deposits inside the cell during tellurite reduction, which results in a darkening of cell cultures as elemental tellurium accumulates (Taylor, Walter, Sherburne, & Bazett-Jones, 1988). The formation of elemental tellurium from tellurate requires an addition step where Te(VI) is first reduced to Te(IV). The reduction of Te(VI) to Te(IV) in *E. coli* is not fully understood, although there is genetic evidence to suggest that a molybdoenzyme is involved (Theisen, Zylstra, & Yee, 2013). Once tellurite is formed, Te(IV) reduction occurs in the cytoplasm of *E. coli* via reactions with intracellular thiols and by the non-specific activity of certain enzymes such as the nitrate reductase (Avazéri et al., 1997; Turner et al., 1999).

The SulT-type sulfate transporter is widely distributed among bacteria, suggesting that this transport system may act as an entryway for tellurate into other bacterial cells. While the SulT-type transporter is not universal in prokaryotes (Shaun M. Baesman et al., 2007; S. M. Baesman, Stolz, Kulp, & Oremland, 2009), this sulfate transport system has been reported in the genomes of a variety of *Proteobacteria*, *Actinobacteria*, *Firmicutes*, *Spirochetes* and *Cyanobacteria* (Aguilar-Barajas et al., 2011). We also found homologs of this transporter in members of the *Chloroflexi*, *Deinococcus-Thermus*, and *Nitrospirae*. In addition to the findings presented here on tellurate transport and toxicity in *E. coli*, a recent study showed that tellurate and tellurite are inhibitory towards important environmental processes such as methanogenesis (Ramos-Ruiz et al., 2016). Because many microorganisms that perform carbon cycling, photosynthesis, and bioremediation harbor the SulT-type transporter system,

further research is warranted to determine tellurate uptake in ecologically-relevant microorganisms to understand toxic effects of tellurium contamination on microbial processes in the environment.

REFERENCES:

Aguilar-Barajas, E., Díaz-Pérez, C., Ramírez-Díaz, M. I., Riveros-Rosas, H., & Cervantes, C. (2011). Bacterial transport of sulfate, molybdate, and related oxyanions. *BioMetals, 24*(4), 687-707. doi:10.1007/s10534-011-9421-x

Avazéri, C., Turner, R. J., Pommier, J., Weiner, J. H., Giordano, G., & Verméglio, A. (1997). Tellurite reductase activity of nitrate reductase is responsible for the basal resistance of Escherichia coli to tellurite. *Microbiology, 143*(4), 1181-1189. doi:doi:10.1099/00221287-143-4-1181

Baba, T., Ara, T., Hasegawa, M., Takai, Y., Okumura, Y., Baba, M., . . . Mori, H. (2006). Construction of Escherichia coli K-12 in-frame, single-gene knockout mutants: the Keio collection. *Molecular Systems Biology, 2*, 2006.0008-2006.0008. doi:10.1038/msb4100050

Baesman, S. M., Bullen, T. D., Dewald, J., Zhang, D., Curran, S., Islam, F. S., . . . Oremland, R. S. (2007). Formation of Tellurium Nanocrystals during Anaerobic Growth of Bacteria That Use Te Oxyanions as Respiratory Electron Acceptors. *Applied and Environmental Microbiology, 73*(7), 2135-2143. doi:10.1128/aem.02558-06

Baesman, S. M., Stolz, J. F., Kulp, T. R., & Oremland, R. S. (2009). Enrichment and isolation of Bacillus beveridgei sp. nov., a facultative anaerobic haloalkaliphile from Mono Lake, California, that respires oxyanions of tellurium, selenium, and arsenic. *Extremophiles, 13*(4), 695-705. doi:10.1007/s00792-009-0257-z

Bébien, M., Kirsch, J., Méjean, V., & Verméglio, A. (2002). Involvement of a putative molybdenum enzyme in the reduction of selenate by Escherichia coli. *Microbiology, 148*(12), 3865-3872. doi:doi:10.1099/00221287-148-12-3865

Chasteen, T. G., Fuentes, D. E., Tantaleán, J. C., & Vásquez, C. C. (2009). Tellurite: history, oxidative stress, and molecular mechanisms of resistance. *FEMS Microbiology Reviews, 33*(4), 820-832. doi:10.1111/j.1574-6976.2009.00177.x

Elías, A., Díaz-Vásquez, W., Abarca-Lagunas, M. J., Chasteen, T. G., Arenas, F., & Vásquez, C. C. (2015). The ActP acetate transporter acts prior to the PitA phosphate carrier in tellurite uptake by Escherichia coli. *Microbiological Research, 177*, 15-21. doi:http://dx.doi.org/10.1016/j.micres.2015.04.010

Farmer, K. L., & Thomas, M. S. (2004). Isolation and Characterization of Burkholderia cenocepacia Mutants Deficient in Pyochelin Production: Pyochelin Biosynthesis Is Sensitive to Sulfur Availability. *Journal of Bacteriology, 186*(2), 270-277. doi:10.1128/jb.186.2.270-277.2004

Hryniewicz, M., Sirko, A., Pałucha, A., Böck, A., & Hulanicka, D. (1990). Sulfate and thiosulfate transport in Escherichia coli K-12: identification of a gene encoding a novel protein involved in thiosulfate binding. *Journal of Bacteriology, 172*(6), 3358-3366. Retrieved from http://www.ncbi.nlm.nih.gov/pmc/articles/PMC209147/

Kranz, L., Buecheler, S., & Tiwari, A. N. (2013). Technological status of CdTe photovoltaics. *Solar Energy Materials and Solar Cells, 119*, 278-280. doi:http://dx.doi.org/10.1016/j.solmat.2013.08.028

Mansilla, M. C., & de Mendoza, D. (2000). The Bacillus subtilis cysP gene encodes a novel sulphate permease related to the inorganic phosphate transporter (Pit) family. *Microbiology, 146*(4), 815-821. doi:doi:10.1099/00221287-146-4-815

Myers, J. A., Curtis, B. S., & Curtis, W. R. (2013). Improving accuracy of cell and chromophore concentration measurements using optical density. *BMC Biophysics, 6*, 4-4. doi:10.1186/2046-1682-6-4

Pérez, J. M., Calderón, I. L., Arenas, F. A., Fuentes, D. E., Pradenas, G. A., Fuentes, E. L., . . . Vásquez, C. C. (2007). Bacterial Toxicity of Potassium Tellurite: Unveiling an Ancient Enigma. *PLOS ONE, 2*(2), e211. doi:10.1371/journal.pone.0000211

Perkins, W. T. (2011). Extreme selenium and tellurium contamination in soils — An eighty year-old industrial legacy surrounding a Ni refinery in the Swansea Valley. *Science of The Total Environment, 412*, 162-169. doi:http://dx.doi.org/10.1016/j.scitotenv.2011.09.056

Ramos-Ruiz, A., Wilkening, J. V., Field, J. A., & Sierra-Alvarez, R. (2017). Leaching of cadmium and tellurium from cadmium telluride (CdTe) thin-film solar panels under simulated landfill conditions. *Journal of Hazardous Materials, 336*, 57-64. doi:http://dx.doi.org/10.1016/j.jhazmat.2017.04.052

Ramos-Ruiz, A., Zeng, C., Sierra-Alvarez, R., Teixeira, L. H., & Field, J. A. (2016). Microbial toxicity of ionic species leached from the II-VI semiconductor materials, cadmium telluride (CdTe) and cadmium selenide (CdSe).

Chemosphere, 162, 131-138. doi:http://dx.doi.org/10.1016/j.chemosphere.2016.07.081

Sirko, A., Hryniewicz, M., Hulanicka, D., & Böck, A. (1990). Sulfate and thiosulfate transport in Escherichia coli K-12: nucleotide sequence and expression of the cysTWAM gene cluster. *Journal of Bacteriology, 172*(6), 3351-3357. Retrieved from http://www.ncbi.nlm.nih.gov/pmc/articles/PMC209146/

Taylor, D. E., Walter, E. G., Sherburne, R., & Bazett-Jones, D. P. (1988). Structure and location of tellurium deposited in Escherichia coli cells harboring tellurite resistance plasmids. *Journal of Ultrastructure and Molecular Structure Research, 99*(1), 18-26. doi:http://dx.doi.org/10.1016/0889-1605(88)90029-8

Theisen, J., Zylstra, G. J., & Yee, N. (2013). Genetic Evidence for a Molybdopterin-Containing Tellurate Reductase. *Applied and Environmental Microbiology, 79*(10), 3171-3175. doi:10.1128/aem.03996-12

Turner, R. J., Aharonowitz, Y., Weiner, J. H., & Taylor, D. E. (2001). Glutathione is a target in tellurite toxicity and is protected by tellurite resistance determinants in Escherichia coli. *Canadian Journal of Microbiology, 47*(1), 33-40.

Turner, R. J., Weiner, J. H., & Taylor, D. E. (1999). Tellurite-mediated thiol oxidation in Escherichia coli. *Microbiology, 145*(9), 2549-2557. doi:doi:10.1099/00221287-145-9-2549

Vrionis, H. A., Wang, S., Haslam, B., & Turner, R. J. (2015). Selenite Protection of Tellurite Toxicity Toward Escherichia coli. *Frontiers in Molecular Biosciences, 2*, 69. doi:10.3389/fmolb.2015.00069

Wray, D. S. (1998). The impact of unconfined mine tailings and anthropogenic pollution on a semi-arid environment – an initial study of the Rodalquilar mining district, south east Spain. *Environmental Geochemistry and Health, 20*(1), 29-38. doi:10.1023/A:1006575127212

Zeng, C., Ramos-Ruiz, A., Field, J. A., & Sierra-Alvarez, R. (2015). Cadmium telluride (CdTe) and cadmium selenide (CdSe) leaching behavior and surface chemistry in response to pH and O2. *Journal of Environmental Management, 154*, 78-85. doi:http://dx.doi.org/10.1016/j.jenvman.2015.02.033

FIGURES:

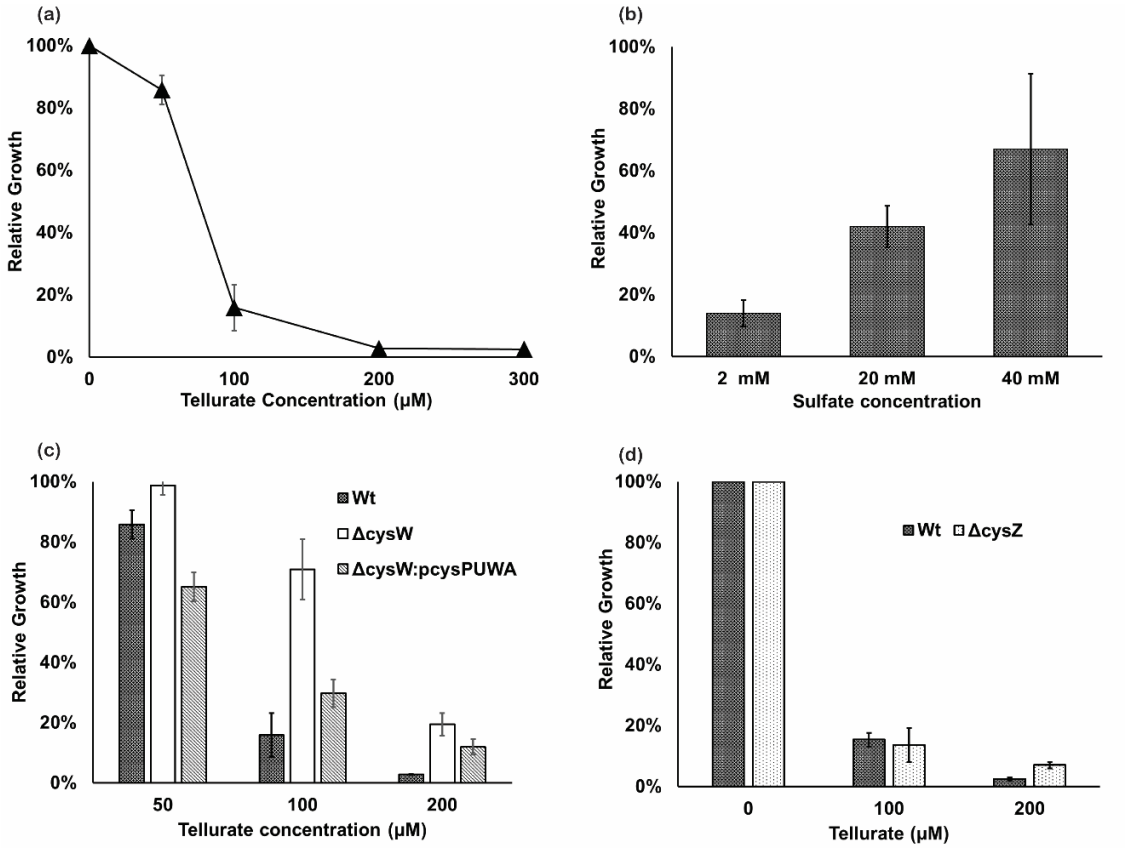

Figure 2.1. Growth of *E. coli* strains in the presence of tellurate. Averages and standard error bars represent the results of experiments performed in triplicate. (**a**) Relative growth of the *E. coli* wild-type strain after 10 h at varying tellurate concentrations. (**b**) Relative growth of the *E. coli* wild-type strain grown with 100 μM tellurate at varying sulfate concentrations. (**c**) Relative growth of the *E. coli* wild-type strain (Wt), Δ*cysW* mutant, and Δ*cysW*:p*cysPUWA* complemented mutant at varying tellurate concentrations. Dark gray bars represent the wild-type, white bars represent Δ*cysW* and hatched bars represent Δ*cysW*:p*cysPUWA*. (**d**) Relative growth of *E. coli* wild-type strain

and Δ*cysZ* mutant at varying tellurate concentrations. Dark gray bars represent the wild-type strain and stippled bars represent the Δ*cysZ* mutant.

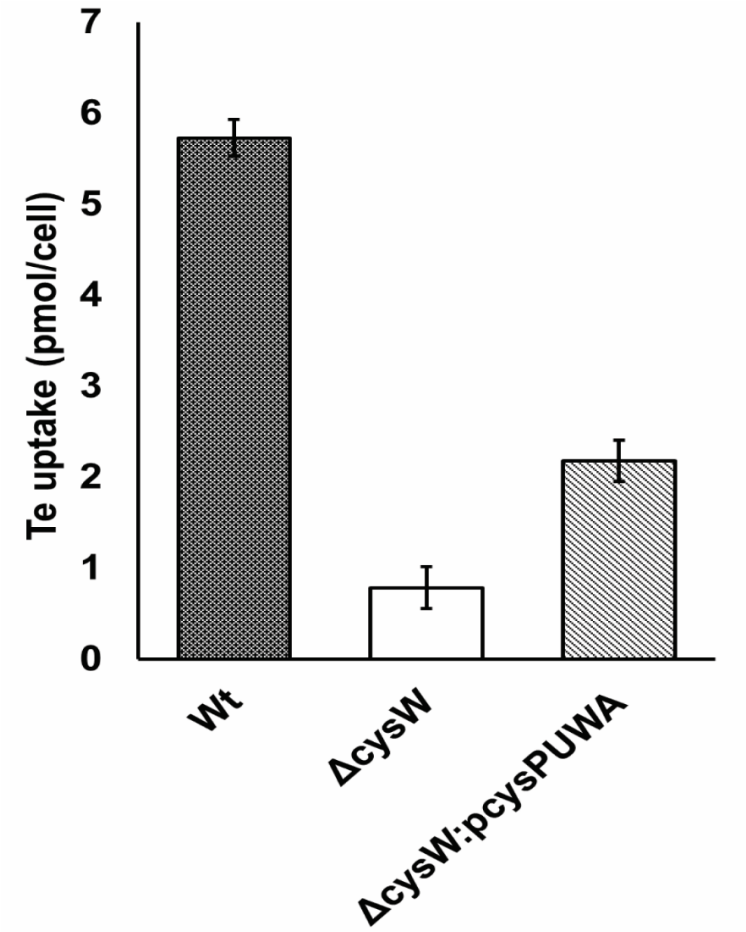

Figure 2.2. Tellurate uptake by the *E. coli* wild-type strain (dark gray bar), Δ*cysW* mutant (white bar) and Δ*cysW*:p*cysPUWA* complimented mutant (hatched bar). Averages and standard error bars represent the results of experiments performed in triplicate.

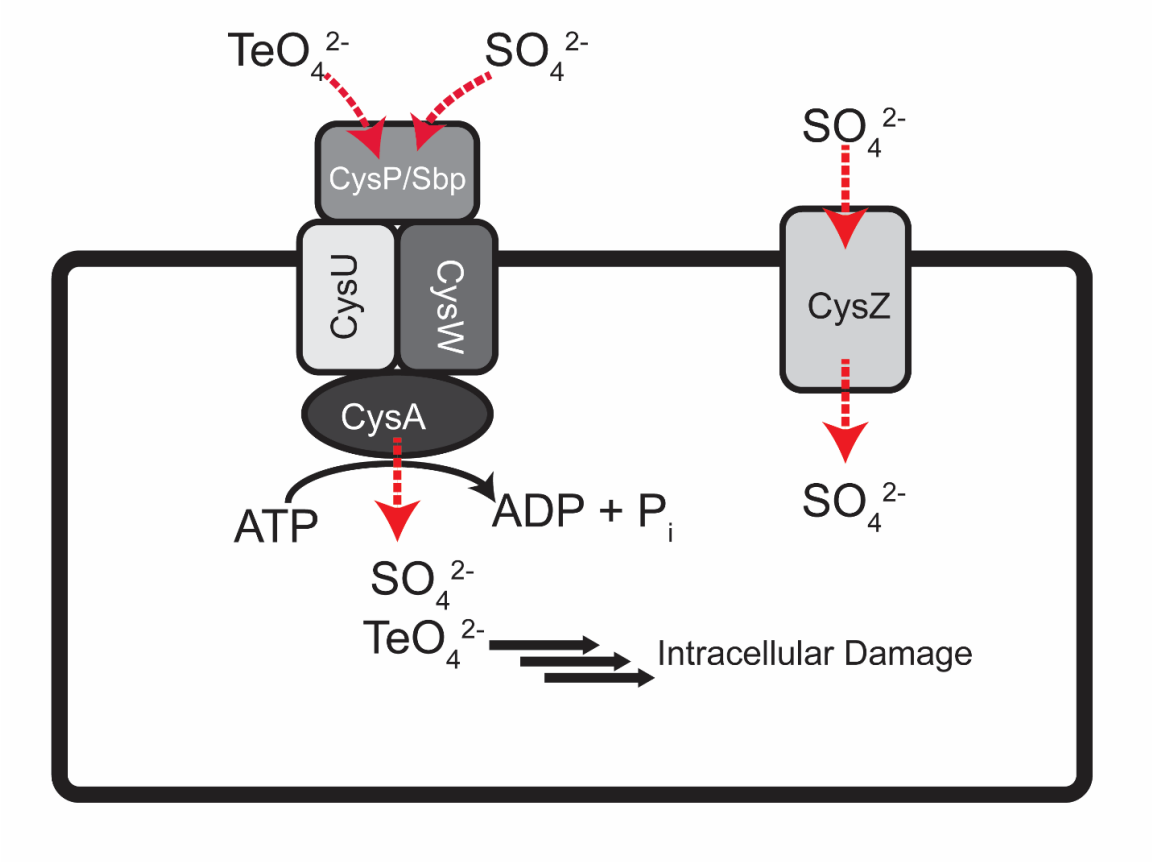

Figure 2.3. Proposed model for the transport-dependent toxicity of tellurate. Tellurate primarily exerts its damagining effects within the cytoplasm of E. coli. Loss of tellurate transport into the cytoplasm limits this damage.

CHAPTER 3
MEDIA EFFECTS ON TELLURATE TOXICITY IN *ESCHERICHIA COLI* K-12

ABSTRACT:

Tellurate reduction and toxicity in *Escherichia coli* has received little attention and are poorly understood processes. Here we studied the underlying basis for the difference in tellurate toxicity in a minimal defined medium (M9) compared to a rich complex medium (LB). Tellurate was more toxic to cells grown on LB medium compared to M9 medium. Cystine in LB was found to be the key component controlling this difference. Inactivation of the cystine transporter YdjN increased the resistance of cells towards tellurate. Cystine amendments to cultures pre-grown with tellurate resulted in a rapid decrease in cell viability. Oxidation of the intracellular thiol pool with the thiol-oxidizing agent diamide resulted in an increase in resistance of cells towards tellurate. Tellurate exposure induced only a modest decrease in the intracellular cysteine pool. In contrast, tellurate exposure dramatically depleted the glutathione pool. In abiotic experiments, cysteine was observed to reduce tellurate to Te(0) while glutathione did not. These data suggest a mechanism whereby tellurate directly interacts with intracellular cysteine, and glutathione is subsequently depleted in a secondary reaction without directly interacting with tellurate.

INTRODUCTION:

The mechanisms of toxicity of tellurium oxyanions – namely, tellurite (Te[IV]) and tellurate (Te[VI])—remain poorly understood despite having been the subject of study for decades. Of the two oxyanions, tellurite is the better studied but even still research on its toxicity towards microorganisms has primarily produced a series of observations on the alterations of various physiological processes while still lacking a unifying mechanism to tie together these observations. Three major themes have emerged from the research on tellurite toxicity in *Escherichia coli*: (1) tellurite depletes intracellular thiol pools (Turner, Aharonowitz, Weiner, & Taylor, 2001); (2) tellurite triggers reactive oxygen species (ROS) formation and related stress and (Pérez et al., 2007); and (3) recent work has shown that tellurite-exposure leads to accumulation of heme biosynthesis pathway intermediates (Morales et al., 2017).

Early studies demonstrated that upon tellurite exposure, the intracellular thiol pool of *E. coli* is depleted concurrent with a loss in cell viability (Turner, Weiner, & Taylor, 1999). A follow-up study demonstrated that glutathione is the main target of the tellurite-induced thiol depletion observed in *E. coli* (Turner et al., 2001). In that study, intracellular thiol pools were monitored following tellurite exposure. Glutathione was the major thiol that was depleted following this exposure. Depletion of acetyl-CoA was also observed following tellurite exposure but cysteine pools remained unchanged (Turner et al., 2001).

Later work has shown that tellurite exposure triggers the formation of ROS in the cytoplasm of *E. coli* (Pérez et al., 2007). The generation of ROS was

accompanied by the development of extensive cellular damage including: increased oxidation of cytoplasmic proteins, oxidation of membrane lipids, and up-regulation of genes involved in the oxidative stress response (Pérez et al., 2007). The source of the ROS is likely, in part, from the reduction of tellurite. The reduction of tellurite *in vitro* by catalase was observed to produce superoxide (Pérez et al., 2007). Similarly, reduction of tellurite *in vitro* by the NADH-dehydrogenase II enzyme produces superoxide (Díaz-Vásquez et al., 2014). This is similar to prior observations that superoxide is produced during the abiotic reduction of selenite with glutathione (Kessi & Hanselmann, 2004). However, the direct reduction of tellurite by glutathione coupled to the production of ROS has not yet been demonstrated. The glutathione pool depletion observed by others could therefore also be secondary to the ROS generation that may accompany the reduction of tellurite in the cytoplasm (Winterbourn & Metodiewa, 1994).

A recent study by Morales et. al. (2017) has shown that *E. coli* cells accumulate the heme biosynthesis pathway intermediates in response to exposure to tellurite (Morales et al., 2017). Wild-type cells were observed to accumulate protoporphyrinogen IX in response to tellurite exposure. However, a mechanism explaining this observation remains unknown. Additionally, hydroxyl radical generation in the cytoplasm following tellurite exposure was observed in that study (Morales et al., 2017). Porphyrin compounds are known to be able to generate ROS and so the hydroxyl radical production was attributed to the accumulated protoporphyrinogen IX (Vatansever et al., 2013). Therefore, protoporphyrinogen IX accumulation triggered by tellurite exposure may lead to

generation of excessive ROS, particularly hydroxyl radicals. Intracellular thiols may also play a role in hydroxyl radical detoxification, which could account for observation that tellurite exposure also depletes intracellular thiol pools (Morales et al., 2017; Vatansever et al., 2013).

While tellurite is considerably more toxic to *E. coli* than selenite, selenite exposure triggers the generation of higher amounts of intracellular ROS compared to tellurite exposure, suggesting that more than just oxidative stress is involved in the toxicity of tellurite (Vrionis, Wang, Haslam, & Turner, 2015). Additionally, tellurite remains toxic to cells grown under anaerobic conditions (Tantaleán et al., 2003). The recent discovery of protoporphyrinogen IX accumulation in tellurite-exposed cells does suggest another important pathway by which ROS might be produced; however, it fails to extend the current working model for tellurite toxicity beyond generation of ROS in the cytoplasm (Morales et al., 2017). While its possible that protoporphyrinogen IX may directly interact with other intracellular components, its targets remain unknown at this time.

Currently, even less is known about the toxicity of tellurate and the cellular response to tellurate exposure. **Chapter 2** demonstrated that tellurate transport into cytoplasm plays an important role in mediating its toxicity in *E. coli* (Goff & Yee, 2017). Additionally, earlier work has suggested that a molybdoenzyme(s) of unknown identity may play a role in tellurate reduction (Theisen, Zylstra, & Yee, 2013). However, it remains unclear what role tellurate and tellurite reduction plays in the toxicity of these oxyanions towards *E. coli* and other tellurate-reducing organisms (Chasteen, Fuentes, Tantaleán, & Vásquez, 2009). On this

point, it is important to note that two highly tellurite-resistant phototrophic bacteria – *Roseococcus thiosulfatophilus* and *Erythromicrobium ezovicum*—do not reduce tellurite to elemental tellurium under certain growth conditions despite maintaining a high level of resistance to the oxyanion under those conditions (Yurkov, Jappe, & Vermeglio, 1996). This suggests that reduction of tellurate and tellurite may not be a detoxification pathway in certain organisms. This idea runs counter to the commonly held notion that microorganisms will reduce or modify toxic metals and other compounds to their less toxic forms (Lloyd & Lovley, 2001).

The study performed here was initiated by our observation that *E. coli* tolerates higher concentrations of tellurate when grown on M9 minimal medium compared to LB medium. A series of experiments were conducted to explore the media dependence on tellurate toxicity as it may provide insight into the toxicity mechanism of tellurate in *E. coli*. The objective of this work was two-fold. First, we sought to determine the component(s) of the LB medium that were primarily responsible for the increase in the toxicity of tellurate relative to M9 medium. Second, we sought to use those findings to understand the cellular response to tellurate exposure. The results indicate that intracellular cysteine plays a key role in tellurate reduction and toxicity.

MATERIALS AND METHODS:

Strains and growth conditions

Experiments were conducted with the wild-type *E. coli* K-12 strain, and the mutant strains JW1905 (Δ*fliY*::kan), JW1718 (Δ*ydjN*::kan), JW2663 (Δ*gshB*::kan) and JW2414 (Δc*ysM*::kan) obtained from the Keio Collection of the National Institute of Genetics, Japan (Baba et al., 2006). YdjN and FliY-YecSC are two characterized cystine transporters which import cystine to the cytosol. (Chonoles Imlay, Korshunov, & Imlay, 2015). FliY-YecSC is an ATP-dependent ABC transporter with a higher affinity for cystine (with a K_m in the nanomolar range) (Butler, Levin, Facchiano, Miele, & Mukherjee, 1993; Chonoles Imlay et al., 2015). YdjN is a recently described transporter with homology to H+/Na+-driven symporters. YdjN has a lower affinity for cystine with a K_m in the micromolar range (Chonoles Imlay et al., 2015). GshB and CysM are proteins involved in glutathione and cysteine biosynthesis, respectively.

All experiments were either performed in LB medium or in M9 medium with amendments as described in later sections. M9 medium composition includes, per liter, 0.68 g Na_2HPO_4, 0.3 g KH_2PO_4, 0.05 g NaCl, 0.1 g NH_4Cl, 0.25 g $MgSO_4$, 0.012 g $CaCl_2$. 0.4% (w/v) glucose was added as a carbon source. For all experiments except for the MIC tests, 0.1% (w/v) yeast extract was added as a nutritional supplement to the M9 medium. For incubations, cultures were routinely grown in a 37°C shaking incubator at 200 RPM.

MIC test

The minimum inhibitory concentration (MIC) was determined by diluting an overnight culture into 96 well plates with an initial cell density of 5 x 10^5 cells/mL. Increasing tellurate concentrations (0, 0.025, 0.05, 0.1, 0.2, 0.3, 0.4, 0.5, 0.7, 0.9, 1, 1.1 mM) were added to each well. Plates were incubated for 18 hours and turbidity was observed. The MIC was defined as the lowest concentration of tellurate needed to inhibit growth under the conditions defined above. Amino acid amendments were added at concentrations calculated for commercial LB medium preparations (**Table A3.1**).

Viable cell counts

Experiments were conducted to examine the effect of cystine amendments, thiol-blocking, and glutathione and cysteine biosynthesis gene mutations on tellurate toxicity in *E. coli*. Overnight cultures were washed in phosphate-buffered saline and diluted into M9 medium. For experiments using diamide to oxidize intracellular thiols, cells were pre-treated with 1 mM diamide. For the experiments to test the effects of cystine exposure on cell viability, cells were pre-treated with 0.5 mM tellurate. For experiments to compare tellurate toxicity in cysteine and glutathione mutants, no pre-treatment was performed.

Cultures were then exposed to different treatments depending on the experiment performed. For experiments testing the effects of cystine exposure, cultures were first pre-grown with tellurate to an optical density of 0.1 and then spiked with cystine (0.04 g/L) (controls were spiked with a Milli Q water blank).

Samples were taken for quantification immediately prior to the cystine spike and then at timepoints after. For experiments with the diamide pre-treatment, cultures were pre-grown with diamide to an optical density of 0.1 and then spiked with 0.5 mM tellurate (controls were spiked with a Milli Q water blank). Diamide is a thiol-oxidizing agent that is used to oxidize intracellular glutathione to glutathione disulfide (Kosower, Kosower, Wertheim, & Correa, 1969). Diamide has also been shown to deplete intracellular cysteine pools in addition to intracellular glutathione pools and to induce s-thiolations (disulfide bond formation between protein cysteine residues and free low-molecular weight thiols) (Pöther et al., 2009). Samples were taken for quantification immediately prior to the tellurate spike and then at timepoints after.

For experiments with the cysteine and glutathione biosynthesis mutants, cultures were spiked with 0.5 mM tellurate after reaching an optical density of 0.1 (controls were spiked with a Milli Q water blank). Knock-out mutant strains Δ*gshB* and Δ*cysM* were used for this experiment. GshB is the glutathione synthetase that catalyzes the final step of glutathione biosynthesis: the condensation of glycine with gamma-L-glutamyl-L-cysteine to form glutathione (Apontoweil & Berends, 1975). CysM catalyzes the final step of cysteine biosynthesis: the formation of cysteine from sulfide and O-acetyl-L-serine (Claus, Zocher, Maier, & Schulz, 2005). A sample was taken for quantification immediately prior to the tellurate spike and then at timepoints after. After these treatments, additional samples were taken for dilution and spot-plating using the methodology described above.

All samples were diluted into phosphate-buffered saline solution in a 96 well plate. Dilutions were then spotted in triplicate in 10 µL volumes onto LB plates. Plates were incubated overnight at 37°C. Following incubation, the number of colonies were counted and used to determine the number of viable cells present in the culture at the sampling point. Viable counts at later time points were normalized against the viable cell count prior to the treatment to obtain a percentage of viable cells remaining following treatment. A student's t-test was used for statistical analysis of data.

Reduction of tellurium compounds with cysteine and glutathione

It was tested whether cysteine and glutathione can reduce tellurate to Te(0). Previously it has been reported that intracellular cysteine concentrations in *E. coli* cells grown in minimal medium with sulfate as a sulfur source and in minimal medium with as a cystine source were 0.2, and 1.5 mM, respectively (Park & Imlay, 2003). For our experiment we selected a range of cysteine concentrations that spanned these reported values. Cysteine at a range of concentrations from 0-4 mM was added to each reactor. Reactors were initially prepared with 0.5 mM tellurate in sterile Milli-Q water and purged with N_2 gas to minimize oxidation of the cysteine. Separately, the cysteine stock was prepared in purged Milli-Q water. The final volume was 20 mL. A similar experimental set-up was used to determine if tellurate reacts with glutathione. Intracellular concentrations of glutathione can reach up to 10 mM (Park & Imlay, 2003). Therefore, the concentrations used here were physiologically relevant (0-4 mM).

A similar series of experiments were performed for reactions between tellurite and cysteine or glutathione. 0.5 mM tellurite was reacted with a range of thiol concentrations (0-4 mM) under the conditions described above.

All reactors were gently shaken at room temperature for 24 hours to allow the reactions to proceed to completion. Following this reaction period, samples were collected from each reactor for analysis of the remaining soluble tellurium and thiol concentrations. Samples for tellurium analysis were filtered with 0.2 μm nylon filters and acidified with 2% nitric acid. Samples for thiol analysis were immediately derivatized using the fluorescent probe monobromobimane (mBBr). mBBr is a weakly fluorescent molecule that reacts with the unpaired electrons of the sulfhydryl group of thiol molecules to form a stable and highly fluorescent thioether bond (Fahey & Newton, 1988). Stock solutions of mBBr (Sigma) were prepared in acetonitrile at a concentration of 50 mM. Using a method adapted from Dupont and Ahner (2005), 84 μL of borate/diethylenetriaminepentaacetic acid (DTPA) buffer (100 mM/10 mM, pH 9) and 3 μL of the 50 mM mBBr stock solution were added to 800 μL of the sample (Dupont & Ahner, 2005). The reaction proceeded for 30 minutes at room temperature in the dark before being stopped by the addition of 60 μL of methanesulfonic acid (MSA). Following mBBr derivatization, samples are stable for storage at -20°C for extended periods of time (Smith, Sessions, Dawson, Dalleska, & Orphan, 2017). Samples were stored at ~4°C with observed stability for at least a month of storage.

Monitoring intracellular cysteine and glutathione

Initially, glutathione and cysteine concentrations were monitored in unexposed cells to validate the extraction procedure and analytical methods. Overnight cultures were washed with phosphate-buffered saline and diluted into LB to a starting OD of ~0.01. Samples were collected at regular intervals for dry weight and intracellular thiol measurements. At each sampling point, 2 mL of sample was collected for dry weight measurements. Samples were dried for ~24 hours in an oven at 90°C prior to weighing. For preparation of intracellular extracts, 800 µL of sample was spun down in a centrifuge at 13,000 RPM. The supernatant was then removed and cells were resuspended in 800 µL of Milli-Q water. Using a modified version of the procedure outlined above, 84 µL of the borate/DTPA buffer and 3 µL of the mBBr stock were added to the sample. The sample was incubated at 90°C in the dark for 30 minutes to release and then immediately derivatize the intercellular contents. To stop the derivatization reaction, 60 µL of MSA was added as described above. Samples were then centrifuged and supernatants were filtered using a 0.2 µm nylon filter. Samples were stored at 4°C until analysis. Analytical methods are described in the following section. Intracellular cysteine and glutathione concentrations were normalized against dry weights. The results of this preliminary trial are given in **Figure A3.1 of Appendix 3.** We compared these values to those reported for intracellular glutathione and cysteine concentrations in *E. coli* cells in the literature. Intracellular cysteine concentrations are reported at a range of 0.26-31 µmol/g

dry cell weight depending on growth conditions (Wheldrake, 1967). Intracellular glutathione concentrations are reported at a range of 7-27 μmol/g dry cell weight depending on growth conditions (Fahey, Brown, Adams, & Worsham, 1978). The values observed here were found to be similar, supporting the validity of our methodology.

To determine the effect of tellurate exposure on intracellular thiol pools, overnight cultures were washed with phosphate-buffered saline. The cells were diluted into fresh LB medium and allowed to grow to mid-log phase. At mid-log growth, samples were taken to determine dry weight and for analysis of intracellular thiols using the methods described and validated above. Cultures were then spiked with 0.1 mM tellurate. At two and four hours following the tellurate spike, samples were taken for dry weight measurements and analysis of intracellular thiols. A student's t-test was used for statistical analysis of data.

Analytical methods

High-performance liquid chromatography analysis of thiol-bimanes

We analyzed the mBBr-derivatized samples to determine concentrations of glutathione and cysteine. Separations of intracellular extracts were performed using reversed-phase high-pressure liquid chromatography (HPLC) on a ZORBAX Extend-C18 column (Agilent) using an Agilent 1260 Infinity II HPLC system equipped with an Agilent 1100 series fluorescence detector. A gradient method was used to achieve separation of the bimane-derivatized compounds.

The same method was used to measure glutathione and cysteine concentrations during the cell-free reaction with tellurate and tellurite. Solvent A was a mixture of 0.25% glacial acetic acid and 1% acetonitrile prepared in Milli-Q water and solvent B was 100% acetonitrile. A gradient method was used for the separations with a flow rate of 0.5 mL/min. The gradient method was as follows: 0-3 minutes 3% B; 3-10 minutes increase to 14% B; 10-34 minutes increase to 20% B; 34-43 minutes increase to 80% B; 43-54 minutes maintain at 80% B; 54-56 minutes decrease to 3% B; 56-59 minutes maintain at 3% B. Cysteine elutes at approximately 14.7 minutes and glutathione elutes at approximately 17.3 minutes. Injections of 60 µL were used. Compounds were detected using a fluorometer with an excitation wavelength of 390 nm and an emission wavelength of 478 nm. Cysteine and glutathione standards were prepared under the same conditions as samples were prepared.

Inductively-coupled plasma optical emission spectroscopy analysis of total soluble tellurium

Total soluble tellurium concentrations were measured using an iCAP 7400 Inductively Coupled Plasma Optical Emission Spectrometer (ICP-OES) (Thermo Fisher) at a wavelength of 214.282 nm. Tellurate or tellurite standards were prepared over a range of concentrations under the same conditions described above for sample preparation.

RESULTS:

Tellurate MICs in different types of media

We observed a difference in the toxicity of tellurate towards *E. coli* when it was cultured on LB medium versus when it was cultured on M9 medium without any additional nutrient enrichment (**Table 3.1**). While *E. coli* grew in M9 medium supplemented with 0.1 mM of tellurate (**Chapter 2**), our attempts to culture *E. coli* in LB medium supplemented with tellurate at the same concentration were unsuccessful. This led to a hypothesis that certain component(s) of the LB medium contributed to the increased toxicity of tellurate compared to the M9 medium. Thus, we conducted a series of experiments to identify the media component(s) and mechanisms of toxicity of tellurate in *E. coli*.

We determined the MIC of tellurate on LB and M9 medium supplemented with glucose as a carbon source. All experiments were performed under aerobic conditions. On LB, the MIC of tellurate was 0.015 mM. On M9 medium, the MIC was much higher at 1 mM (**Table 3.1**). From there we considered each component of the LB medium individually to determine which one(s) was responsible for the lower MIC of tellurate on LB medium. The manufacturer for our standard LB medium mix did not provide a detailed breakdown of the chemical components (i.e. amino acids) of the mix. Therefore, we had to base our amino acid amendment concentrations off those reported by BD for their yeast extract and tryptone products. As such, we wanted to confirm that LB medium prepared from these products ("LB #2" in **Table 3.1**) produced comparable results to previously-used LB mix ("LB #1" in **Table 3.1**). The MIC of tellurate in

this second version of the LB recipe (using the same concentrations of ingredients but different manufacturers) was also 0.015 mM. Thus, results were replicated even between LB mixes that likely have some variation in their nutritional components.

The standard LB recipe consists of 10 g/L NaCl, 5 g/L yeast extract, and 10 g/L tryptone. We tested the effect of each component of the medium on the toxicity of tellurate in *E. coli.* Supplementation with either yeast extract or tryptone in M9 medium decreased the MIC from 1.0 to 0.3 mM. M9 supplemented with a higher concentration of NaCl produced a similar MIC as M9 medium alone. To determine if the amino acid components of the tryptone and yeast extract were the major contributors towards the lower MIC on LB medium, the M9 medium was supplemented with casamino acids (**Table 3.1**). The MIC decreased from 1 mM to 0.2 mM when casamino acids were added to M9 medium. Based on examination of the amino acids present in a standard LB medium (calculated based on manufacturer-reported values) we found that the LB contained approximately 0.04 g/L of cystine, the oxidized form of cysteine (**Appendix 3, Table A3.1**). The addition of cystine to M9 medium decreased the MIC of tellurate from 1 mM to 0.05 mM. This value is on the order of magnitude of the 0.015 mM MIC observed when the test was performed in LB medium (**Table 3.1**).

We also performed MIC measurements for tellurite, selenite, and selenate on LB, M9 medium, and M9 medium amended with cystine. Interestingly, a similar trend was observed with tellurite where the MIC for tellurate in LB and

M9 amended with cystine was lower (0.005 mM) compared to the MIC in unamended M9 (0.3 mM). However, the trend was reversed for both selenate and selenite. The presence of cystine resulted in a large increase in the MIC for both compounds (**Table 3.2**). These results indicate that the mechanism of tellurium toxicity is fundamentally different that selenium toxicity.

Inactivation of the *E. coli* cystine transporter YdjN increases resistance to tellurate

The MIC of tellurate in different media was determined for *ΔydjN* and *ΔfliY* knock-out strains. The MICs of both *ΔydjN* and *ΔfliY* on M9 remained the same as the wild-type strain (**Table 3.3).** However, on LB medium the MIC of *ΔydjN* was higher at 0.1 mM (compared to 0.015 mM for the wild-type strain) but was unchanged in the *ΔfliY* mutant (0.020 mM). On M9 medium supplemented with cystine the MIC for the *ΔydjN* mutant was increased compared to the MIC in the wild-type strain (0.6 vs. 0.015 mM). The MIC for the *ΔfliY* mutant on M9 medium supplemented with cystine was the same as the wild-type strain (**Table 3.3**). These results suggest that deletion of the YdjN transporter increases the resistance of *E. coli* to tellurate by decreasing cystine transport into the cytosol of the cells.

Addition of cystine to cultures rapidly kills cells

To further examine the synergistic interactions between tellurate and cystine in *E. coli*, we performed an experiment in which cells were pre-grown with 0.5 mM tellurate and then cultures were spiked with cystine (0.04 g/L). Spiking cultures with cystine significantly decreased the viability of the cells pre-treated with tellurate (**Figure 3.1**). The tellurate pre-treated cultures that were spiked with cystine showed a significantly lower normalized viable cell count (2.36% ± 1%) compared to the tellurate pre-treated cultures that were not spiked with cystine (113%±8%) ($p<0.001$) (**Figure 3.1**). Additionally, the controls indicate that cystine additions by themselves in non-tellurate-treated cells were not toxic **(Figure 3.1)**

Reactions of tellurate and tellurite with thiol compounds

In the cytosol of *E. coli* cystine is reduced to cysteine (Chonoles Imlay et al., 2015). In cell-free experiments, we found that tellurate is rapidly reduced in a reaction with cysteine. Reduction of the tellurate to elemental tellurium (Te(0)) by the cysteine was indicated by the formation of a dark brown/black precipitate was visually observed within seconds of the addition of cysteine to a tellurate solution (**Figure 3.2C**). Supporting this observation, at increasing cysteine concentrations we observed a decrease in the concentration of soluble tellurium remaining in the reactors. This indicates that tellurium is being reduced to the insoluble Te(0). At a concentration of 3 mM cysteine, 96.3% of the tellurate had been reduced to Te(0). Additionally, we found that soluble tellurium concentrations decreased linearly ($R^2=0.94$) with increasing starting

cysteine:tellurate ratios up to a 6:1 ratio (**Figure 3.2A**). This ratio is consistent with the six electron reduction of tellurate (6+) to Te(0) according to following reaction stoichiometry (CSH = cysteine and CSSC = cystine):

$$TeO_4^{2-} + 6CSH + 2H^+ \rightarrow Te(0) + 3CSSC + 4H_2O$$

These results indicate that six moles of cysteine are required for the reduction of one mole of tellurate to Te(0).

We then conducted experiments to determine if tellurate reacts with glutathione. No Te(0) formation was observed when 0.5 mM of tellurate was reacted with up to 4 mM of glutathione (**Figure 3.2D).** To examine if soluble tellurium intermediates were formed through a reaction with glutathione, experiments were then conducted to monitor the concentration of free glutathione in the reaction vessel over time. While we did observe minor loss of glutathione in solution (~15% in each reactor) this was similar to the amount lost in a tellurate-free control reactor (**Figure 3.2B).** In contrast, cysteine was almost entirely depleted in reactors containing tellurate when it was added at ratios up to and including 6:1 cysteine: tellurate. Once cysteine was in excess of that ratio, no further cysteine depletion was observed **(Figure 3.2B).**

Since tellurite may form as an intermediate of tellurate reduction and as reactions of tellurite with cellular thiols remain poorly characterized, we then performed a similar set of experiments using tellurite. Similar to tellurate, when cysteine or glutathione was reacted with tellurite, we observed reduction to Te(0) by cysteine but not by glutathione **(Figure 3.3A,C,D)**. In contrast to the tests with tellurate, when glutathione concentrations were monitored in these reactors,

we observed substantial depletion of glutathione compared to the control **(Figure 3.3B**). These results suggest that a soluble reduced tellurium species is being formed rather than the insoluble Te(0). When cysteine and tellurite are reacted at a 4:1 ratio, 99.8% of the tellurite was reduced to Te(0) (**Figure 3.3A)**. Furthermore, we found soluble tellurium concentrations decreased linearly (R^2 =0.97) with increasing starting ratios of cysteine:tellurite, up to a 4:1 ratio. Additionally, cysteine is almost entirely depleted in reactors where it is added up to and including 4:1 cysteine:tellurite ratio (**Figure 3.3B**). Once cysteine is in excess of this ratio, complete depletion is no longer observed **(Figure 3.3B)**. This ratio is consistent with the four electron reduction of tellurite (4+) to Te(0) according to following reaction stoichiometry

$$TeO_3^{2-} + 4CSH + 2H^+ \rightarrow Te(0) + 2CSSC + 3H_2O$$

Disulfide stress increases resistance to tellurate

As cysteine reduces tellurate *in vitro*, we next determined the effect of blocking this reaction *in vivo* on the toxicity of tellurate in *E. coli*. Diamide had a drastic impact on cell-survival following tellurate exposure (**Figure 3.4A)**. At thirty minutes, 63%±13% of cells pre-treated with diamide remained alive compared to 1%±0.26% of non-treated cells ($p<0.05$). Similarly, at 2 hours, 67%±31% of pre-treated cells remained alive compared to 0.1%±0.04% in the non-treated cells. Additionally, we observed less darkening of the medium (Te(0) formation) following tellurate additions in the diamide pre-treated cultures compared to the non-pre-treated cultures (**Figure 3.4B**).

Effects of inactivation of genes involved in thiol metabolism on tellurate resistance

The *cysM* knock-out strain showed a modest increase in the percentage of viable cells remaining over the wild-type strain at two hours following tellurate exposure ($p<0.01$). At later time points, the percentage of viable cells remaining in the *ΔcysM* cultures was decreased but still greater than the control ($p<0.05$) (**Figure 3.5B**). The *ΔgshB* mutant did show increased resistance to tellurate exposure at 6 hours but this did not achieve statistical significance (**Figure 3.5A**).

Tellurate exposure causes depletion of intracellular thiol pools

In LB medium, tellurate exposure caused a decrease in intracellular concentrations of glutathione and cysteine. After two hours of tellurate-exposure, we observed a significant decrease in the intracellular glutathione content of *E. coli* compared to the unexposed controls ($p<0.001$). The glutathione concentration in unexposed controls 38.6±2.72 μmol/g compared to 0.96±0.17 μmol/g in the tellurate exposed cells. Similar results were observed at four hours of tellurate exposure (**Figure 3.6A**). Cysteine concentrations also decreased but to a lesser extent than glutathione concentrations. After four hours of tellurate exposure, cysteine concentrations were 0.15±0.02 μmol/g compared to 0.24±0.02 μmol/g in the unexposed controls ($p<0.05$)(**Figure 3.6B**).

DISCUSSION:

The results demonstrate that the media background has a significant influence on the toxicity of tellurate in *E. coli*. Tellurate was ~60 times more toxic towards *E. coli* when cells were grown on LB medium compared to when grown on M9 medium with glucose added as a carbon source. When tryptone (10 g/L) or yeast extract (5 g/L) were used to supplement the M9 medium, the MIC for tellurate decreased from 1 mM to 0.3 mM (**Table 3.1**). Similar results were also observed when the M9 medium was supplemented with casamino acids (2 g/L). Additions of sodium chloride (10 g/L) had no impact on the MIC of tellurate in M9 medium, indicating that the nutritional supplements are the main controllers of tellurate toxicity in the LB medium (**Table 3.1**). The addition of cystine decreased the MIC of tellurate on M9 medium to 0.05, similar to the value for LB medium (0.015) (**Table 3.1**).

Similar results were observed by Moore and Kaplan (1992) in the purple non-sulfur bacterium *Rhodobacter sphaeroides* using tellurite. The MIC for tellurite was ~45 times higher on minimal medium without a nutritional supplement compared to the two types of rich media used (LB and YP media) (Moore & Kaplan, 1992). We also observed here that the MIC of tellurite was ~60 times higher on M9 medium compared to LB medium (**Table 3.2**). These results suggest a commonality between the mechanisms of toxicity of tellurite and tellurate. However, in *R. sphaeroides*, cystine supplementation was only found to increase toxicity of tellurite by approximately 2-fold while cysteine supplementation produced a similar increase in tellurite toxicity as the rich

medium. Likely the cysteine and cystine have similar effects intracellularly as the cystine is expected be imported and reduced to cysteine in the cystoplasm (Park & Imlay, 2003). Differences in the effects of cysteine and cystine on tellurite toxicity in *R. sphaeroides* may be due to lower rates of cystine transport or intracellular cystine reduction in this organism compared to *E. coli*. We did not test the effects of cysteine amendments here because of the observation that cysteine will reduce tellurate *in vitro* (**Figure 3.2A).** We did not want extracellular reactions to confound the results. Similar to our results here for tellurate, Scala and Williams (1963) found that cystine supplementation greatly increased tellurite toxicity in *E. coli* (Scala & Williams, 1963). They also observed that the amino acid methionine enhances tellurite toxicity in *E. coli* (Scala & Williams, 1963). However, we found that supplementation with methionine had no impact on tellurate toxicity (**Table 3.1**).

Inactivation of the YdjN cystine transporter decreased the toxicity of tellurate when the cells were grown on LB medium and M9 medium supplemented with cystine. Inactivation of the FliY component of the FliY-Yec produced similar growth profiles as the wild-type strain (**Table 3.3**). The difference in the results for the two transporters is unsurprising as YdjN is the primary cystine transporter under cystine-rich conditions (Chonoles Imlay et al., 2015). YdjN is expected to be the primary cystine transporter when the cells are growing in LB medium and in M9 medium supplemented with cystine. Inactivation of either transporter had no effect on the toxicity of tellurate in M9 medium without cystine supplementation. This data is consistent with the

hypothesis that cystine transport into the cells is important in mediating its interactions with tellurate.

Once within the cytosol of *E. coli*, cystine is rapidly reduced by glutathione to cysteine (Chonoles Imlay et al., 2015). As demonstrated above, transport inside the cell is necessary for cystine to amplify the toxicity of tellurate (**Table 3.3)**. Therefore, cysteine is most likely mediating the toxicity effects that are attributed to the cystine present in the medium. Once inside the cells, cystine is reduced to cysteine in a glutathione-dependent manner. This reaction is enzyme-catalyzed although a singular enzyme has not been implicated as *E. coli* carries a number of functionally redundant enzymes that can carry out this reaction (Chonoles Imlay et al., 2015). Given prior observations that cysteine can enhance tellurite toxicity in other organisms and the fact that *E. coli* will reduce cystine intracellular to cysteine, we determined whether cysteine and tellurate will react *in vitro*. We observed the *in vitro* reduction of tellurate to Te(0) with biologically-relevant concentrations of cysteine (**Figure 3.2A**). Blocking this reaction *in vivo* using the thiol-oxidizing agent diamide increased the resistance of *E. coli* to tellurate (**Figure 3.4A**). This suggests that the interactions between intracellular thiols—including cysteine— and tellurate is, in part, contributing to its toxicity. Since cysteine will reduce tellurate to Te(0), we predict that this reaction is also occurring *in vivo* and contributing to the toxicity of tellurate.

When cells pre-grown with tellurate were exposed to concentrations of cystine commonly found in LB medium, there was a reduction in the number of viable cells present in the culture 30 minutes after the treatment compared to

cells not spiked with cystine (**Figure 3.1**). The sulfur source in the medium prior to cystine exposure was sulfate. It has previously been demonstrated that when *E. coli* is switched from sulfate as its sulfur source to cystine that the cells will massively import cystine resulting in a large burst of intracellular cysteine (Chonoles Imlay et al., 2015). Whether this same process may be occurring in the cells when they are transferred to LB medium and can account for the lower MIC of tellurate on LB compared to M9 medium remains unclear. Chonoles Imlay et. al. (2015) only observed massive cystine import in response to switching cells from cystine-limited (sulfate as the only sulfur source) to cystine-rich conditions (Chonoles Imlay et al., 2015). In that study, when cells were transferred from cystine-rich to cystine-rich conditions, there was no massive import of cystine. However, it is important to note that in the work performed by Chonoles Imlay et. al. (2015), cells were only grown for 4-5 generations under the initial conditions before being transferred to the cystine-rich conditions (Chonoles Imlay et al., 2015). For our experiments, cells were grown overnight on LB before being diluted into fresh medium. It is likely that in our LB precultures cystine had become limiting during overnight growth. This would then lead to the rapid over-import of cystine once they are switched to cystine-rich medium. In these cultures, the rapid expansion of the intracellular cysteine pool following the cystine exposure may result in a temporary increase in the intracellular tellurate reduction rates.

Why the intracellular reduction of tellurate by thiols plays a role in its toxicity is still unknown. Importantly, Te(0) is generally believed be non-toxic

(Ba, Döring, Jamier, & Jacob, 2010) and so it is unlikely that the actual production of the Te(0) is contributing to the cysteine/cystine-mediated toxicity of tellurate. The toxicity of both tellurite and selenite has, in part, been attributed to the formation of reactive oxygen species during the reduction of these oxyanions to Te(0) and Se(0), respectively. Superoxide production has been measured concurrent to the abiotic reduction of selenite with glutathione (Kessi & Hanselmann, 2004). Likewise, when tellurite is reduced *in vitro* by the enzyme catalase, superoxide is produced (Pérez et al., 2007). If ROS production does occur during the reduction of tellurate, this could result in a burst of intracellular ROS. Future work should focus on measuring ROS in tellurate-exposed cells but also during the reaction between cysteine and tellurate *in vitro*.

Given our observation that cysteine reduces tellurate *in vitro* and that oxidation of intracellular thiols with diamide increases tellurate resistance, we next monitored intracellular concentrations of cysteine and glutathione following tellurate exposure. We observed modest depletion of cysteine when cells were grown in the presence of tellurate. In contrast to cysteine, a much more dramatic depletion of glutathione was observed in tellurate-exposed cells. A previous study with tellurite demonstrated that tellurite exposure results in a similar extent of depletion of the glutathione pool in *E. coli* when grown on LB medium (Turner et al., 2001). However, that study did not observe any depletion of the cysteine pool following tellurite exposure. The connection between the two thiol pools and their responses to tellurate exposure may be attributed to one or a combination of the following four processes: (1) depletion of glutathione pools to maintain

cysteine homeostasis, (2) depletion of glutathione in response to an increase in ROS stress following tellurate exposure, (3) direct oxidation of glutathione by tellurate, and (4) direct oxidation of glutathione by tellurite that forms from tellurate reduction.

As mentioned previously, the reduction of cystine to cysteine is a glutathione-dependent process that is catalyzed by a number of functionally redundant enzymes (Chonoles Imlay et al., 2015). Glutathione is also directly converted to cysteine when the cysteine becomes limiting within the cells via the γ-glutamyl cycle. The enzyme γ-glutamyltranspeptidase catalyzes the hydrolysis of glutathione to L-cysteinylglycine and L-glutamate (H. Suzuki, Hashimoto, & Kumagai, 1993). Aminopeptidases then catalyze the cleavage of the L-cysteinylglycine to L-cysteine and glycine (Hideyuki Suzuki, Kamatani, Kim, & Kumagai, 2001). If tellurate reduction—similar to tellurite reduction-- is coupled to ROS production, then glutathione oxidation could also be occurring secondary to that (Carmel-Harel & Storz, 2000; Chasteen et al., 2009; Pérez et al., 2007; Winterbourn & Metodiewa, 1994). All these processes could potentially deplete the glutathione pool secondary to the oxidation of cysteine by tellurate.

Inactivation of the glutathione synthetase (GshB) --which catalyzes the second of two steps in the glutathione biosynsthesis pathway (Apontoweil & Berends, 1975)—did not have a significant impact on cell survival immediately following tellurate exposure **(Figure 3.5A)**. This supports a model whereby there are no direct interactions between tellurate and glutathione that contributes towards the toxicity of tellurate. In contrast, inactivation of cysteine

synthase produced a modest increase in survival following tellurate exposure, supporting an early role for cysteine in the toxicity of tellurate (**Figure 3.5B**).

We next tested whether tellurate can directly oxidize glutathione. *E. coli* can accumulate up to 10 mM of glutathione in its cytosol and so we tested glutathione concentrations within this range (Fahey et al., 1978). Despite the observation that tellurate exposure induces intracellular glutathione depletion, we found tellurate does not directly react with glutathione *in vitro* (**Figure 3.2B).** It is interesting that cysteine but not glutathione will reduce tellurate *in vitro*. The standard reduction potentials of the cystine/cysteine and glutathione disulfide/glutathione redox couples are very similar (-250 and -264 mV, respectively) and the standard reduction potentials for the tellurate/tellurite and tellurite/elemental tellurium redox couples are relatively high (+892 mV, and +827 mV, respectively)(Bouroushian, 2010; Park & Imlay, 2003). Both reactions appear energetically favorable. This suggests that some other factor must be controlling the differences in their reactivities with tellurate (Jones et al., 2000). Interestingly, cysteine and glutathione also differ enormously in their abilities to reduce free intracellular iron (Park & Imlay, 2003). The reason for this observation remains unclear but may be related to how the thiols coordinate around the ferric iron during the reactions and resulting differences in rates of electron transfer (McAuliffe & Murray, 1972; Park & Imlay, 2003). In our system we predict that cysteine, being less structurally hindered, reacts more readily with tellurate compared to the bulkier tripeptide glutathione. Taken together with the observation that inactivation of GshB does not have a significant impact

on tellurate sensitivity, these results support a model where there are no direct intracellular interactions between tellurate and glutathione. Depletion of the glutathione pool occurs through a secondary process.

As tellurate may be reduced to a tellurite intermediate within the cells, we sought to further explore the mechanisms of interaction between tellurite and cellular thiols. It is known that tellurite exposure will lead to a loss of reduced glutathione in *E. coli* (Turner et al., 2001). However, it is unknown if the two can directly interact and if that reaction leads to the formation of Te(0). Similar to when tellurate was reacted with glutathione, we did not observe formation of large quantities of Te(0) in our reactors with tellurite and glutathione (**Figure 3.3C)**. This was supported by measurements of soluble tellurium in the reactors which showed no or only minor depletion of soluble tellurium following reaction with glutathione **(Figure 3.3A**). However, despite the fact that little Te(0) was formed, we measured significant depletion of glutathione in reactors that were prepared with glutathione:tellurite ratios up to and including a 4:1 ratio **(Figure 3.3B).** At higher ratios, excess glutathione remains. In contrast, cysteine reduces tellurite to Te(0) at a 4:1 ratio **(Figure 3.3A,B,D).** These findings are significant because glutathione is commonly reported in the literature to reduce tellurite to Te(0) (Chasteen et al., 2009). However, these findings rest on the observation of Turner et. al. (2001) that tellurite exposure results in a depletion of the intracellular glutathione pool of *E. coli* and the general observation of darkening of the medium of tellurite-exposed *E. coli* cells (Turner et al., 2001). We can use the well-established mechanism for selenite reduction by glutathione to make

predictions for tellurite reduction by glutathione in combination with our observations. Selenite reduction by glutathione produces several soluble reduced selenium compounds including selenodiglutathione, glutathiolselenol, and hydrogen selenide (Tarze et al., 2007). Our results support a model where tellurite reacts with glutathione to form tellurodiglutathione:

$$TeO_3^{2-} + 4GSH + 2H+ \rightarrow 2GS\text{-}Te\text{-}GS + 2GSSG + 3H_2O$$

With our data alone, it cannot be determined whether the tellurodiglutathione is further reduced to other intermediates. However, since excess glutathione remains unreacted when added at a ratio above 4:1 (glutathione:tellurite) it seems that, at least, *in vitro,* the reaction may end at a stable tellurodiglutathione intermediate. The increased toxicity of selenite in the presence of exogenous glutathione in yeast has been attributed to the toxicity of the selenide that forms from this reaction (Tarze et al., 2007). Additionally, selenodiglutathione formed from the reaction between selenite and glutathione has been shown to be toxic to mammalian cell lines (Wallenberg et al., 2014; Wu, Lanfear, & Harrison, 1995). Tellurite reduction by glutathione appears to form similar soluble intermediates that may also be toxic to the cells. Te(0) may eventually form from this reaction but this may be a kinetically-slow and possibly oxygen-dependent step. Indeed, we did visually observe slight darkening of some of our glutathione-tellurite reactors suggesting that some Te(0) is forming **(Figure 3.3C).**

Regarding our observation that tellurate exposure produces a significant decrease in the glutathione pool but only a modest decrease in the cysteine pool, our data suggests that tellurate and glutathione are non-reactive. This is

supported by the observation that a GshB knockout strain retains a similar level of tellurate sensitivity as the wild-type strain whereas the CysM knock-out strain is less sensitive than the wild-type strain. The data presented above supports a model where glutathione is consumed in order to maintain the cysteine pool within the cell following tellurate exposure **(Figure 3.7)**. Cysteine reduces tellurate with Te(0) as an end product. Glutathione may also be consumed in the reduction of the resulting tellurite if tellurite accumulates to sufficient quantities during tellurate reduction. As the reaction of glutathione with tellurite likely results in the formation of a soluble tellurodiglutathione species, this would also serve to remove glutathione from the recyclable intracellular pool of glutathione/glutathione disulfide. This loss of recyclable glutathione/glutathione disulfide may contribute to the toxicity of tellurium oxyanions in *E. coli* by removing a cellular buffer against oxidative stress. However, it is important to note that some have suggested that glutathione is not critical in ROS-defense in *E. coli* (Carmel-Harel & Storz, 2000). Glutathione, though, has been suggested to play a role in other cellular systems beyond thiol homeostasis and oxidative stress defense. In eukaryotic organisms, glutathione plays a role in iron metabolism through buffering the cytosolic ferrous iron pool and participation in iron-sulfur cluster maturation (Hider & Kong, 2011; Kumar et al., 2011). The loss of glutathione in this role in *E. coli* is interesting in light of the observation that tellurite exposure apparently results in a dysregulation of cellular iron and heme metabolism in *E. coli* (Morales et al., 2017).

In summary, we found that the interactions between thiols (cysteine and possibly other non-glutathione thiols) and tellurate contributes to the toxicity of tellurate in *E. coli*. This work is important for the general understanding of cellular interactions of tellurium oxyanions. Just as the extensive literature on tellurite toxicity informs this work, developing a better understanding of tellurate toxicity will likely further our knowledge of the toxicity of tellurite and possibly other tellurium-containing compounds. Indeed, we have demonstrated here for—to our knowledge—the first time that tellurite is reduced by glutathione to form a soluble tellurium species whereas previously it was assumed this reaction proceeded to a Te(0) end-product (Chasteen et al., 2009). These results are also important for experimental microbiology because it also identifies cystine as the main precipitating factor in the increased toxicity of tellurate on rich medium compared to minimal medium. The media background, alone, contributed to an approximately 60-fold difference in the MIC of tellurate in *E. coli*. This difference is important and needs to be considered when performing studies on tellurate (and tellurite) toxicity in *E. coli* and other organisms. The media background has the potential to control the effect of various genetic manipulations on tellurite/tellurate toxicity. For example, when a YdjN knockout strain is grown on minimal medium, it has the same MIC as the wild-type strain. In contrast, when the same strain was grown on rich medium or minimal medium with cystine supplemented, the MIC was much higher compared to the wild-type strain. Thus, this study lays the groundwork for further investigations into the interactions of tellurate with other environmentally-relevant microorganisms.

REFERENCES:

Apontoweil, P., & Berends, W. (1975). Glutathione biosynthesis in Escherichia coli K 12. Properties of the enzymes and regulation. *Biochimica et biophysica acta, 399*(1), 1-9.

Ba, L. A., Döring, M., Jamier, V., & Jacob, C. (2010). Tellurium: an element with great biological potency and potential. *Organic & Biomolecular Chemistry, 8*(19), 4203-4216. doi:10.1039/C0OB00086H

Baba, T., Ara, T., Hasegawa, M., Takai, Y., Okumura, Y., Baba, M., . . . Mori, H. (2006). Construction of Escherichia coli K-12 in-frame, single-gene knockout mutants: the Keio collection. *Molecular Systems Biology, 2*, 2006.0008-2006.0008. doi:10.1038/msb4100050

Bouroushian, M. (2010). Electrochemistry of the Chalcogens. In M. Bouroushian (Ed.), *Electrochemistry of Metal Chalcogenides* (pp. 57-75). Berlin, Heidelberg: Springer Berlin Heidelberg.

Butler, J. D., Levin, S. W., Facchiano, A., Miele, L., & Mukherjee, A. B. (1993). Amino acid composition and N-terminal sequence of purified Cystine Binding Protein of Escherichia coli. *Life Sciences, 52*(14), 1209-1215. doi:https://doi.org/10.1016/0024-3205(93)90103-A

Carmel-Harel, O., & Storz, G. (2000). Roles of the Glutathione- and Thioredoxin-Dependent Reduction Systems in the Escherichia Coli and Saccharomyces Cerevisiae Responses to Oxidative Stress. *Annual Review of Microbiology, 54*(1), 439-461. doi:10.1146/annurev.micro.54.1.439

Chasteen, T. G., Fuentes, D. E., Tantaleán, J. C., & Vásquez, C. C. (2009). Tellurite: history, oxidative stress, and molecular mechanisms of resistance. *FEMS Microbiology Reviews, 33*(4), 820-832. doi:10.1111/j.1574-6976.2009.00177.x

Chonoles Imlay, K. R., Korshunov, S., & Imlay, J. A. (2015). Physiological Roles and Adverse Effects of the Two Cystine Importers of Escherichia coli. *Journal of Bacteriology, 197*(23), 3629. doi:10.1128/JB.00277-15

Claus, M. T., Zocher, G. E., Maier, T. H. P., & Schulz, G. E. (2005). Structure of the O-Acetylserine Sulfhydrylase Isoenzyme CysM from Escherichia coli. *Biochemistry, 44*(24), 8620-8626. doi:10.1021/bi050485+

Díaz-Vásquez, W. A., Abarca-Lagunas, M. J., Arenas, F. A., Pinto, C. A., Cornejo, F. A., Wansapura, P. T., . . . Vásquez, C. C. (2014). Tellurite reduction by Escherichia coli NDH-II dehydrogenase results in superoxide production

in membranes of toxicant-exposed cells. *BioMetals, 27*(2), 237-246. doi:10.1007/s10534-013-9701-8

Dupont, C. L., & Ahner, B. A. (2005). Effects of copper, cadmium, and zinc on the production and exudation of thiols by Emiliania huxleyi. *Limnology and Oceanography, 50*(2), 508-515. doi:10.4319/lo.2005.50.2.0508

Fahey, R. C., Brown, W. C., Adams, W. B., & Worsham, M. B. (1978). Occurrence of glutathione in bacteria. *Journal of Bacteriology, 133*(3), 1126-1129. Retrieved from https://jb.asm.org/content/jb/133/3/1126.full.pdf

Fahey, R. C., & Newton, G. L. (1988). Determination of low molecular weight thiols using monobromobimane fluorescent labeling and high-performance liquid chromatography - NASA-CR-182932. In.

Goff, J., & Yee, N. (2017). Tellurate enters Escherichia coli K-12 cells via the SulT-type sulfate transporter CysPUWA. *FEMS Microbiology Letters, 364*(24). doi:10.1093/femsle/fnx241

Hider, R. C., & Kong, X. L. (2011). Glutathione: a key component of the cytoplasmic labile iron pool. *BioMetals, 24*(6), 1179-1187. doi:10.1007/s10534-011-9476-8

Jones, D. P., Carlson, J. L., Mody, V. C., Cai, J., Lynn, M. J., & Sternberg, P. (2000). Redox state of glutathione in human plasma. *Free Radical Biology and Medicine, 28*(4), 625-635. doi:https://doi.org/10.1016/S0891-5849(99)00275-0

Kessi, J., & Hanselmann, K. W. (2004). Similarities between the Abiotic Reduction of Selenite with Glutathione and the Dissimilatory Reaction Mediated by Rhodospirillum rubrum and Escherichia coli. *Journal of Biological Chemistry, 279*(49), 50662-50669. doi:10.1074/jbc.M405887200

Kosower, N. S., Kosower, E. M., Wertheim, B., & Correa, W. S. (1969). Diamide, a new reagent for the intracellular oxidation of glutathione to the disulfide. *Biochemical and Biophysical Research Communications, 37*(4), 593-596. doi:https://doi.org/10.1016/0006-291X(69)90850-X

Kumar, C., Igbaria, A., D'Autreaux, B., Planson, A.-G., Junot, C., Godat, E., . . . Toledano, M. B. (2011). Glutathione revisited: a vital function in iron metabolism and ancillary role in thiol-redox control. *The EMBO Journal, 30*(10), 2044-2056. doi:10.1038/emboj.2011.105

Lloyd, J. R., & Lovley, D. R. (2001). Microbial detoxification of metals and radionuclides. *Current opinion in biotechnology, 12*(3), 248-253. doi:https://doi.org/10.1016/S0958-1669(00)00207-X

McAuliffe, C. A., & Murray, S. G. (1972). Metal complexes of sulphur-containing amino acids. *Inorganica Chimica Acta Reviews, 6*, 103-121. doi:https://doi.org/10.1016/0073-8085(72)80013-5

Moore, M. D., & Kaplan, S. (1992). Identification of intrinsic high-level resistance to rare-earth oxides and oxyanions in members of the class Proteobacteria: characterization of tellurite, selenite, and rhodium sesquioxide reduction in Rhodobacter sphaeroides. *Journal of Bacteriology, 174*(5), 1505-1514. doi:10.1128/jb.174.5.1505-1514.1992

Morales, E. H., Pinto, C. A., Luraschi, R., Muñoz-Villagrán, C. M., Cornejo, F. A., Simpkins, S. W., . . . Vásquez, C. C. (2017). Accumulation of heme biosynthetic intermediates contributes to the antibacterial action of the metalloid tellurite. *Nature Communications, 8*(1), 15320. doi:10.1038/ncomms15320

Park, S., & Imlay, J. A. (2003). High Levels of Intracellular Cysteine Promote Oxidative DNA Damage by Driving the Fenton Reaction. *Journal of Bacteriology, 185*(6), 1942-1950. doi:10.1128/jb.185.6.1942-1950.2003

Pérez, J. M., Calderón, I. L., Arenas, F. A., Fuentes, D. E., Pradenas, G. A., Fuentes, E. L., . . . Vásquez, C. C. (2007). Bacterial Toxicity of Potassium Tellurite: Unveiling an Ancient Enigma. *PLOS ONE, 2*(2), e211. doi:10.1371/journal.pone.0000211

Pöther, D.-C., Liebeke, M., Hochgräfe, F., Antelmann, H., Becher, D., Lalk, M., . . . Hecker, M. (2009). Diamide Triggers Mainly S Thiolations in the Cytoplasmic Proteomes of Bacillus subtilis and Staphylococcus aureus. *Journal of Bacteriology, 191*(24), 7520-7530. doi:10.1128/jb.00937-09

Scala, J., & Williams, H. H. (1963). A comparison of selenite and tellurite toxicity in Escherichia coli. *Arch Biochem Biophys, 101*, 319-324. doi:10.1016/s0003-9861(63)80019-3

Smith, D. A., Sessions, A. L., Dawson, K. S., Dalleska, N., & Orphan, V. J. (2017). Rapid quantification and isotopic analysis of dissolved sulfur species. *Rapid Commun Mass Spectrom, 31*(9), 791-803. doi:10.1002/rcm.7846

Suzuki, H., Hashimoto, W., & Kumagai, H. (1993). Escherichia coli K-12 can utilize an exogenous gamma-glutamyl peptide as an amino acid source, for which gamma-glutamyltranspeptidase is essential. *Journal of Bacteriology, 175*(18), 6038. doi:10.1128/jb.175.18.6038-6040.1993

Suzuki, H., Kamatani, S., Kim, E.-S., & Kumagai, H. (2001). Aminopeptidases A, B, and N and Dipeptidase D Are the Four Cysteinylglycinases of Escherichia coli K-12. *Journal of Bacteriology, 183*(4), 1489-1490. doi:10.1128/jb.183.4.1489-1490.2001

Tantaleán, J. C., Araya, M. A., Saavedra, C. P., Fuentes, D. E., Pérez, J. M., Calderón, I. L., . . . Vásquez, C. C. (2003). The Geobacillus stearothermophilus V iscS gene, encoding cysteine desulfurase, confers resistance to potassium tellurite in Escherichia coli K-12. *Journal of Bacteriology, 185*(19), 5831-5837.

Tarze, A., Dauplais, M., Grigoras, I., Lazard, M., Ha-Duong, N. T., Barbier, F., . . . Plateau, P. (2007). Extracellular production of hydrogen selenide accounts for thiol-assisted toxicity of selenite against Saccharomyces cerevisiae. *J Biol Chem, 282*(12), 8759-8767. doi:10.1074/jbc.M610078200

Theisen, J., Zylstra, G. J., & Yee, N. (2013). Genetic Evidence for a Molybdopterin-Containing Tellurate Reductase. *Applied and Environmental Microbiology, 79*(10), 3171-3175. doi:10.1128/aem.03996-12

Turner, R. J., Aharonowitz, Y., Weiner, J. H., & Taylor, D. E. (2001). Glutathione is a target in tellurite toxicity and is protected by tellurite resistance determinants in Escherichia coli. *Canadian Journal of Microbiology, 47*(1), 33-40.

Turner, R. J., Weiner, J. H., & Taylor, D. E. (1999). Tellurite-mediated thiol oxidation in Escherichia coli. *Microbiology, 145*(9), 2549-2557. doi:doi:10.1099/00221287-145-9-2549

Vatansever, F., de Melo, W. C. M. A., Avci, P., Vecchio, D., Sadasivam, M., Gupta, A., . . . Hamblin, M. R. (2013). Antimicrobial strategies centered around reactive oxygen species – bactericidal antibiotics, photodynamic therapy, and beyond. *FEMS Microbiology Reviews, 37*(6), 955-989. doi:10.1111/1574-6976.12026

Vrionis, H. A., Wang, S., Haslam, B., & Turner, R. J. (2015). Selenite Protection of Tellurite Toxicity Toward Escherichia coli. *Frontiers in Molecular Biosciences, 2*, 69. doi:10.3389/fmolb.2015.00069

Wallenberg, M., Misra, S., Wasik, A. M., Marzano, C., Björnstedt, M., Gandin, V., & Fernandes, A. P. (2014). Selenium induces a multi-targeted cell death process in addition to ROS formation. *Journal of cellular and molecular medicine, 18*(4), 671-684. doi:10.1111/jcmm.12214

Wheldrake, J. F. (1967). Intracellular concentration of cysteine in Escherichia coli and its relation to repression of the sulphate-activating enzymes. *The Biochemical journal, 105*(2), 697-699. doi:10.1042/bj1050697

Winterbourn, C. C., & Metodiewa, D. (1994). The Reaction of Superoxide with Reduced Glutathione. *Archives of Biochemistry and Biophysics, 314*(2), 284-290. doi:https://doi.org/10.1006/abbi.1994.1444

Wu, L., Lanfear, J., & Harrison, P. R. (1995). The selenium metabolite selenodiglutathione induces cell death by a mechanism distinct from H2O2 toxicity. *Carcinogenesis, 16*(7), 1579-1584. doi:10.1093/carcin/16.7.1579

Yurkov, V., Jappe, J., & Vermeglio, A. (1996). Tellurite resistance and reduction by obligately aerobic photosynthetic bacteria. *Applied and Environmental Microbiology, 62*(11), 4195-4198. Retrieved from https://www.ncbi.nlm.nih.gov/pubmed/16535446

FIGURES:

Table 3.1. Tellurate MICs on different types of media

Media	**MIC (mM)**
LB #1*	0.015
LB #2**	0.015
M9 + 0.4% Glucose	1
M9 + 1% NaCl	1
M9 + 0.4% Glucose + 0.5% yeast extract	0.3
M9 + 0.4% Glucose + 1% tryptone	0.3
M9 + 0.4% Glucose + 0.5% yeast extract + 1% tryptone	0.4
M9 + 0.4% Glucose + 0.3% casamino acids	0.2
Amino Acids (M9 + 0.4% Glucose + AA)	
Glutamate	0.7
Methionine	1
Arginine	1
Leucine	>1
Isoleucine	>1
Histidine	>1
Tryptophan	>1
Threonine	>1.1
Cystine	0.05

*LB mix from

**LB prepared in lab using yeast extract and tryptone from BD

Table 3.2. MICs for tellurite, selenate, and selenite

	Tellurite MIC (mM)	**Selenite MIC (mM)**	**Selenate MIC (mM)**
LB	0.005	>100	>100
M9 + 0.4% Glucose	0.3	0.5	0.07
M9 + 0.4% Glucose + cystine (0.04 g/L)	0.005	100	>100

Table 3.3. Tellurate MICs for cystine transporter knock-out strains

	K-12 Wild-type	ΔydjN	ΔfliY
LB	0.015	0.1	0.02
M9 + 0.4% Glucose	1	1	1.1
M9 + 0.4% Glucose + cystine (0.04 g/L)	0.050	0.6	0.05

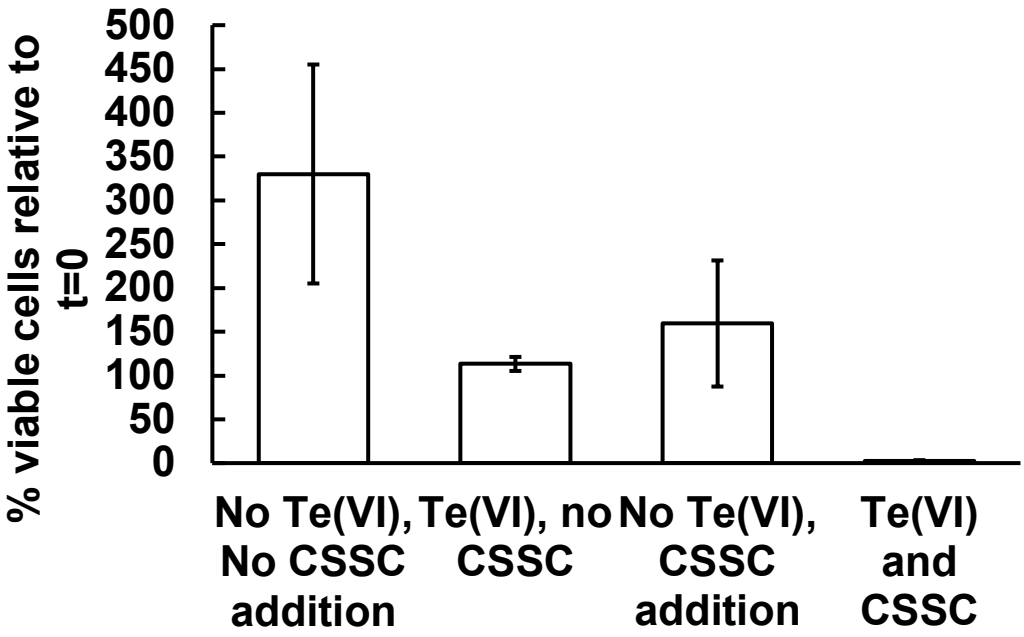

Figure 3.1. *E. coli* cultures pre-grown with Te(VI) and spiked with cystine (CSSC). *E. coli* was grown on M9 minimal medium with glucose as a carbon source. In half the cultures, 0.5 mM of tellurate was added initially and in the other half a Milli-Q water blank was added. Cultures were grown until they reached a density of ~OD_{600} = 0.1. A sample was collected at this point for dilution and plating to quantify the number of viable cells in the culture. Immediately after, half the cultures were spiked with cystine (0.04 g/L) and the other half were spiked with a Milli-Q water blank. Cultures were grown an additional 30 minutes and then a second sample was collected for dilution and plating. The numbers here represent the 30 minute counts normalized against the 0 minute counts. Each bar represents the average of triplicate replicates. Standard error bars are shown.

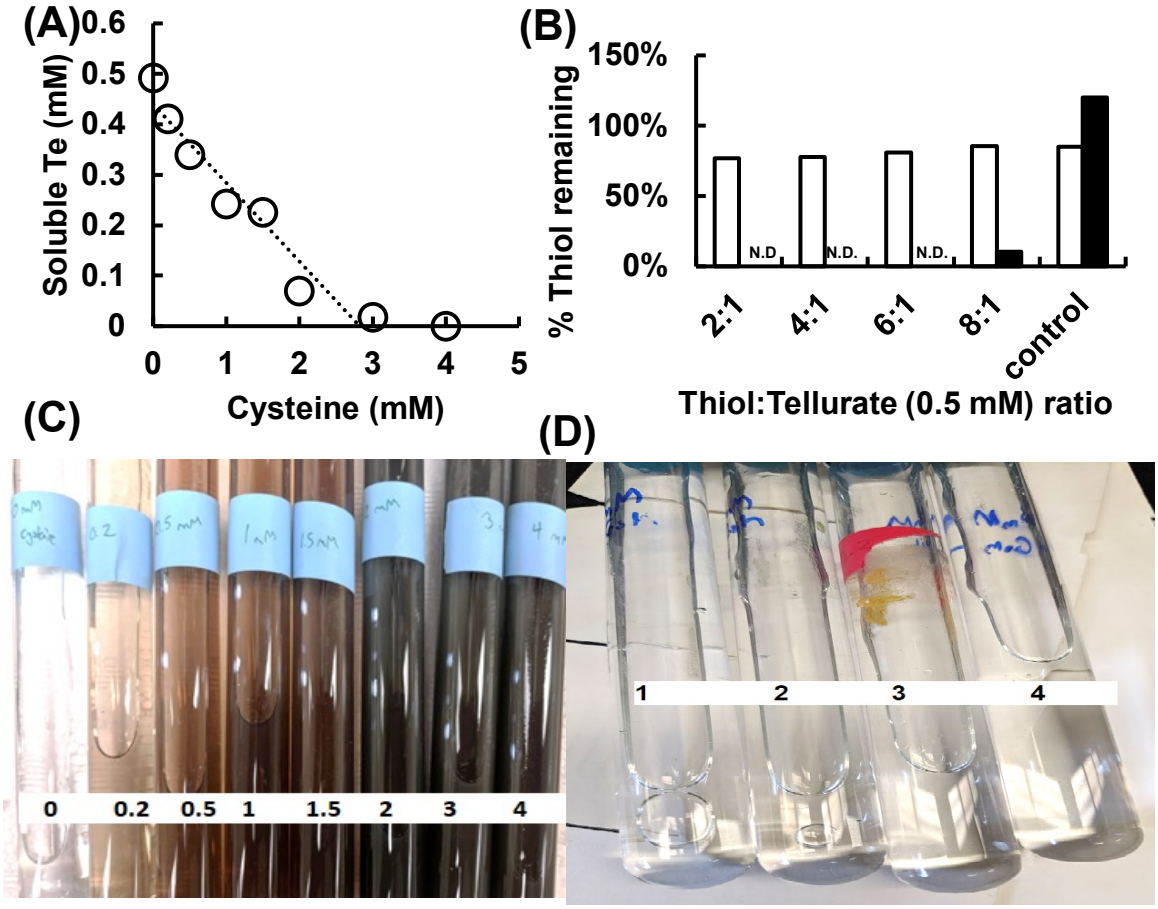

Figure 3.2. Reactions of tellurate with cysteine and glutathione *in vitro*. (A) Soluble tellurium remaining following 24 hour reaction of 0.5 mM tellurate with varying concentrations (0-4 mM) of cysteine. A linear regression line is fit to the data points from 0-3 mM of cysteine (R^2=0.94). (B) % thiols remaining in the reactors. The y-axis shows the starting ratio of thiol (either glutathione or cysteine) to tellurate (0.5 mM). The white bars represent glutathione and the black bars represent cysteine. (C) Image of reactors showing increased darkening of the medium with increasing cysteine concentrations. Cysteine concentrations in each reactor are given in the photo and are reported in

mM. (D) Image of reactors containing glutathione and tellurate showing the darkening of the solution. Glutathione concentrations in each reactor are given in the photo and are reported in mM.

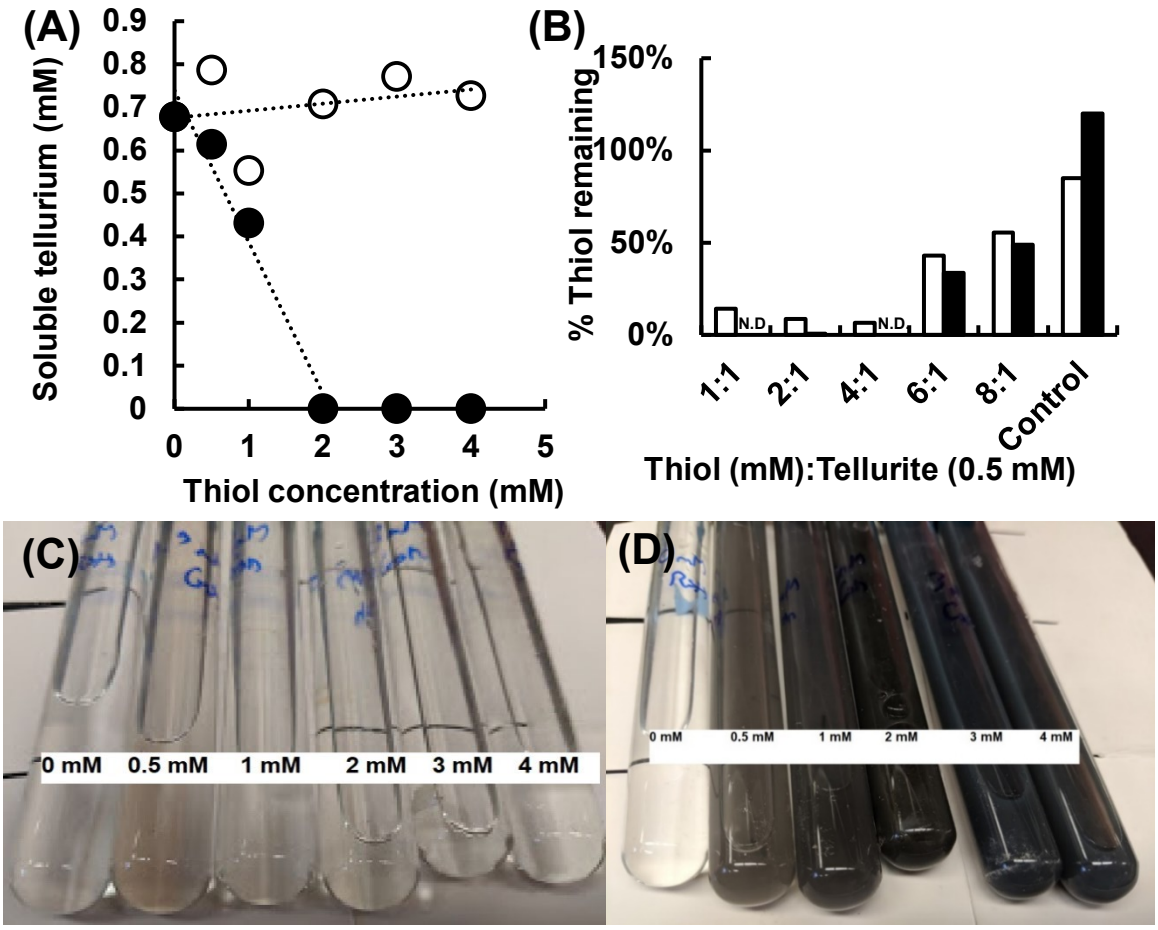

Figure 3.3. Reactions of tellurite with cysteine and glutathione *in vitro*. Tellurite (0.5 mM) was reacted with cysteine or glutathione at varying concentrations (0-4 mM) under anaerobic conditions to prevent O_2-mediated oxidation of thiols. After 24 hours, reactors were sampled and analyzed for total dissolved tellurium species (A) in the presence of cysteine (black circles) or glutathione (unfilled circles) and concentrations of cysteine (black bars) and glutathione (unfilled bars) (B). The x-axis of panel B represents the starting ratio of thiol to tellurite in the reactors. (C) The reactors with glutathione added. Starting cysteine concentrations are indicated. (D) The reactors with cysteine added showing the darkening of the solution. Starting glutathione concentrations are indicated.

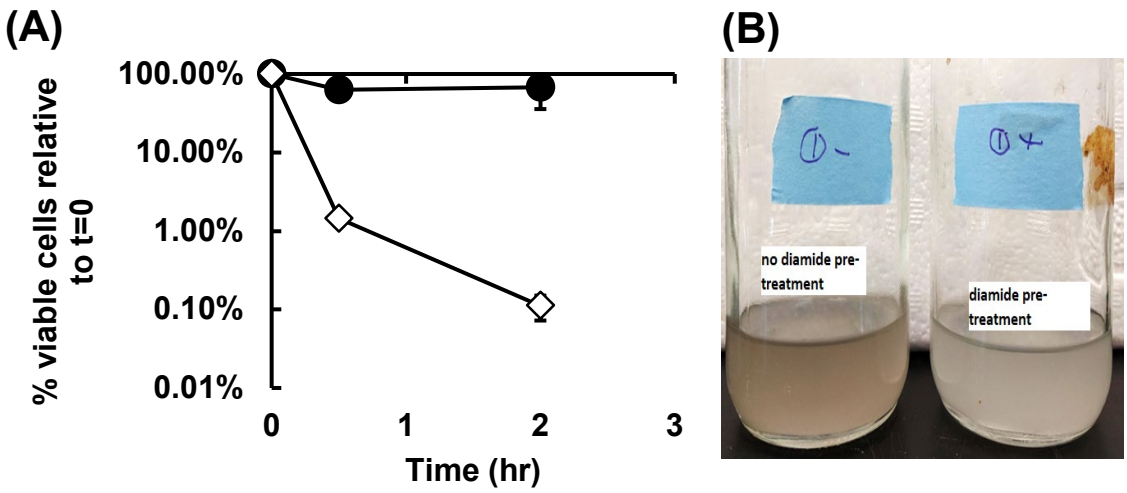

Figure 3.4. Effect of diamide pre-treatment on cell viability following tellurate exposure. (A) The number of viable cells in the cultures was determined at several time points using a spot-plating method. Cell numbers were normalized against cell numbers at 0 hours (immediately prior to tellurate exposure). Cells were either pre-treated with 1 mM diamide (filled circles) or were not pre-treated (open diamonds) and were grown in M9 medium until they reached an optical density of ~0.1. At that point, cells were spiked with 0.5 mM tellurate. Points on the graph are plotted on a log-10 scale and are the averages of three replicates. Standard error bars are shown. (B) Darkening of cultures caused by Te(0) formation following treatment with tellurate. The culture on the left was pre-treated with diamide prior to tellurate exposure. The culture on the right was not pre-treated.

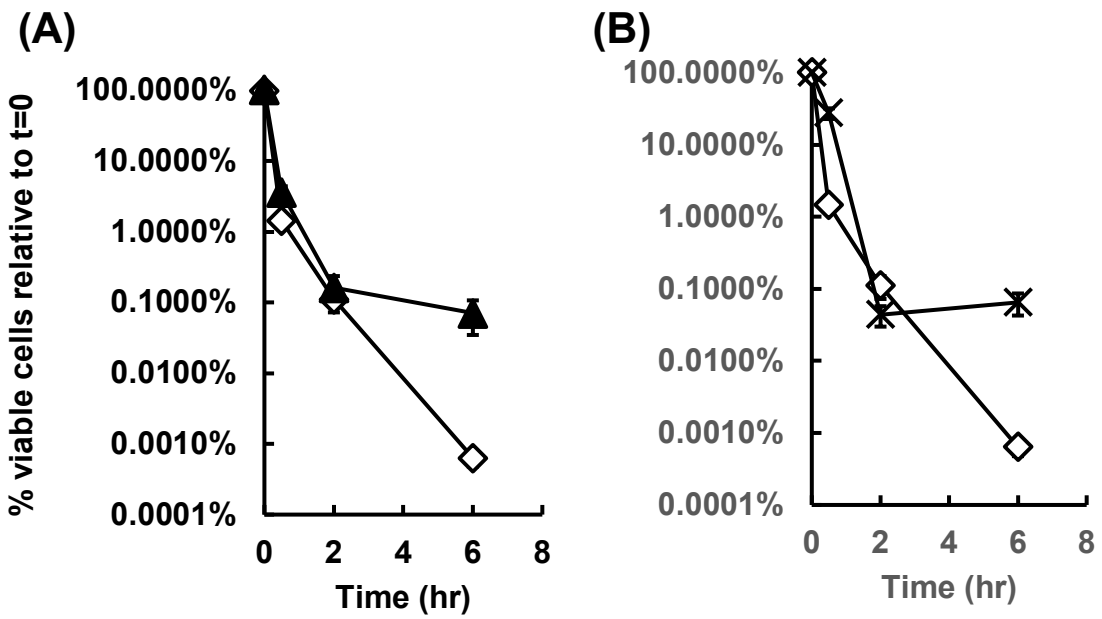

Figure 3.5. Tellurate toxicity in thiol biosynthesis pathway mutants. The number of viable cells in the cultures was determined at several time points using a spot-plating method. Cell numbers were normalized against cell numbers at 0 hours (immediately prior to tellurate exposure). All strains were grown on M9 medium until they reached an optical density of ~0.1. At that point, cells were spiked with 0.5 mM tellurate. Points on the graph are plotted on a log-10 scale and are the averages of three replicates. Standard error bars are shown. (A) *ΔgshB* knock-out mutant (closed triangles) and the wild-type strain (open diamonds). (B) *ΔcysM* knock-out mutant (crosses) and the wild-type strain (open diamonds).

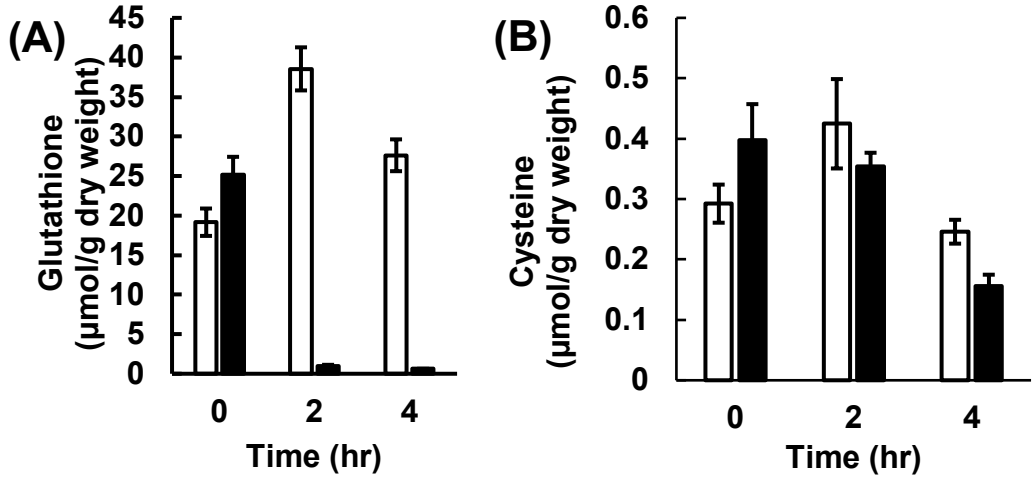

Figure 3.6. Intracellular thiol concentrations in cells grown with and without tellurate. Cells were grown in LB. Intracellular extracts were derivatized with mBBr, separated by HPLC. Glutathione (A) and cysteine (B) were quantified using fluorescence detection. White bars represent the average of triplicate cultures of cells grown without tellurate. Black bars represent the average of triplicate cultures grown with tellurate. Standard error bars are shown.

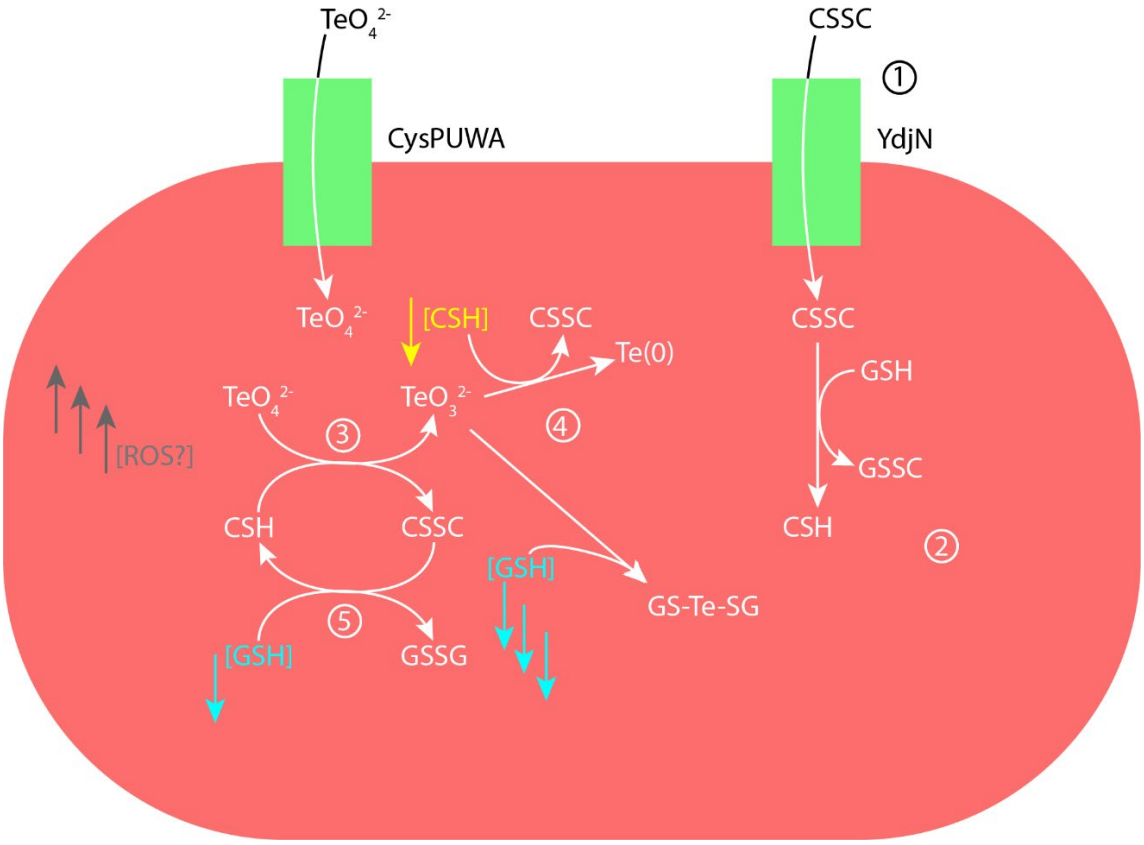

Figure 3.7. Proposed schematic for reactions of tellurate with the intracellular thiols of *E. coli* when transferred to cystine-rich medium. (1) Cystine (CSSC) is transported into the cells by the transporter YdjN in response to the shift from low- to high-cystine conditions. (2) In a glutathione-dependent step, cystine is reduced to cysteine (CSH). (3) Simultaneously tellurate (TeO_4^{2-}) is transported into the cell and reacts with intracellular cysteine residues (and possibly other thiols) and is reduced to tellurite (TeO_3^{2-}). (4) Tellurite is further reduced by cysteine to Te(0) or by glutathione (GSH) to a predicted tellurodiglutathione (GS-Te-GS) intermediate, depleting the glutathione pool (5) Glutathione may also be oxidized to glutathione disulfide (GSSG) in order to

maintain the intracellular cysteine pool and also in its activity as a buffer against ROS damage (not shown).

CHAPTER 4

ROLE OF EXTRACELLULAR REACTIVE SULFUR METABOLITES IN MICROBIALLY-MEDIATED SE(0) DISSOLUTION

Published in Geobiology as "Role of extracellular reactive sulfur metabolites on microbial Se(0) dissolution" (*Geobiology,* 2019, 17(3): 320-329)

ABSTRACT:

The dissolution of elemental selenium [Se(0)] during chemical weathering is an important step in the global selenium cycle. While microorganisms have been shown to play a key role in selenium dissolution in soils, the mechanisms of microbial selenium solubilization are poorly understood. In this study, we isolated a *Bacillus* species, designated as strain JG17, that exhibited the ability to dissolve Se(0) under oxic conditions and neutral pH. Growth of JG17 in a defined medium resulted in the production and accumulation of extracellular compounds that mediated Se(0) dissolution. Analysis of the spent medium revealed the presence of extracellular sulfite, sulfide, and thiosulfate. Abiotic Se(0) dissolution experiments with concentrations of sulfite, sulfide, and thiosulfate relevant to our system showed similar extents of selenium solubilization as the spent medium. Together, these results indicate that the

solubilization of Se(0) by JG17 occurs via the release of extracellular inorganic sulfur compounds followed by chemical dissolution of Se(0) by the reactive sulfur metabolites. Our findings suggest that production of reactive sulfur metabolites by soil microorganisms and the formation of soluble selenosulfur complexes can promote selenium mobilization during chemical weathering.

INTRODUCTION:

Microorganisms are major drivers of the selenium (Se) biogeochemical cycle (Stolz, Basu, Santini, & Oremland, 2006; Stüeken et al., 2015). The biological reduction of soluble selenite [Se(IV) as SeO_3^{2-}] and selenate [Se(VI) as SeO_4^{2-}] to poorly soluble elemental selenium [Se(0)] is catalyzed by bacteria (Nancharaiah & Lens, 2015; Oremland et al., 1989), archaea (Huber, Sacher, Vollmann, Huber, & Rose, 2000), and fungi (Rosenfeld, Kenyon, James, & Santelli, 2017). The oxidation of selenium is also known to be mediated by microorganisms, however very little is known about the microbial pathways that control this process (Dowdle & Oremland, 1998; Losi & Frankenberger, 1998; Sarathchandra & Watkinson, 1981). In the global selenium cycle, Se(0)-oxidizing microbial communities are generally thought to play a central role in the dissolution of selenium-bearing minerals and the production of soluble selenium oxyanions that are transferred from continental to marine reservoirs (Haygarth, 1994; Nriagu, 1989). Furthermore, the transformations of selenium during continental weathering and transport to marine depositional settings have been used to infer

the redox state of the early Earth and oxygenation of the Archean oceans (Stueken, 2017; Stueken, Buick, & Anbar, 2015). Thus, an accurate understanding of how microorganisms affect selenium mobilization during chemical weathering has important implications for the development of reliable models that describe modern and ancient selenium biogeochemical cycles.

Sarathchandra and Watkinson (1981) reported the isolation of a heterotrophic *Bacillus megaterium* strain from a seleniferous soil that was capable of oxidizing Se(0) to Se(IV) during aerobic growth. Later, Losi and Frankenberger (1998) showed that Se(0)-solubilization and oxidation in natural soils is a microbially-driven process mediated by both heterotrophic and autotrophic communities. At the same time, Dowdle and Oremland (1998) demonstrated that Se(0) oxidation by the chemoheterotrophic bacteria *Thiobacillus* sp. ASN-1 and *Leptothrix* sp. MnB1 and by oxic soil slurries resulted in the formation of a mixture of Se(IV) and Se(VI). It was speculated that microbial Se(0)-oxidation may occur (1) by an unknown mechanism in heterotrophic cultures or (2) by enzymatic oxidation mediated via sulfur-oxidizing enzymes capable of non-specifically oxidizing Se(0) in sulfur-oxidizing microorganisms (Dowdle & Oremland, 1998). To date, the mechanisms controlling this process remain unknown.

Se(0) is known to react with various inorganic sulfur compounds [e.g. sulfite (SO_3^{2-}), thiosulfate ($S_2O_3^{2-}$), and sulfide (S^{2-})] to form aqueous selenosulfur complexes that increase selenium solubility (Ball & Milne, 1995; Rahim & Milne, 1996; Weres, Jaouni, & Tsao, 1989). Above pH 7, sulfide reacts with Se(0) to form

selenium sulfide (SeS^{2-}) in a manner similar to the reaction of sulfide with elemental sulfur to form polysulfide anions (Weres et al., 1989):

(1) $$Se_n + HS^- + OH^- \rightarrow Se_{n-1} + SeS^{2-} + H_2O$$

Additionally, Se(0) has been demonstrated to dissolve at pH 7 in the presence of sulfite through the formation of selenosulfate ($SeSO_3^{2-}$) in a reaction analogous to the formation of thiosulfate from elemental sulfur, according to the reaction (Ball & Milne, 1995; Kulp & Pratt, 2004; Velinsky & Cutter, 1990):

(2) $$Se + SO_3^{2-} \leftrightarrow SeSO_3^{2-}$$

Finally, Se(0) can react with thiosulfate leading to the formation of selenothiosulfate ($SeS_2O_3^{2-}$), following the reaction (Rahim & Milne, 1996):

(3) $$Se + S_2O_3^{2-} \leftrightarrow SeS_2O_3^{2-}$$

Therefore, reactions with sulfide, sulfite, and thiosulfate can strongly affect selenium dissolution, and impact the mobility of selenium in soil and sedimentary environments.

Reactive sulfur metabolites are produced by microorganisms but their role in microbial Se(0) solubilization is poorly understood. While it is well established that significant amounts of sulfide are produced by anaerobic sulfate-respiring bacteria (Muyzer & Stams, 2008), little is known about the production of extracellular sulfide and other reactive sulfur metabolites by aerobic bacteria. Many eukaryotic yeasts have been shown to produce extracellular sulfide and sulfite as a by-product of their central sulfur metabolism (Donalies & Stahl, 2002; Huang, Roncoroni, & Gardner, 2014). Given the homology between the pathways

for sulfate assimilation in yeasts and bacteria, it is possible that aerobic bacteria may also be capable of producing similar extracellular sulfur metabolites (Thomas & Surdin-Kerjan, 1997). Currently, the production of reactive sulfur metabolites by aerobic bacteria and their interactions with Se(0) have not been investigated in detail.

In this study, we examined the role of extracellular metabolites in microbial Se(0) dissolution. The objective was to isolate a Se(0)-solubilizing bacterial strain from seleniferous soil and to use the bacterial isolate to characterize the mechanism of microbially-mediated Se(0)-dissolution. We tested the hypothesis that Se(0)-solubilizing bacteria produce reactive sulfur metabolites, and that extracellular reactions between sulfide, sulfite, and thiosulfate with Se(0) increase selenium solubility. The results of this study indicate that the microbial production of extracellular sulfur metabolites can affect the chemical weathering of selenium and the formation of mobile aqueous selenium complexes.

MATERIALS AND METHODS:

Isolation of a Se(0)-solubilizing *Bacillus* strain

Because a *Bacillus* species has previously been reported to dissolve Se(0) (Sarathchandra & Watkinson, 1981), we isolated *Bacillus* species from seleniferous soil collected at Punjab, India (Schilling, Johnson, Dhillon, & Mason, 2015). Approximately one gram of dry soil was added to test tubes containing a

mineral salts medium with glucose (0.4% w/v) as the carbon source. The mineral salts medium contained (per liter): 4.0 g Na_2HPO_4, 1.5 g KH_2PO_4, 1.0 g NH_4Cl, 0.2 g $MgSO_4 \cdot 7H_2O$, 15 mg $FeSO_4 \cdot 7H_2O$, 3.0 g NaCl, 1.0 mg $NaSeO_4$, 8.0 mg $FeCl_3$, 0.1 g yeast extract, 0.1 mL of a metal supplement solution, and 1.0 mL of a trace elements solution. The trace elements solution contained (per liter): 2.8 g H_3BO_3, 0.24 g $ZnSO_4 \cdot 7H_2O$, 0.75 g $Na_2MoO_4 \cdot 2H_2O$, 0.042 g $CuSO_4 \cdot 5H_2O$, and 0.17 g $MnSO_4 \cdot H_2O$. The metal supplement contained (per 100 mL): 1.41 g $CoSO_4 \cdot 7H_2O$, and $NiCl_2 \cdot 6H_2O$. The pH was adjusted to 7.0 with 10 M NaOH.

After 4 days of aerobic growth at room temperature, the enrichment culture was incubated at 80°C for 10 minutes to select for spore-forming organisms and then spread onto agar plates to isolate viable cells. Colonies which exhibited visually unique morphologies were picked and repeatedly streaked on lysogeny broth (LB) plates to obtain cultural purity. Individual colonies were then selected for further characterization, including phylogenetic determination and their ability to solubilize Se(0), as described below.

The isolates were screened for their ability to dissolve Se(0). First, a stock solution of red Se(0) was synthesized by chemical reduction of Se(IV) using a method modified from Pettine et. al. (2013). Briefly, a liter of deoxygenated 30 mM Na_2SeO_3 was mixed with 200 mL of 0.4 M ascorbic acid, bubbled with N_2 gas for 30 minutes, capped, and then stirred for 90 minutes. The appearance of red coloration in the mixture indicated the formation of Se(0). The suspension was centrifuged at 5,000 rpm (Sorvall LegendT) for 5 minutes and the supernatant was decanted followed by three washing steps according to the protocol of

Oremland et al. (2004). The washing steps included: (1) 70% ethanol, (2) 10 mM Na_2HPO_4 and (3) double deionized H_2O. For each step, one of the washing solutions was added to the Se(0) suspension, vortexed, sonicated in a water bath for 5 minutes, centrifuged again, and the supernatant discarded. The final washing step was repeated until dissolved selenium was no longer measurable in subsamples of the Se(0) preparation. After the last washing step, the Se(0) particles were re-suspended with 500 mL of sterilized double deionized H_2O. Atomic force microscopy images indicated that the spherical globules of selenium were aggregated into clusters of approximately 800 nm in size. The particles were determined to have a BET specific surface area of 8.93 ± 0.08 m^2/g.

The bacterial isolates were screened for their ability to dissolve the synthesized Se(0). Individual isolates were streaked on an agar plate and grown aerobically for 24 hours. When single colonies were visible, a few drops of red Se(0) suspension was added to the agar plates. The agar plates were incubated at 30°C and monitored for the next several days. Isolate strains capable of dissolving Se(0) were identified by the gradual clearance of the red Se(0) particles immediately surrounding the colonies

The isolates were grown overnight aerobically in LB broth for genomic DNA extraction and 16S rRNA gene analysis. DNA extraction was performed using the PowerSoil® DNA Isolation Kit (MO BIO). PCR amplification of the 16S rRNA gene was performed using the universal 27F (AGAGTTTGATCMTGGCTCAG) and 1492R (TACGGYTACCTTGTTACGACTT) primers. PCR products were purified using the UltraClean PCR Clean-Up Kit

(MO BIO). Sanger sequencing of the PCR products was performed by Genewiz (South Plainfield, NJ). BLAST was used to search for annotated sequences with high sequence homology to the 16S sequences to determine phylogeny. Partial 16S rRNA gene sequences of isolates and representative *Bacillus* species were aligned with MUSCLE. Alignments were trimmed to aligned regions and a phylogenetic tree was constructed with MEGA 7 using the Maximum Likelihood Method with 100 bootstraps.

Se(0) dissolution experiments

An isolate that solubilized Se(0) was selected for further characterization. Cultures of this isolate were grown in G1 medium supplemented with 25 mM sucrose as the carbon source. G1 medium contained (per liter): 20.9 g MOPS, 0.1 g NaCl, 0.182 g NH_4Cl, 0.06 g $CaCl_2 \cdot 2H_2O$, 0.03 g KH_2PO_4, 0.2 g $MgSO_4 \cdot 7H_2O$, and 1 mL SL10 trace elements solution (Widdel & Pfennig, 1981). The sulfate concentration was approximately 0.8 mM. The pH of the medium was adjusted to 7.0 with 10 M NaOH. All cultures were grown at 30°C under aerobic conditions in a shaking incubator.

Se(0) dissolution experiments with whole cells were conducted in triplicate with an overnight inoculum diluted into fresh G1 media containing approximately 1.5 mg/L of Se(0). The amount of Se(0) was added in excess such as over 95% of the selenium was expected to remain in the solid phase throughout in the incubation. All experiments were conducted in the dark at room temperature. At periodic intervals, the culture was sampled to determine

the concentration of dissolved selenium. An abiotic control experiment was performed using sterile medium under identical conditions but without any added cell suspensions. For both the active and control experiments, samples were filtered through 0.2 μm nylon membrane syringe filters, acidified with 2% (v/v) HNO_3, and total soluble selenium was measured with an iCAP 7400 ICP-OES Analyzer (Thermo Scientific) at a detection wavelength of 196.09 nm.

Experiments with cell-free filtrates were conducted to determine the role of extracellular metabolites in selenium solubilization. To obtain cell-free filtrates, triplicate cultures were grown on G1 media in the absence of Se(0). Cells were grown to the desired growth phase with optical density monitored at 600 nm on a Shimadzu Bio Mini Spectrophotometer. Cultures were then filtered through 0.45 μm nylon membrane filters. To determine the kinetics of selenium solubilization, experiments were conducted with filtrates obtained from a late log phase culture. All selenium dissolution experiments were performed by adding an aliquot of Se(0) particles to the cell-free filtrates at a final Se(0) concentration of 1.5 mg/L. The formation of soluble selenium was monitored over the course of 6 hours and total dissolved selenium was determined using the method described above. Additionally, several experiments were conducted to characterize the reactive molecules in the filtrates. Cell-free filtrates that were prepared as described above were obtained from stationary phase cultures. The involvement of reactive oxygen species (ROS) in the extracellular dissolution of Se(0) was examined by amending filtrates with 5 μM of the ROS scavenger superoxide dismutase (SOD) or 1 mM of the hydroxyl radical (OH·) scavenger dimethyl

sulfoxide (DMSO) prior to reaction with Se(0). Control experiments were conducted with sterile medium without the addition of cells or filtrates. To determine the thermal stability of Se(0)-solubilizing molecules, filtrates were heated in a hot water bath for 1 hour at 80°C then cooled to room temperature prior to reaction with Se(0) for six hours.

To quantify the solubility of Se(0) in the presence of inorganic sulfur compounds, batch dissolution experiments were conducted with sulfite, sulfide, and thiosulfate at different concentrations (0.5 to 2.0 μM). A known amount of each sulfur compound was mixed with approximately 1.5 mg/L Se(0) in an aqueous solution adjusted to pH 7.0 with 0.1 M HNO_3 or 0.1 M NaOH. Preliminary experiments with sulfite were conducted in G1 media or 0.001 M $NaNO_3$ electrolyte. No differences in reaction kinetics were observed and subsequent experiments were performed with background sodium nitrate solutions. Experiments with sulfide were conducted in sealed bottles purged with N_2 to maintain anoxic conditions. Samples were collected periodically and filtered using a 0.20 μm nylon syringe filter. The filtrate was acidified with 2% (v/v) HNO_3 and total dissolved selenium was analyzed using ICP-OES as described above.

Measurement of extracellular sulfur metabolites

To examine the production of extracellular sulfur metabolites by the isolate, triplicate cultures were grown in the G1 medium described above. Se(0) was not added to these cultures. At regular time intervals, samples were collected for sulfite, thiosulfate, cysteine, and glutathione analysis. Samples were filtered using a 0.45 μm syringe filter and stored in a -20°C freezer until analysis. Prior to

analysis samples were thawed and derivatized by the addition of 50 µL 2,2,'-dithiobis(5-nitropyridine) (DTNP) solution (2 mM solution in 100% acetonitrile) and 50 µL of sodium acetate buffer (0.2 M solution with pH adjusted to 6.0) according to the method described by Valravamurthy & Mopper (1990). The samples were reacted for 5 minutes prior to high performance liquid chromatography (HPLC) analysis. Standards were prepared using dilutions of sodium thiosulfate (Sigma-Aldrich), sodium sulfite (Sigma-Aldrich), L-cysteine (SAFC), and L-glutathione (Fisher Scientific) in G1 medium.

Thiosulfate and sulfite in the samples were analyzed on a Shimadzu SL-10A HPLC system equipped with a Shimadzu STD-10AV UV-Vis detector. A reversed-phase C18 column (250 mm × 4.60 mm) containing 5 µm fully porous silica packing (Phenomenex Luna) was used for separation of compounds. A gradient elution method was used for the HPLC separations with a flow rate of 0.8 mL min^{-1}. The first eluent was a solution of 0.05 M sodium acetate and 7.5 mM tetrabutylammonium hydrogen sulfate prepared in double deionized water with the pH adjusted to 3.5 with 6 M HCl. The second eluent was 100% acetonitrile (ACN). The gradient used was as follows: 10% ACN for 1 minute; 10% to 35% ACN in 4 minutes; 35% to 100% ACN in 10 minutes; 100% ACN for 7 minutes; and back to 10% ACN in 3 minutes.

To measure extracellular sulfide, cultures were incubated under standard conditions described above. Samples were taken at regular time intervals for sulfide analysis. Sulfide measurements were made using the methylene blue assay (Ang, Konigstorfer, Giles, & Bhatia, 2012). Samples were centrifuged at

16,100 × *g* for 2 minutes. 500 µL of the supernatant was used to measure extracellular sulfide content. Five hundred µL of the supernatant was mixed with 350 µL of zinc acetate solution (1% w/v solution in deionized water), 133 µL of N,N-dimethyl-p-phenylenediamine (NNDP) solution (20 mM solution in 7.2 M HCl), 133 µL ferric chloride solution (30 mM solution in 1.2 M HCl), and 250 µL of trichloroacetic acid solution (10% w/v solution). The samples were then allowed to react for 10 minutes to allow the coloration to develop. The spectrophotometric absorbance of methylene blue was measured at 670 nm. Standards were prepared using dilutions of a sodium sulfide solution (Sigma-Aldrich) prepared in a sodium carbonate buffer with pH adjusted to 9.2.

RESULTS:

Twenty-six bacterial isolates obtained from the Punjab soils were screened their ability to solubilize red Se(0). Four isolates formed clearing zones around colonies indicating the dissolution of red Se(0). One isolate, designated as JG17, formed a clearing zone that extended distally from growing colonies (**Figure 4.5**). Based on the 16S rRNA gene sequence, JG17 grouped with members of the *Bacillus* genus and was closely related to *Bacillus megaterium* ATCC 14581 (99% sequence identity) and *Bacillus aryabhattai* B8W22 (100% sequence identity) **(Figure 4.1)**. Additional physiological information is provided in **Appendix 4.**

To test if Se(0) dissolution is an extracellular process, cell-free filtrates were harvested during growth of JG17. Se(0) particles reacted with spent medium collected at late exponential phase showed rapid formation of dissolved selenium

with an initial Se(0) dissolution rate of 0.43 μM h^{-1} **(Figure 4.2A).** Extensive solubilization occurred within the first hour of the reaction, and then the dissolution rate gradually decreased to 0.07 μM h^{-1} before approaching steady state at approximately 3 hours. Triplicate experiments yielded an average of 0.71 μM (±0.03) of dissolved selenium after 25 hours. While the remaining Se(0) appeared red, microscopic characterization of the particles was not undertaken following the dissolution experiments. Abiotic control experiments had no detectable Se(0)-solubilizing activity.

The extent of Se(0) dissolution by the cell-free filtrates was dependent on the growth-stage of the culture **(Figure 4.2B)**. Se(0) reacted with early-log filtrates generated very low levels of dissolved selenium. Stationary phase filtrates produced the greatest amount of soluble selenium, with intermediate values for mid-log phase cultures. These results indicate that the reactive compounds that solubilized Se(0) were released during growth and accumulated in the spent medium. Untreated filtrates collected at stationary phase formed soluble selenium (0.71 μM ± 0.03) at similar amounts compared to cultures containing whole cells (0.80 μM ± 0.05), and also to filtrates treated with either SOD (0.91 μM ± 0.01) or DMSO (0.82 μM ± 0.09), and filtrates treated with heat (0.78 μM ± 0.05) **(Figure 4.2C)**.

Analysis of extracellular metabolites in the spent medium showed that JG17 produced inorganic sulfur compounds during growth **(Figure 4.3A,B)**. Sulfite, sulfide, and thiosulfate were detected in the cell-free filtrates, reaching maximum concentrations at mid-log, late log/early stationary, and stationary

phase, respectively. The dominant extracellular sulfur compound during early-log phase growth (12 hours) was sulfite, which peaked at mid-log phase at a concentration of 0.61 μM ± 0.21, then dropped at late-log phase, and remained low for the remainder of the experiment **(Figure 4.3A,B)**. Sulfide was not detected until 18 hours (late-log phase) and peaked at 24 hours when it was measured at a concentration of 1.75 μM ± 0.22. While sulfide concentrations were highly variable at some time points, the concentrations in most replicates remained elevated from mid-log to stationary phase **(Figure 4.3A, C)**. Finally, a rapid rise in thiosulfate concentrations occurred at 24 hours and then gradually increased during stationary phase to 0.76 μM ± 0.02 at 40 hours **(Figure 4.3A, D)**. Extracellular cysteine and glutathione were not detected at any of the time points. Sulfite, sulfide, and thiosulfate were also not detected in control experiments with sterile uninoculated medium.

Abiotic experiments with either sulfite, sulfide or thiosulfate reacting with Se(0) resulted in selenium solubilization **(Figure 4.4A-C)**. The data showed that sulfide was the most reactive solubilizing compound followed by sulfite and then thiosulfate. At the lowest concentration tested (0.5 μM), reactions with sulfite, sulfide, and thiosulfate resulted in total dissolved selenium concentrations of 0.26, 0.42, and 0.14 μM respectively. The extent of Se(0) dissolution increased linearly with increasing concentrations of sulfide, sulfite, and thiosulfate between 0.5 to 2.0 μM. Se(0) solubilization by sulfite and thiosulfate was rapid occurring mostly in the first hour of the reaction and reaching equilibrium within 6 hours. Se(0) dissolution by sulfide was slower and continued for the duration of the

experiment. Using the concentrations of sulfide, sulfite, and thiosulfate measured in the spent medium of JG17 at early stationary phase (0.22 μM sulfite, 2.1 μM sulfide, and 0.65 μM thiosulfate), we estimate that these reactive sulfur metabolites would result in total dissolved selenium of 0.98 μM, which is comparable to the maximum soluble selenium concentration of 0.91 μM observed in the cell-free filtrate experiments. These reactive sulfur metabolites can also account for 98% to 113% of the dissolved selenium measured in the mid-log and late-stationary Se(0) dissolution experiments **(Figure 4.2B)**.

DISCUSSION

The results of this study indicate that the isolate *Bacillus* sp. JG17 solubilizes Se(0) via extracellular reactions with reactive sulfur metabolites. This finding is consistent with previous observations that sulfide, sulfite, and thiosulfate react with Se(0) to form the aqueous species selenosulfide (SeS^{2-}), selenosulfate ($SeSO_3^{2-}$), and selenothiosulfate ($SeS_2O_3^{2-}$), respectively (Ball & Milne, 1995; Rahim & Milne, 1996; Weres et al., 1989). While these previous studies used the black amorphous Se(0) in their experiments, our results show that the red selenium allotrope also readily reacts with inorganic sulfur compounds to form aqueous selenosulfur complexes (**Figure 4.4**). Furthermore, when the concentrations of dissolved selenium from the abiotic dissolution experiments are taken together with the observed extent of reactive sulfur metabolite production by JG17, the solubilization of Se(0) by the microbially-generated sulfite, sulfide, and thiosulfate can fully account for

selenium dissolution observed in mid-log, early-stationary, and late-stationary filtrate experiments. The absence of organic thiols in the spent medium further supports the hypothesis that the three identified inorganic sulfur metabolites are the primary reactive compounds mediating extracellular Se(0) dissolution.

The extent of Se(0) dissolution by JG17 is in the same order of magnitude as the microbial selenium solubilization reported by Dowdle and Oremland (1998) in heterotrophic enrichment cultures and pure cultures of *Leptothrix* sp. MnB1 and *Thiobacillus* sp. ASN-1. The measurements by Dowdle and Oremland (1998) made at six and nine days showed similar levels of soluble selenium as JG17 stationary phase filtrates. Our results indicate that JG17 dissolves Se(0) dissolution via reactions with sulfur metabolites, but does not preclude alternate selenium dissolution mechanisms such as direct contact and non-specific enzymatic Se(0) oxidation. Nonetheless, it is interesting to note that Dowdle and Oremland (1998) observed significant stimulation of Se(0) solubilization through the addition of sulfide and thiosulfate to biological cultures. While the authors attributed the increased Se(0) solubilization to stimulation of microbial processes by the sulfur compounds, it is unclear whether abiotic interactions between the sulfur compounds and selenium may have also played a role.

Our findings suggest that the production of reactive sulfur metabolites by soil microorganisms can promote selenium mobilization during chemical weathering. Because Se(0) is the dominant form of selenium in certain soils (Favorito, Luxton, Eick, & Grossl, 2017) and rock deposits (Wen, Carignan, Qiu, & Liu, 2006), water-rock interactions with reactive sulfur metabolites may lead to

the formation of soluble selenosulfur complexes that are subject to transport by surface- and ground-water flow. Furthermore, Se(0) represents up to 50 to 60% of the total selenium in sediments (Belzile, Chen, & Xu, 2000; Velinsky & Cutter, 1991; Wiramanaden, Liber, & Pickering, 2010) and thus reactions with sulfite, thiosulfate, and sulfide would also be expected to mobilize selenium during early diagenesis. Since pore water concentrations of total dissolved selenium in sediments are typically in the nanomolar range (Belzile et al., 2000; Velinsky & Cutter, 1991), our experiments suggest that selenosulfur compounds may potentially represent a significant fraction of soluble selenium in pore waters containing micromolar levels of sulfite and thiosulfate (Valravamurthy & Mopper, 1990). While selenosulfate has been detected in flue gas desulfurization waste-waters (Petrov, Charters, & Wallschläger, 2012), detailed analyses to examine selenosulfur complexes in natural waters have not yet been carried out. Our preliminary efforts to separate and measure selenosulfur compounds using HPLC-ICP-MS were unsuccessful (data not shown). Future work should be aimed at speciating soluble selenium complexes formed by microbial sulfur metabolites and determining the occurrence of inorganic selenosulfur compounds in soil and sediment pore waters.

The stability of selenosulfur complexes in natural systems is not fully understood, but will likely depend on secondary microbial and redox processes. For example, the presence of oxygen may lead to the formation of selenite and selenate. The selenothiosulfate formed from the reaction of Se(0) and thiosulfate [reaction (3)] may react similarly to disulfane-monosulfonic acid ($S_3O_3^{2-}$) which

at neutral pH in the presence of oxygen will degrade to tritionate ($S_3O_6^{2-}$) (Schippers, Jozsa, & Sand, 1996). Analogously, selenothiosulfate may form selenodithionate ($SeS_2O_6^{2-}$) in the presence of oxygen:

(4) $$SeS_2O_3^{2-} + \frac{3}{2}O_2 \rightarrow SeS_2O_6^{2-}$$

This selenodithionate ion formed may subsequently be hydrolyzed to thiosulfate and selenate, equivalent to the hydrolysis of trithionate to form sulfate and thiosulfate (Schippers, 2004)**:**

(5) $$SeS_2O_6^{2-} + H_2O \rightarrow S_2O_3^{2-} + SeO_4^{2-} + 2H^+$$

The selenosulfide ion (SeS^{2-}) formed from the reaction of Se(0) with sulfide [reaction (1)] (Weres et al., 1989) may be oxidized in a mechanism similar to the oxidation of the polysulfide ion at pH values between 7.0 and 9.0, forming selenosulfate ($SeSO_3^{2-}$) as a product (Kleinjan, Keizer, & Janssen, 2005):

(6) $$Se_nS^{2-} + \frac{3}{2}O_2 \rightarrow SeSO_3^{2-} + (n-2)Se_0$$

The -SS-, -SeS- and -SeSe- bonds are very similar and the total energy change for the interconversion reaction between these bonds is so small that the rearrangement reactions between various $-Se_nS_{8-n}$, molecules are possible in solution (Laitinen & Pakkanen, 1983). Thus, the selenium moiety may be oxidized instead and form the thioselenate ion ($SSeO_3^{2-}$). However, thioselenate is unstable in aqueous solution and will readily isomerize to selenosulfate (Bouroushian, 2010).

Selenosulfate formed from the reaction between sulfite and Se(0) [reaction (2)] and possibly by the mechanism described in reaction (6) is expected to behave similarly to thiosulfate in oxygen-rich aqueous environments. The oxidation of thiosulfate in aqueous systems by oxygen is an extremely slow process with tetrathionate ($S_4O_6^{2-}$) and sulfate as the main end-products (Aylmore & Muir, 2001; Naito, Shieh, & Okabe, 1970). However, free metal ions can catalyze the oxidation of thiosulfate to tetrathionate, trithionate, and sulfate (Aylmore & Muir, 2001). Likewise, selenosulfate may be oxidized to selenate and sulfate, or various mixed-valence selenosulfur complexes analogous to polythionates (Aylmore & Muir, 2001; Byerley, Fouda, & Rempel, 1973).

Strain JG17 produced extracellular sulfite, sulfide, and thiosulfate using sulfate as the sole sulfur source in the medium. A temporal progression of the sulfur compounds was observed where *Bacillus* sp. JG17 produces sulfite first during early- to mid-log phase growth, followed by sulfide mainly during the transition from log- to stationary phase growth. Thiosulfate formed later and was detectable at late-log phase. Because JG17 was grown aerobically and does not respire sulfate (Castro, Williams, & Ogram, 2000), the production of reactive sulfur metabolites must have originated from sulfate assimilation pathways. We note that only a small fraction of the sulfate added to the growth media was converted to extracellular sulfite, sulfide, and thiosulfate (<1%). Although the concentrations of these metabolites are at the micromolar concentration range, the compounds are highly reactive and their production by bacteria under aerobic growth conditions has largely been ignored. In contrast, yeasts have been long

known to produce extracellular sulfite and sulfide as a by-product of sulfur assimilation (Dott & Trüper, 1976; Eschenbruch, 1974). Components of the sulfate assimilation pathway in yeast are homologous to their bacterial counterparts (Thomas & Surdin-Kerjan, 1997), and may be useful in informing the mechanism of reactive sulfur metabolite production by JG17. Strains of yeast that over-produce sulfite often have genetic defects in enzymes for sulfate assimilation. During sulfate assimilation, sulfate is reduced to sulfite via APS and PAP intermediates. In a key step in cysteine biosynthesis, sulfite is then reduced to sulfide by sulfite reductase (Dott & Trüper, 1976). Defects of the sulfite reductase enzyme have been shown in engineered yeast to slow the process of sulfite reduction to sulfide, allowing for significant amounts of sulfite to accumulate (Hansen & Kielland-Brandt, 1996). Other engineered sulfite-overproducing strains overexpress the genes encoding APS kinase and sulfate adenylyltransferase (Donalies & Stahl, 2002; Korch, Mountain, Gyllang, Winge, & Brehmer, 1991).

Similar to strain JG17, yeasts also produce sulfide as a by-product of their central sulfur metabolism. In *Saccharomyces cerevisiae* this production occurs when cysteine is absent in the growth medium and is caused by the dysregulation of the sulfate-assimilation pathway under nitrogen-limiting conditions (Giudici & Kunkee, 1994; Jiranek, Langridge, & Henschke, 1995). Depending on growth conditions, commercial wine-producing yeasts will produce ~13-2000 nM sulfide during growth in the absence of cysteine (Jiranek et al., 1995), on the same order of magnitude as the levels of sulfide production observed in our experiments. We

observed a large amount of variability in the sulfide measurements at certain time points. This could be explained by several reasons. At neutral pH, a portion of the sulfide produced by JG17 during log and stationary phases may have been lost due to volatilization to the gas phase in the form of H_2S. Alternatively, the sulfide may have reacted with oxygen to form sulfite and/or thiosulfate (Zhang & Millero, 1993).

The thiosulfate which accumulated in the spent medium of JG17 is likely the result of a chemical reaction between biogenic sulfite and sulfide. This thiosulfate formation mechanism is supported by the fact that sulfite is the primary reactive sulfur metabolite in the media until the appearance of sulfide during late-log growth, after which point the concentration of thiosulfate begins to increase at a greater rate and the concentration of sulfite drops to a lower concentration. The reaction between sulfite and sulfide to produce thiosulfate in the presence of oxygen is a well-characterized geochemical reaction (Zhang & Millero, 1993).

Bacillus sp. JG17 was isolated from seleniferous soils where we expect extracellular reactive metabolites to have the greatest influence on selenium mobilization. Although soils naturally enriched in selenium have been found around the world (e.g. Fernández-Martínez & Charlet, 2009) and *Bacillus* species are commonly found in seleniferous soils (e.g. Sarathchandra & Watkinson, 1981), more work is needed to examine the production of reactive sulfur metabolites in different *Bacillus* species and other genera of bacteria in order to elucidate the environmental relevance of this process. Extracellular

production of reactive sulfur metabolites has been extensively described in yeasts (Eschenbruch, 1974), and may also occur in diverse bacteria. This is not a topic that has been well-studied with most focus being on the sulfur species produced by anaerobic sulfate-respiring bacteria. If the ability to produce extracellular reactive sulfur metabolites is wide-spread among bacteria, it would have implications for not only the geochemical cycling of selenium but also for other sulfur-reactive elements in chemical weathering environments.

REFERENCES:

Ang, A. D., Konigstorfer, A., Giles, G. I., & Bhatia, M. (2012). Measuring free tissue sulfide. *Advances in Biological Chemistry, Vol.02No.04*, 6. doi:10.4236/abc.2012.24044

Aylmore, M. G., & Muir, D. M. (2001). Thiosulfate leaching of gold—A review. *Minerals Engineering, 14*(2), 135-174. doi:https://doi.org/10.1016/S0892-6875(00)00172-2

Ball, S., & Milne, J. (1995). Studies on the interaction of selenite and selenium with sulfur donors. Part 3. Sulfite. *Canadian Journal of Chemistry, 73*(5), 716-724. doi:10.1139/v95-091

Belzile, N., Chen, Y. W., & Xu, R. (2000). Early diagenetic behaviour of selenium in freshwater sediments. *Applied Geochemistry, 15*(10), 1439-1454. doi:https://doi.org/10.1016/S0883-2927(00)00011-1

Bouroushian, M. (2010). Chalcogens and Metal Chalcogenides *Electrochemistry of Metal Chalcogenides* (pp. 1-52): Springer.

Byerley, J. J., Fouda, S. A., & Rempel, G. L. (1973). The oxidation of thiosulfate in aqueous ammonia by copper (II) oxygen complexes. *Inorganic and Nuclear Chemistry Letters, 9*(8), 879-883. doi:https://doi.org/10.1016/0020-1650(73)90041-X

Castro, H. F., Williams, N. H., & Ogram, A. (2000). Phylogeny of sulfate-reducing bacteria1. *FEMS Microbiology Ecology, 31*(1), 1-9. doi:10.1111/j.1574-6941.2000.tb00665.x

Donalies, U. E. B., & Stahl, U. (2002). Increasing sulphite formation in Saccharomyces cerevisiae by overexpression of MET14 and SSU1. *Yeast, 19*(6), 475-484. doi:10.1002/yea.849

Dott, W., & Trüper, H. G. (1976). Sulfite formation by wine yeasts. *Archives of Microbiology, 108*(1), 99-104. doi:10.1007/BF00425098

Dowdle, P. R., & Oremland, R. S. (1998). Microbial Oxidation of Elemental Selenium in Soil Slurries and Bacterial Cultures. *Environmental Science & Technology, 32*(23), 3749-3755. doi:10.1021/es970940s

El-Ramady, H. R., Domokos-Szabolcsy, É., Shalaby, T. A., Prokisch, J., & Fári, M. (2015). Selenium in Agriculture: Water, Air, Soil, Plants, Food, Animals and Nanoselenium. In E. Lichtfouse, J. Schwarzbauer, & D. Robert (Eds.), *CO2 Sequestration, Biofuels and Depollution* (pp. 153-232). Cham: Springer International Publishing.

Eschenbruch, R. (1974). and Sulfide Formation during Winemaking -- A Review. *American Journal of Enology and Viticulture, 25*(3), 157.

Favorito, Sulfite J. E., Luxton, T. P., Eick, M. J., & Grossl, P. R. (2017). Selenium speciation in phosphate mine soils and evaluation of a sequential extraction procedure using XAFS. *Environmental Pollution, 229*, 911-921. doi:https://doi.org/10.1016/j.envpol.2017.07.071

Fernández-Martínez, A., & Charlet, L. (2009). Selenium environmental cycling and bioavailability: a structural chemist point of view. *Reviews in Environmental Science and Bio/Technology, 8*(1), 81-110. doi:10.1007/s11157-009-9145-3

Giudici, P., & Kunkee, R. E. (1994). The Effect of Nitrogen Deficiency and Sulfur-Containing Amino Acids on the Reduction of Sulfate to Hydrogen Sulfide by Wine Yeasts. *American Journal of Enology and Viticulture, 45*(1), 107.

Hansen, J., & Kielland-Brandt, M. C. (1996). Inactivation of MET10 in brewer's yeast specifically increases SO2 formation during beer production. *Nat Biotech, 14*(11), 1587-1591.

Haygarth, P. M. (1994). Global importance and global cycling of selenium. In J. W.T. Frankenberger & S. Benson (Eds.), *Selenium in the Environment* (pp. 1-18). New York, New York: Marcel Dekker, Inc.

Huang, C., Roncoroni, M., & Gardner, R. C. (2014). MET2 affects production of hydrogen sulfide during wine fermentation. *Applied Microbiology and Biotechnology, 98*(16), 7125-7135. doi:10.1007/s00253-014-5789-1

Huber, R., Sacher, M., Vollmann, A., Huber, H., & Rose, D. (2000). Respiration of arsenate and selenate by hyperthermophilic archaea. *Systematic and Applied Microbiology, 23*(3), 305-314. doi:10.1016/s0723-2020(00)80058-2

Jiranek, V., Langridge, P., & Henschke, P. A. (1995). Regulation of hydrogen sulfide liberation in wine-producing Saccharomyces cerevisiae strains by assimilable nitrogen. *Applied and Environmental Microbiology, 61*(2), 461-467.

Kleinjan, W. E., Keizer, A. d., & Janssen, A. J. H. (2005). Kinetics of the chemical oxidation of polysulfide anions in aqueous solution. *Water Research, 39*(17), 4093-4100. doi:https://doi.org/10.1016/j.watres.2005.08.006

Korch, C., Mountain, H. A., Gyllang, H., Winge, M., & Brehmer, P. (1991). *A mechanism for sulfite production in beer and how to increase sulfite levels by recombinant genetics*. Paper presented at the Proc. 23rd Congr. Eur. Brew. Conv., Lisbon.

Kulp, T. R., & Pratt, L. M. (2004). Speciation and weathering of selenium in upper cretaceous chalk and shale from South Dakota and Wyoming, USA. *Geochimica et Cosmochimica Acta, 68*(18), 3687-3701. doi:https://doi.org/10.1016/j.gca.2004.03.008

Laitinen, R., & Pakkanen, T. (1983). A theoretical investigation of the sulfur—selenium bond. *Journal of Molecular Structure: THEOCHEM, 91*(3), 337-352. doi:https://doi.org/10.1016/0166-1280(83)80079-7

Losi, M. E., & Frankenberger, W. T. (1998). Microbial Oxidation and Solubilization of Precipitated Elemental Selenium in Soil. *Journal of Environmental Quality, 27*(4), 836-843. doi:10.2134/jeq1998.00472425002700040018x

Muyzer, G., & Stams, A. J. M. (2008). The ecology and biotechnology of sulphate-reducing bacteria. *Nature Reviews Microbiology, 6*, 441. doi:10.1038/nrmicro1892

Naito, K., Shieh, M.-C., & Okabe, T. (1970). The Chemical Behavior of Low Valence Sulfur Compounds. V. Decomposition and Oxidation of Tetrathionate in Aqueous Ammonia Solution. *Bulletin of the Chemical Society of Japan, 43*(5), 1372-1376. doi:10.1246/bcsj.43.1372

Nancharaiah, Y. V., & Lens, P. N. L. (2015). Ecology and Biotechnology of Selenium-Respiring Bacteria. *Microbiology and Molecular Biology Reviews, 79*(1), 61-80. doi:10.1128/mmbr.00037-14

Nriagu, J. O. (1989). Global Cycle of Selenium. In M. Ihnat (Ed.), *Occurence and Distribution of Selenium* (pp. 327-340). Boca Raton, Florida: CRC Press.

Oremland, R. S., Herbel, M. J., Blum, J. S., Langley, S., Beveridge, T. J., Ajayan, P. M., . . . Curran, S. (2004). Structural and Spectral Features of Selenium Nanospheres Produced by Se-Respiring Bacteria. *Applied and Environmental Microbiology, 70*(1), 52-60. doi:10.1128/AEM.70.1.52-60.2004

Oremland, R. S., Hollibaugh, J. T., Maest, A. S., Presser, T. S., Miller, L. G., & Culbertson, C. W. (1989). Selenate Reduction to Elemental Selenium by Anaerobic Bacteria in Sediments and Culture: Biogeochemical Significance of a Novel, Sulfate-Independent Respiration. *Applied and Environmental Microbiology, 55*(9), 2333-2343.

Petrov, P. K., Charters, J. W., & Wallschläger, D. (2012). Identification and Determination of Selenosulfate and Selenocyanate in Flue Gas Desulfurization Waters. *Environmental Science & Technology, 46*(3), 1716-1723. doi:10.1021/es202529w

Pettine, M., Gennari, F., & Campanella, L. (2013). The reaction of selenium (IV) with ascorbic acid: Its relevance in aqueous and soil systems. *Chemosphere, 90*(2), 245-250. doi:https://doi.org/10.1016/j.chemosphere.2012.06.061

Rahim, S., & Milne, J. (1996). Studies on the interaction of selenite and selenium with sulphur donors. Part 4. Thiosulfate. *Canadian Journal of Chemistry, 74*(5), 753-759. doi:10.1139/v96-082

Rosenfeld, C. E., Kenyon, J. A., James, B. R., & Santelli, C. M. (2017). Selenium (IV,VI) reduction and tolerance by fungi in an oxic environment. *Geobiology, 15*(3), 441-452. doi:10.1111/gbi.12224

Sarathchandra, S. U., & Watkinson, J. H. (1981). Oxidation of elemental selenium to selenite by Bacillus megaterium. *Science, 211*(4482), 600.

Schilling, K., Johnson, T. M., Dhillon, K. S., & Mason, P. R. D. (2015). Fate of Selenium in Soils at a Seleniferous Site Recorded by High Precision Se Isotope Measurements. *Environmental Science & Technology, 49*(16), 9690-9698. doi:10.1021/acs.est.5b00477

Schippers, A. (2004). Biogeochemistry of metal sulfide oxidation in mining environments, sediments, and soils. In J. P. Amend, K. J. Edwards, & T. W. Lyons (Eds.), *Sulfur Biogeochemistry - Past and Present*: Geological Society of America.

Schippers, A., Jozsa, P., & Sand, W. (1996). Sulfur chemistry in bacterial leaching of pyrite. *Applied and Environmental Microbiology, 62*(9), 3424-3431.

Stolz, J. F., Basu, P., Santini, J. M., & Oremland, R. S. (2006). Arsenic and Selenium in Microbial Metabolism. *Annual Review of Microbiology, 60*(1), 107-130. doi:10.1146/annurev.micro.60.080805.142053

Stueken, E. E. (2017). Selenium Isotopes as a Biogeochemical Proxy in Deep Time. *Reviews in Mineralogy and Geochemistry, 82*(1), 657-682. doi:10.2138/rmg.2017.82.15

Stueken, E. E., Buick, R., & Anbar, A. D. (2015). Selenium isotopes support free O2 in the latest Archean. *Geology, 43*(3), 259-262. doi:10.1130/G36218.1

Stüeken, E. E., Buick, R., Bekker, A., Catling, D., Foriel, J., Guy, B. M., . . . Poulton, S. W. (2015). The evolution of the global selenium cycle: Secular trends in Se isotopes and abundances. *Geochimica et Cosmochimica Acta, 162*, 109-125. doi:https://doi.org/10.1016/j.gca.2015.04.033

Thomas, D., & Surdin-Kerjan, Y. (1997). Metabolism of sulfur amino acids in Saccharomyces cerevisiae. *Microbiology and Molecular Biology Reviews, 61*(4), 503-532.

Valravamurthy, A., & Mopper, K. (1990). Determination of sulfite and thiosulfate in aqueous samples including anoxic seawater by liquid chromatography after derivatization with 2,2'-dithiobis(5-nitropyridine). *Environmental Science & Technology, 24*(3), 333-337. doi:10.1021/es00073a007

Velinsky, D. J., & Cutter, G. A. (1990). Determination of elemental selenium and pyrite-selenium in sediments. *Analytica Chimica Acta, 235*, 419-425. doi:https://doi.org/10.1016/S0003-2670(00)82102-9

Velinsky, D. J., & Cutter, G. A. (1991). Geochemistry of selenium in a coastal salt marsh. *Geochimica et Cosmochimica Acta, 55*(1), 179-191. doi:https://doi.org/10.1016/0016-7037(91)90410-7

Wen, H., Carignan, J., Qiu, Y., & Liu, S. (2006). Selenium Speciation in Kerogen from Two Chinese Selenium Deposits: Environmental Implications. *Environmental Science & Technology, 40*(4), 1126-1132. doi:10.1021/es051688o

Weres, O., Jaouni, A.-R., & Tsao, L. (1989). The distribution, speciation and geochemical cycling of selenium in a sedimentary environment, Kesterson Reservoir, California, U.S.A. *Applied Geochemistry, 4*(6), 543-563. doi:https://doi.org/10.1016/0883-2927(89)90066-8

Widdel, F., & Pfennig, N. (1981). Studies on dissimilatory sulfate-reducing bacteria that decompose fatty acids. *Archives of Microbiology, 129*(5), 395-400. doi:10.1007/BF00406470

Wiramanaden, C. I. E., Liber, K., & Pickering, I. J. (2010). Selenium Speciation in Whole Sediment using X-ray Absorption Spectroscopy and Micro X-ray Fluorescence Imaging. *Environmental Science & Technology, 44*(14), 5389-5394. doi:10.1021/es100822z

Zhang, J.-Z., & Millero, F. J. (1993). The products from the oxidation of H2S in seawater. *Geochimica et Cosmochimica Acta, 57*(8), 1705-1718. doi:https://doi.org/10.1016/0016-7037(93)90108-9

FIGURES:

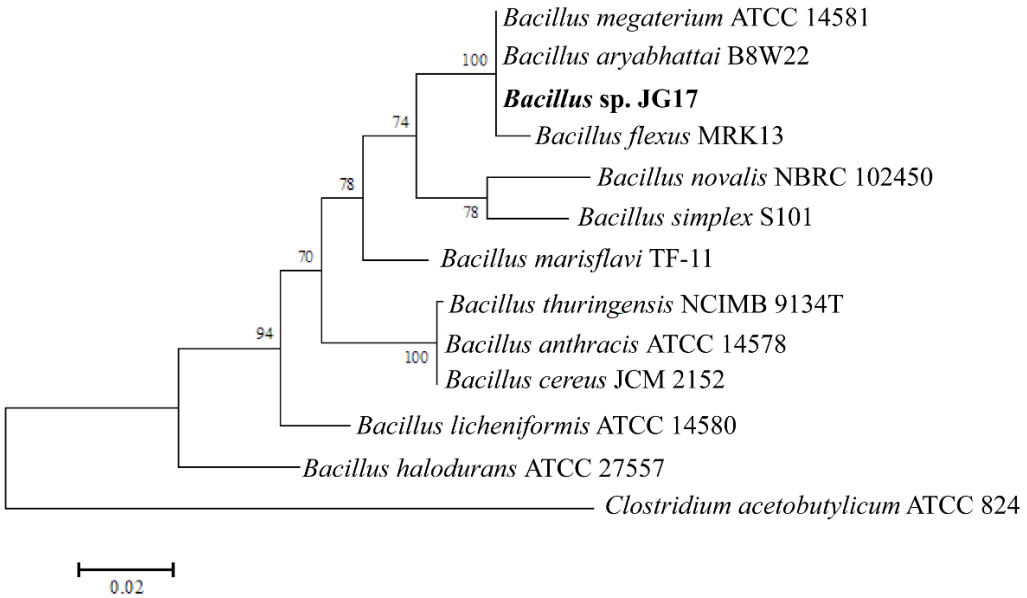

Figure 4.1. Maximum-likelihood phylogenetic tree of the 16S rRNA gene sequences showing the relationship of strain JG17 and representative *Bacillus* species. The tree is drawn to scale with branch lengths measured in the number of nucleotide substitutions per site.

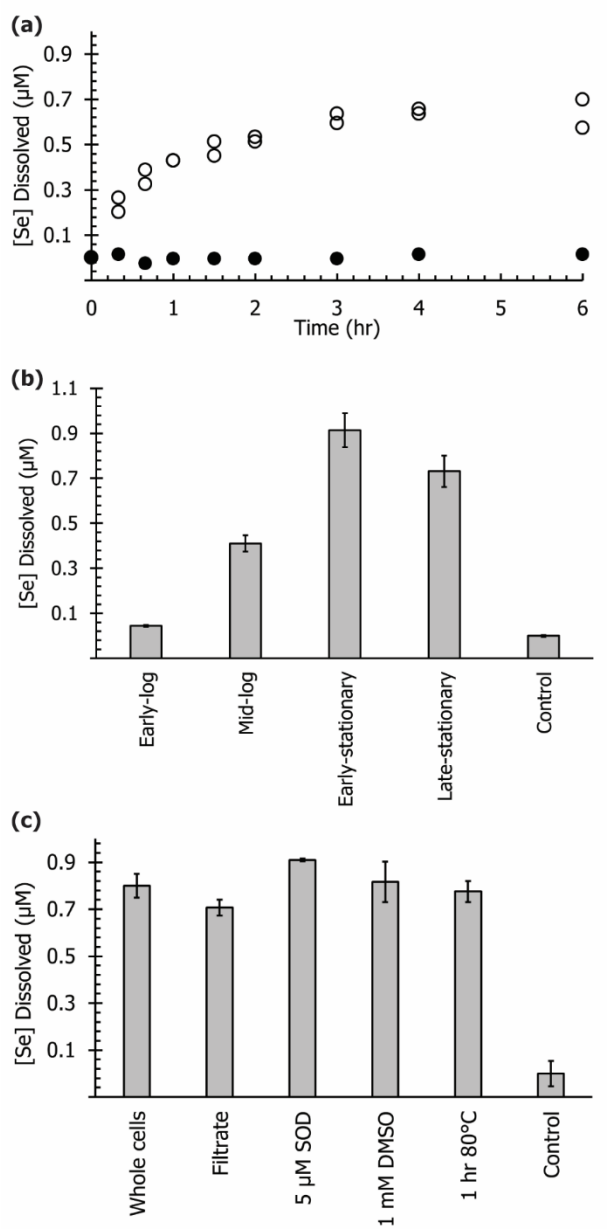

Figure 4.2. Elemental selenium dissolution by cell-free filtrates. (A) Soluble selenium formed during reaction with filtrates derived from late-exponential cultures (open circles represent two separate replicate experimentss) and an abiotic control (closed circle). Symbols represent individual batch reactors that were sacrificed for analysis at each time point. (B) Se(0) dissolution by cell-free filtrates according to the growth phase of JG17 cultures**.** (C) Soluble selenium formed during reaction by whole cells at stationary phase, untreated

filtrates, filtrates treated with superoxide dismutase, filtrates treated with dimethyl sulfoxide, filtrates heated at 80°C, and uninoculated media controls.. For figures B and C bar graphs show the total dissolved selenium measured after 6 hours of reaction. Bars represent the mean of triplicate experiments. Error bars represent ±1 standard deviation.

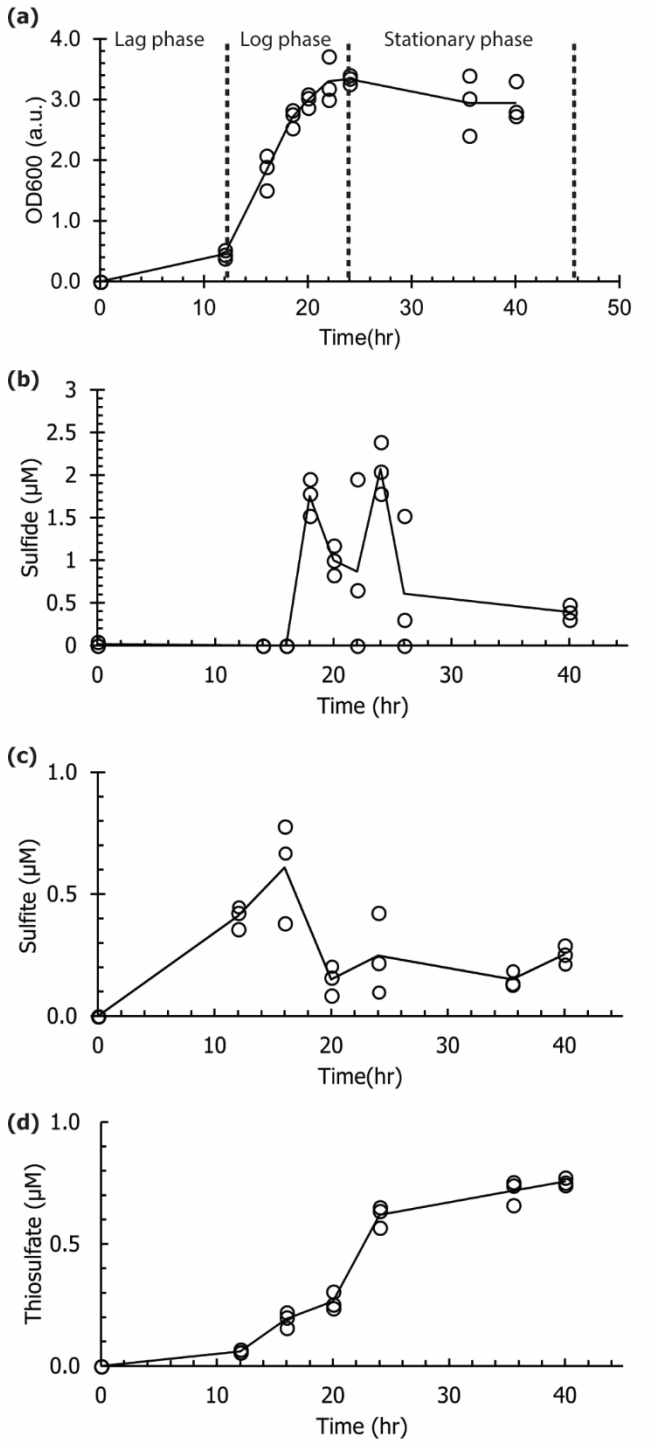

Figure 4.3. Reactive sulfur metabolites in the spent medium. (A) Growth of JG17, (B) sulfite, (C) sulfide, and (D) thiosulfate. Individual replicates are plotted as points and lines represent the average of the three replicates.

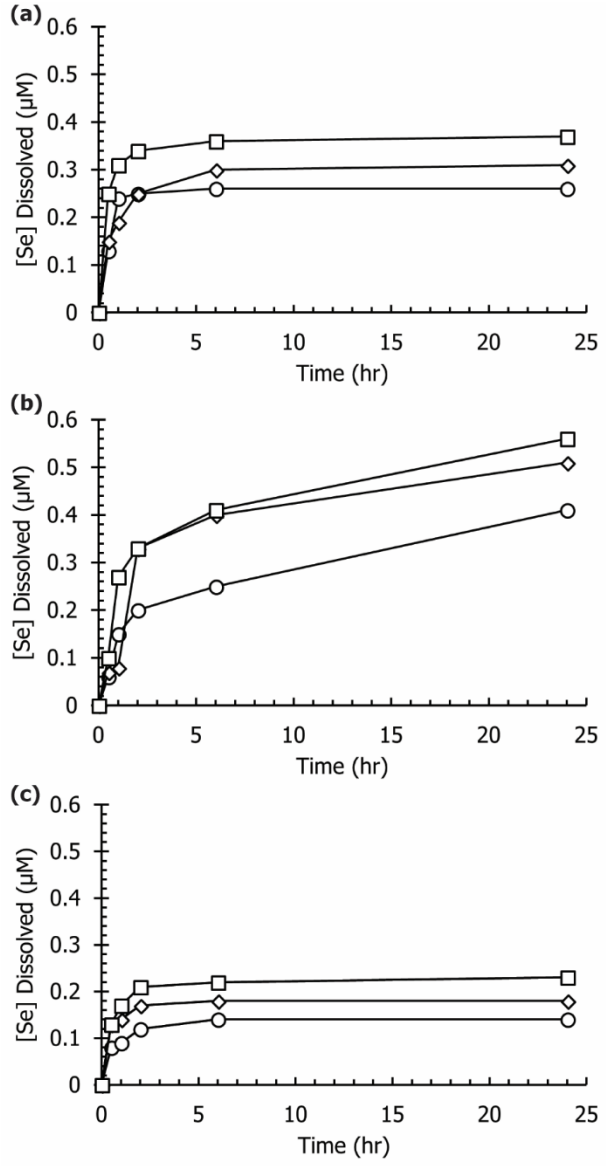

Figure 4.4. Chemical dissolution of Se(0) by (A) sulfite (B) sulfide, and (C) thiosulfate. Varying concentrations of the indicated sulfur compound was used: 0.5 μM (circle), 1 μM (triangle), 2 μM (square).

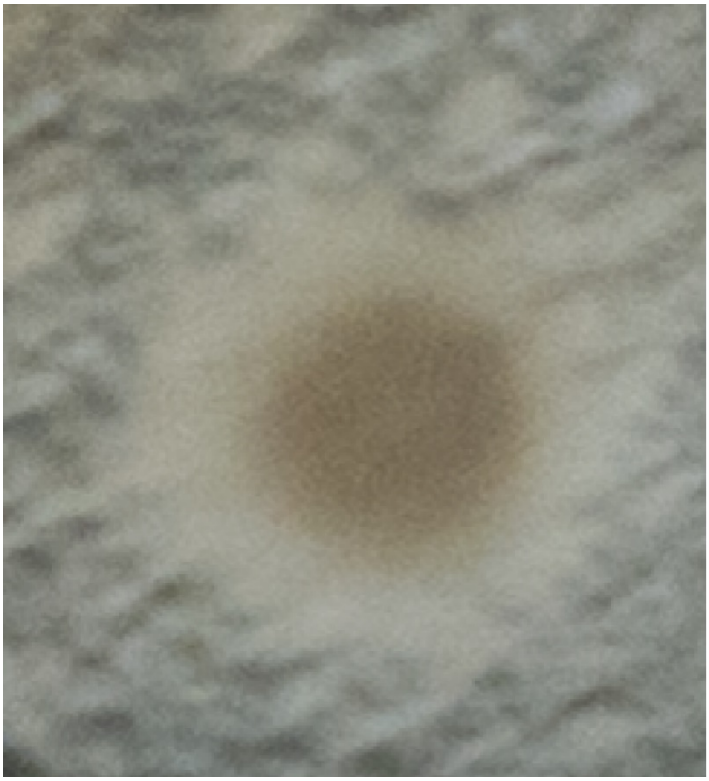

Figure 4.5. *Bacillus* sp. JG17 colony growing on an agar plate. A suspension of particulate Se(0) was spotted onto the plate around where the colony is growing. The clear ring around the colony is the area where the particulate Se(0) was solubilized by JG17.

CHAPTER 5

CHARACTERIZATION OF THE EXTRACELLULAR SULFUR METABOLITES PRODUCED BY SHEWANELLA ONEIDENSIS MR-1

ABSTRACT:

In this study, the production extracellular sulfur metabolites produced by the model dissimilatory metal-reducing organism *Shewanella oneidensis* MR-1 was characterized. Sulfur compounds were produced and released during exponential growth when sulfate was provided as a sulfur source. Sulfite was the major extracellular sulfur metabolite produced under both aerobic conditions and anaerobic conditions with fumarate as an electron acceptor. Low concentrations of thiosulfate, sulfide, glutathione, and cysteine were also detected under anaerobic conditions. When cysteine was instead added as a sulfur source under anaerobic conditions, sulfite production was repressed and sulfide was the major metabolite, suggesting that sulfite is not a product of cysteine degradation. Analysis of the *S. oneidensis* MR-1 genome also indicated the absence of the sulfite-producing enzyme cysteine dioxygenase. Together, this data supports a model where sulfite is produced from the assimilatory sulfate reduction pathway and is released during growth. These sulfur metabolites described herein have the potential to impact the speciation, solubility, and bioavailability of metals and metalloids in the environment.

INTRODUCTION:

Microorganisms can alter the chemistry of their surrounding environment by releasing reactive sulfur compounds. Inorganic sulfur metabolites such as sulfite (Millero, Gonzalez-Davila, & Santana-Casiano, 1995; Van Loon, Mader, & Scott, 2001; Xue, Goncalves, Reutlinger, Sigg, & Stumm, 1991), sulfide (Flynn, O'Loughlin, Mishra, DiChristina, & Kemner, 2014; Kramer, Bell, & Smith, 2007; Lohmayer, Kappler, Lösekann-Behrens, & Planer-Friedrich, 2014), and thiosulfate (Aylmore & Muir, 2001; Fortin & Campbell, 2001; Martínez, Jacobson, & McBride, 2004) and organic sulfur metabolites such as glutathione, cysteine (Doong & Schink, 2002; Martínez et al., 2004), and other biogenic thiols (J. Zhang, Wang, House, & Page, 2004) strongly impact the solubility and speciation of metals and metalloids in microbial ecosystems through their actions as ligands and via redox reactions. The work presented in **Chapter 4** describes how biogenic thiosulfate, sulfite, and sulfide impact elemental selenium solubility (Goff et al., 2019).

Since both organic and inorganic sulfur species are known to be important ligands and redox-active compounds in natural environments, it is important to understand the sources of these compounds in the environment. Following the study detailed in **Chapter 4,** we were interested in determining if other microorganisms were also able to produce extracellular inorganic sulfur metabolites under non-sulfur-respiring conditions. Given the known reactivity of several sulfur metabolites with iron oxides and other metals,the dissimilatory metal-reducing bacterium *Shewanella oneidensis* MR-1 was the focus of this

study. *S. oneidensis* MR-1 is capable of reducing solid external electron acceptors including iron oxides, managanese oxides, and elemental sulfur (Tiedje, 2002). *S. oneidensis* MR-1 has previously been shown to interact with solid minerals via sulfur metabolites. During elemental sulfur respiration *S. oneidensis* MR-1 produces sulfide which then chemically reduces the ferric iron in goethite (α-FeOOH) to Fe(II) (Flynn et al., 2014). Exogenous cysteine or cystine amendments were also shown to stimulate the rate and extent of reduction of the ferric iron in the clay mineral smectite by *S. oneidensis* MR-1 (Liu, Dong, Zhao, & Wang, 2014).

The objective of this study was to characterize the extracellular sulfur metabolites of *S. oneidensis* MR-1 produced during growth. We sought to determine how growth conditions impact sulfur species production and to determine a possible functional role for sulfite production. By derivatizing the reactive sulfur metabolites with the fluorescent probe monobromobimane, we detected high levels of sulfite and simultaneously lower levels of cysteine, thiosulfate, and glutathione in the culture medium of S *oneidensis* MR-1.

MATERIALS AND METHODS:

Cultures and growth conditions

Shewanella oneidensis MR-1 is a dissimilatory metal-reducing bacterium isolated from Lake Oneidea, New York, USA (Myers & Nealson, 1988). *S. oneidensis* MR-1 was routinely grown in LB medium at 30°C in a 200 rpm shaking incubator. For

all experiments, overnight LB cultures of *S. oneidensis* MR-1 were washed with phosphate-buffered saline and then transferred to MR1 lactate medium adapted from Myers and Nealson (1988). This medium contains, per liter, 1.19 g $(NH_4)_2SO4$, 0.99 g K_2HPO_4, 0.45 g KH_2PO4, 0.25 g $MgSO_4{\cdot}7H_2O$, 0.07 g $CaCl_2{\cdot}2H_2O$, 0.17 g $NaHCO_3$, 10 mL of a trace metals solution (100X), 1 mL of a sodium selenite solution (6 mM), 14.8 mL of a sodium lactate solution (30%), and 20 mL of an amino acids solution. The trace metals solution (100X) contains, per liter, 2.5 g Na_2EDTA, 0.35 g H_3BO_3, 0.06 g NaCl, 0.15 g $FeSO_4{\cdot}7\ H_2O$, 0.12 g $CoCl_2{\cdot}6\ H_2O$, 0.13 g $NiSO_4{\cdot}6\ H_2O$, 0.08 g Na_2MoO_4, 0.02 g $MnSO_4{\cdot}7H_2O$, 0.03 g $ZnSO_4{\cdot}7\ H_2O$, and 0.005 g $CuSO_4{\cdot}7H_2O$. The amino acids solution contains, per 100 milliliters, 0.2 g each of serine, arginine, and glutamate. When grown anaerobically, media was purged of oxygen using N_2 gas and fumarate (30 mM) was provided as an electron acceptor.

For experiments performed under low-sulfate conditions, non-sulfate salts were substituted for the sulfate salts in the main medium (ut not in the trace metals solution. This medium contained, per liter, 0.48 g NH_4Cl, 0.99 g K_2HPO_4, 0.45 g KH_2PO4, 0.097 g $MgCl_2$, 0.07 g $CaCl_2{\cdot}2H_2O$, 0.17 g $NaHCO_3$, 10 mL of a trace metals solution (100X), 1 mL of a sodium selenite solution (6 mM), 14.8 mL of a sodium lactate solution (30% (v/v)), and 20 mL of the amino acids solution. The trace metals solution had the same composition as described above and, thus, the final composition of the medium includes ~12 μM of sulfate. In addition to the amino acids solution, cysteine was also added to the medium as a sulfur source at a concentration of 0.5 mM.

Sulfur metabolite production by MR-1

S. oneidensis MR1 was grown under either aerobic conditions or anaerobic conditions with fumarate as the electron acceptor on either MR1 lactate medium or the modified low-sulfate MR1 lactate medium with cysteine added as a sulfur source. At regular intervals, samples were collected for determination of culture density and analysis of extracellular sulfur metabolites. To determine culture density, absorbance readings at 600 nm were taken on a BioSpec-Mini UV-Vis spectrophotometer (Shimadzu). The remainder of the sample was filtered through 0.22 μm nylon filters and the filtrate was used for measurement of extracellular sulfur metabolites.

Filtered samples were immediately derivatized using the fluorescent probe monobromobimane (mBBr), a weakly fluorescent molecule that reacts with the unpaired electrons of the sulfhydryl group of thiol molecules to form a stable and highly fluorescent thioether bond (Fahey & Newton, 1988). Stock solutions of mBBr (Sigma) were prepared in acetonitrile at a concentration of 50 mM. Using a method adapted from Dupont and Ahner (2005), 84 μL of borate/diethylenetriaminepentaacetic acid (DTPA) buffer (100 mM/10 mM, pH 9) and 3 μL of the 50 mM mBBr stock solution were added to 800 μL of the sample (Dupont & Ahner, 2005). The reaction proceeded for 30 minutes at room temperature in the dark before being stopped by the addition of 60 μL of methanesulfonic acid (MSA).

In the cysteine-amended cultures, samples had to first be diluted prior to derivatization in order to (1) maintain an excess of mBBr relative to mBBr-

reactive metabolite concentrations and (2) to avoid interference from a large cysteine-bimane peak with a significantly smaller sulfite-bimane peak during HPLC analysis as the two elute within less than a minute of each other (12.9 min for cysteine and 13.6 min for sulfite). A 1:9 dilution of the sample into Milli-Q water was performed. Dilution factors were determined gravimetrically. Following dilution, derivatization proceeded as described above.

Following mBBr derivatization, samples are stable for storage at -20°C for extended periods of time (Smith, Sessions, Dawson, Dalleska, & Orphan, 2017). Samples are stored at ~4°C with observed stability for at least a month of storage (longer periods of time have not been tested). Samples were analyzed using high-performance liquid chromatography (HPLC). Analytical methods are described below

Abiotic transformations of biogenic sulfite

To determine if sulfite is oxidized to sulfate under aerobic conditions, a 1 mM solution of sulfite was prepared in Milli-Q water. Water was used rather than the MR1 lactate medium due to the high concentration of sulfate already present in that medium. Samples were collected over the course of several hours and immediately analyzed by ion chromatography to minimize further oxidation of the sulfite.

Analytical Methods

High performance liquid chromatography analysis of mBBr-derivatized compounds

The mBBr-derivatized samples were analyzed to determine sulfur metabolite concentrations. Separations of samples were performed using reversed-phase high-performance liquid chromatography (HPLC) on a ZORBAX Extend-C18 column (Agilent) using an Agilent 1260 Infinity II HPLC system equipped with an Agilent 1100 series fluorescence detector. A gradient method was used to achieve separation of the extracellular mBBr-derivatized compounds. Eluent A was 1% acetonitrile and 0.25% glacial acetic acid prepared in Milli-Q water and Eluent B was 100% acetonitrile. Separation was performed at a flow rate of 0.5 mL per minute by the following gradient method: 3% B from 0-3 minutes, increase to 12.5% B from 3-5 minutes, increase to 26.4% B from 5-18 minutes, increase to 80% B from 18-23 minutes, hold at 80% B from 23-33 minutes, decrease to 3% B from 33 to 35 minutes, and hold at 3% B from 35 to 40 minutes. Cysteine elutes at 12.9 minutes, sulfite elutes at 13.6 minutes, glutathione elutes at 14.1 minutes, thiosulfate elutes at 17.9 minutes, sulfide elutes at 26.3 minutes. All standards were prepared in a matrix that matched that of the samples being analyzed.

Ion chromatography analysis of products of sulfite oxidation

Sulfate formation in aerobic sulfite solutions was determined using ion chromatography (IC). Samples were analyzed on a Dionex Aquion Ion Chromatography System (Thermo Scientific) equipped with a Dionex IonPac AS-9 HC column (4 x 250 mm) (Thermo Scientific). Anions were detected using

suppressed conductivity detection with a DS6 Conductivity Cell (Thermo Scientific). Injection volume was 25 µL. A 20 minute isocratic method was used for sample separation with a 9 mM sodium carbonate buffer as the eluent at a flow rate of 1 mL per minute. Sulfite eluted at approximately 14.1 minutes and sulfate eluted at approximately 15.7 minutes. Standards were prepared in deoxygenated Milli-Q water and stored under an N_2 gas atmosphere until analysis to minimize oxidation of the sulfite.

RESULTS:

Detection of sulfur metabolites in the spent medium of *S. oneidensis* MR-1

Sulfite was the major mBBr-derivatizable sulfur metabolite present in the spent medium of the cultures under anaerobic conditions. Sulfate was used as the sulfur source in these cultures. Under these conditions, we detected sulfite (13.6 minute peak), thiosulfate (17.9 minute peak), cysteine (12.9 minute peak), glutathione (14.1 minute peak), and sulfide (26.3 minute peak) **(Figure 5.1).** The increase in sulfite concentration was concurrent to increases in cell density and plateaued when the culture reached stationary phase. **(Figures 5.2B,D)**. Under aerobic conditions, the sulfite concentrations (**Figure 5.2A**) peaked at the beginning of stationary phase at an average concentration of 17.2 µM. Under anaerobic conditions, the maximum concentration of sulfite was an average of 44.7 µM **(Figure 5.2B).** During anaerobic growth, the concentrations of thiosulfate, cysteine, glutathione, and sulfide also increased with increasing cell

density **(Figure 5.3).** Cysteine was present under anaerobic conditions in low quantities and was detected from 12.5 hours onward. The highest amount was measured late in the growth of *S. ondeidensis* MR-1 at a concentration of 0.21 µM **(Figure 5.3A)**. Glutathione was also present under anaerobic conditions from 12.5 hours onwards. Its maximum concentration was 0.086 µM at the end of the experiment **(Figure 5.3C).** Sulfide and thiosulfate are both undetectable in the pent medium until 23.5 hours of growth **(Figure 5.3B, D)**. Thiosulfate concentrations peak at 0.258 µM and sulfide concentrations at 0.197 µM. Cysteine, glutathione, and sulfide were not observed in the spent medium under aerobic conditions. Low concentrations of thiosulfate were detected in the aerobic culture but the thiosulfate levels could not be reliably quantified (data not shown).

Oxygen degrades sulfur metabolites

We observed more than a 2.5-fold greater extent of sulfite production in the anaerobic cultures compared to the aerobic cultures despite the fact that the aerobic cultures achieve a maximum cell density that is approximately 7.5-fold greater than the anaerobic cultures (**Figure 5.2C,D)**. We hypothesized that the difference was attributable to differences in the stability of sulfite in the presence of oxygen, and that under aerobic conditions sulfite was oxidized to sulfate. Thus, a solution of sulfite was prepared under aerobic conditions and analyzed using ion chromatography to allow for the detection of both sulfite and sulfate. Over the

course of 6 hours, 700 μM of sulfite was oxidized concurrent to the formation of 628 μM sulfate **(Figure 5.5)**.

Cysteine represses sulfite production by *S. oneidensis* MR-1

To determine how sulfur-source effects sulfur metabolite production, we performed the experiments described in the prior section using a low-sulfate medium amended with cysteine (0.5 mM) as a sulfur source. Experiments demonstrated that growth on cysteine repressed sulfite production. Sulfite remained below detection throughout the experiment with the exception of one replicate at a single timepoint (**Figure 5.4A**). Large quantities of sulfide were produced by these cultures. Sulfide first appears after 20 hours of growth and peaked at the end of the experiment at an average concentration of 25 μM (**Figure 5.4C**). Nanomolar quantities of thiosulfate were also detectable at the 20 hour time point (**Figure 5.4B**). Glutathione was not observed in the spent medium of these cultures (data not shown).

DISCUSSION:

Here we report an analysis of the extracellular sulfur metabolites of the model dissimilatory metal-reducing bacterium *S. oneidensis* MR-1. All the detected compounds originated from the central sulfur metabolic pathways of *S. oneidensis* MR-1 and not through any respiratory pathway as the cells were either grown with oxygen or fumarate as terminal electron acceptors (**Figure 5.6**). The

production of the sulfite, in particular, is of interest as a physiological role for sulfite production by bacteria under non-sulfur-respiring conditions has, to our knowledge, not been reported.

We observed micromolar quantities of sulfite produced by actively growing *S. oneidensis* MR-1 cells. We hypothesize that sulfite is directly produced from the assimilatory sulfate reduction pathway and released to the extracellular medium. (**Figure 5.6A).** *S. oneidensis* MR-1 has homologs to all the enzymes of this same pathway found in *E. coli.* Based on what is known about assimilatory sulfate reduction in *E. coli*, sulfate first reacts with ATP in a reaction catalyzed by ATP sulfurylase to form adenosine phosphosulfate (APS) (Sekowska, Kung, & Danchin, 2000). APS is then phosphorylated by a second molecule of ATP to form 3'phosphoadinosine phosphosulfate (PAPS) in a reaction catalyzed by APS kinase (Sekowska et al., 2000). PAPS is then reduced to sulfite by PAPS reductase, releasing adenosine 3'-5' diphosphate (PAP) as a byproduct (Sekowska et al., 2000). Sulfite is then reduced to sulfide in an NADPH-dependent step by the enzyme NADPH-sulfite reductase (Sekowska et al., 2000). The sulfide then reacts with O-acetyl-L-serine (OAS) to form cysteine (Sekowska et al., 2000). The production and release of sulfite from this pathway in eukaryotic yeasts is well-documented but a similar process has not been described in detail in bacteria (Dott & Trüper, 1976).

Sulfite production by wine yeasts is heavily influenced by the cysteine and methionine content of the grapes used for fermentation. Cysteine and methionine are known to suppress sulfite production in both high sulfite-producing yeast

strains and in low sulfite-producing strains through the inhibition of sulfate uptake and decreased flux through the sulfate assimilation pathway (Eschenbruch, 1972; Kleinzeller, Kotyk, & Kovac, 1959). Therefore we investigated the role of cysteine in sulfite production in *S. oneidensis* MR-1. In our experiments, we observed that when grown on sulfate-limited medium with cysteine added as a sulfur source, sulfite production by *S. oneidensis* MR-1 is significantly diminished compared to cells grown with sulfate as the sulfur source. When grown on cysteine as a sulfur source, the assimilatory sulfate reduction pathway would be entirely bypassed resulting in no sulfite production via that pathway (**Figure 5.6B**).

We have also ruled out the possibility of sulfite production via the cysteine dioxygenase pathway. Some bacteria have homologs to the eukaryotic cysteine dioxygenase (CDO) enzyme (Dominy, Simmons, Karplus, Gehring, & Stipanuk, 2006). Cysteine dioxygenase oxidizes cysteine to cysteine sulfinic acid which is further broken down to sulfite and pyruvate by the enzyme aspartate aminotransferase (Dominy et al., 2006). *S. oneidensis* MR-1 does have an aspartate aminotransferase homolog in its genome (SO_2046). There are four major subfamilies of CDO: the Proteobacteria, Actinobacteria, Firmicutes, and Eukarya CDO lineages (Dominy et al., 2006). We searched the genome of *S. oneidensis* MR-1 for homologs of these enzymes using the amino acid sequence for a representative CDO from each lineage: *Rattus norvegicus* CDO (BAA11925.1), *Mycobacterium tuberculosis* CDO (WP_079012717.1), *Bacillus cereus* (NP_832375.1) CDO, and *Vibrio splendidus* CDO (ZP_00991440). No

homologs of any of these CDO enzymes were found in the genome of MR-1. Taken together with the observation that sulfite is evolved under both aerobic and anaerobic conditions, and its production is suppressed by the presence of cysteine, we propose that the sulfite produced by *S. oneidensis* MR-1 originates from the assimilatory sulfate reduction pathway.

We observed a large difference in the formation of sulfite between aerobic and anaerobic conditions when cells were grown with sulfate as a sulfur source despite the lower production of biomass under anaerobic conditions. While the possibility that sulfite production was increased in response to a switch to anaerobic respiration was intriguing, we also had to consider the possibility that the presence of oxygen may influence stability of the sulfite. We hypothesized that the sulfite is likely oxidized to sulfate under aerobic conditions by the following reaction:

$$2SO_3^{2-} + O_2 \rightarrow 2SO_4^{2-}$$

We observed sulfite oxidation concomitant to the appearance of sulfate under aerobic conditions. Half the starting sulfite was oxidized to sulfate after 4 hours under aerobic conditions (**Figure 5.5**). Thus, sulfite oxidation to sulfate under aerobic conditions occurs to an extent and on a timescale that is applicable to these experiments. This suggests that it is most likely that the differences in sulfite concentrations between our aerobic and anaerobic cultures are mainly attributable to the further oxidation of sulfite to sulfate by the oxygen in the atmosphere.

In addition to sulfite, we detected other biogenic sulfur compounds in the medium. Cysteine and glutathione were both detected in the extracellular medium in nanomolar quantities under anaerobic conditions with sulfate as a sulfur source (**Figure 3A,C**). Since these metabolites were not present in the medium, they would have originated from the cysteine and glutathione biosynthesis pathways and been released by *S. oneidensis* MR-1 (**Figure 5.6**). However, it is unclear why *S. oneidensis* MR-1 cells are releasing these compounds. It is known that other gammaproteobacteria-- namely *Escherichia coli* and *Salmonella typhimurium* – will accumulate glutathione in their growth medium (Owens & Hartman, 1986a). This activity appears to play a role in the protection of cells against extracellular reactive oxygen species (ROS) stress (Smirnova, Muzyka, Ushakov, Tyulenev, & Oktyabrsky, 2015). In one study, exposure to exogenous superoxide or hydrogen peroxide stimulated glutathione efflux by *E. coli* (Smirnova et al., 2015). In an earlier study, exogenous additions of micromolar quantities of glutathione protected *Salmonella* Typhimurium from growth inhibition by equimolar quantities of the chemical mutagen M-methyl-N'-nitro-N-nitrosoguanidine. In the same study, exogenous additions of micromolar quantities of glutathione protected *E. coli* from growth inhibition by equimolar quantities of mercuric chloride, methylmercuric chloride, silver nitrate, cisplatin, cadmium chloride, cadmium sulfate, and iodoacetamide (Owens & Hartman, 1986b). Whether there is a similar protective role for glutathione produced by *S. ondeidensis* MR-1 is unknown and would be interesting to explore. However, we will note that the observed glutathione production by *S. ondeidensis* MR-1 is in the sub-100 nanomolar range whereas production of glutathione by *E. coli* and

Salmonella Typhimurium in those studies was measured in the micromolar range (Owens & Hartman, 1986a; Smirnova et al., 2015). Cysteine was also observed to be produced by *S. ondeidensis* MR-1 under anaerobic conditions with sulfate as a sulfur source. Cysteine, while an essential amino acid, can be toxic towards cells if present at a high enough concentration intracellularly (Park & Imlay, 2003). To regulate its intracellular levels of cysteine, *E. coli* secretes cysteine extracellular (Chonoles Imlay, Korshunov, & Imlay, 2015). A similar phenomenon may be occurring in *S. oneidensis* MR-1.

Sulfide production by *S. oneidensis* MR-1 has been previously reported by another group; however, precise concentrations and temporal dynamics were not reported (Wu, Li, Mao, Zhou, & Gao, 2015). Here we measured sulfide concentrations of up to 0.197 μM when sulfate is provided as the sole sulfur source under anaerobic conditions. However, under the same growth conditions, but with cysteine added as the sulfur source, sulfide concentrations of up to 25 μM are observed. It is important to note, though, that at circumneutral pH, sulfide exists in almost equal quantities as bisulfide (HS^-) and the volatile hydrogen sulfide (H_2S) (Lewis, 2010). As we did not attempt to trap and quantify volatile species, these numbers are likely an underestimate of the sulfide produced by *S. oneidensis* MR-1.

Sulfide production likely occurs through the degradation of cysteine by the enzymes MdeA, MetY, and SseA (Wu, Li, et al., 2015). Indeed, we observe here that when sulfate is provided as a sulfur source, only extremely low quantities of sulfide are produced but when cysteine is provided as a sulfur source, sulfide

production increases. Sulfide production is known to occur in other bacteria under non-sulfur-respiring conditions (Carbonero, Benefiel, Alizadeh-Ghamsari, & Gaskins, 2012). However, in many of these studies, sulfide is only detected qualitatively or semi-quantitatively and so it can difficult to draw comparisons between different organisms. Nonetheless, in *E. coli*, *Staphylococcus aureus*, *Bacillus anthracis*, and *Pseudomonas aeruginosa*, it is known that both exogenously-supplied and endogenous sulfide play a role in defense against antibiotics and general reactive oxygen species (ROS) stress (Shatalin, Shatalina, Mironov, & Nudler, 2011). Sulfide increases antibiotic resistance by increasing the cells' resistance to oxidative stress through the induction of the expression of antioxidant enzymes and suppression of Fenton chemistry by sequestration of intracellular iron (Shatalin et al., 2011). However, in *S. oneidensis* MR-1 the role of sulfide in oxidative stress response remains less clear. Depending on the timing of when exogenous sulfide is amended to cultures, it was observed to either increase or decrease sensitivity of cells to ROS (Wu, Wan, Fu, Li, & Gao, 2015). It seems likely that the exogenous sulfide was not added at physiologically-relevant concentrations in that particular study. Those authors did not report the exact concentration of sulfide produced by *S. oneidensis* MR-1, but here we report maximal sulfide production by *S. oneidensis* at 25 μM. However, that study used substantially higher concentrations (0.5-2 mM) of sulfide for their exogenous amendments (Wu, Wan, et al., 2015). It may be that the protective effect of sulfide on the cells is concentration-dependent and lower concentrations may produce a different response. Thus, the physiological role for sulfide production by MR-1 warrants further study.

We also detected nanomolar concentrations of thiosulfate extracellularly regardless of growth conditions. The origin of the thiosulfate is unclear. It is known that in the presence of O_2, sulfite and sulfide will react to form thiosulfate (J. Z. Zhang & Millero, 1993). Indeed, thiosulfate production is only observed concurrent to sulfide production which was also an observation we made in **Chapter 4**. However, here the thiosulfate was also observed in our anaerobic cultures. Others have reported that sulfide will react with sulfite under neutral and alkaline conditions in the absence of oxygen to form thiosulfate (Siu & Jia, 1999). The thiosulfate observed here under anaerobic conditions could orginate from this reaction.

As roles for biogenic glutathione and sulfide in tempering ROS-stress have been reported previously, we postulate that sulfite may have a similar function. In a preliminary experiment we observed that addition of an equimolar concentration of sulfite increased cell survival following exposure to H_2O_2 (**Appendix 5, Figure A5.1)**. The simplest interpretation of this result is that sulfite detoxifies the H_2O_2 through a reaction that degrades H_2O_2 to form sulfate and water (Hoffmann, 1977). However it is unknown if sulfite exposure also effects the resistance of cells to ROS stress in other ways such as how sulfide exposure enhances the ROS stress response systems of some bacteria (Shatalin et al., 2011). *S. oneidensis* MR-1 is particularly sensitive to H_2O_2 with an MIC substantially lower than that of *E. coli* (Jiang et al., 2014). Indeed, we also observed a high sensitivity to H_2O_2 with 100 μM amendments being enough to reduce the viable cell count to zero (**Figure A5.1**). This high level of sensitivity

has been attributed, in part, to the fact that *S. oneidensis* MR-1, unlike *E. coli*, does not import manganese into the cytoplasm in response to H_2O_2 exposure (Wu, Wan, et al., 2015). *E. coli* replaces the iron cofactor of its mononuclear iron enzymes with manganese to minimize damaging Fenton chemistry (Anjem & Imlay, 2012; Sobota & Imlay, 2011). This is a major mechanism by which *E. coli* resists oxidative stress. Instead, *S. oneidensis* MR-1 must rely on scavenging H_2O_2 and sequestering iron to minimize the toxicity of H_2O_2 (Wu, Wan, et al., 2015). H_2O_2-scavenging metabolites such as sulfide, glutathione, and sulfite may constitute one of arm of *S. oneidensis* MR-1's defense against ROS. Thus, while biogenic sulfite certainly has importance from a geochemical perspective in respect to its ability to affect the speciation and solubility of metals and metalloids in the environment, it also potentially plays a role in the ROS-defense in microorganisms. The mechanisms by which sulfite imparts H_2O_2-resistance to *S. oneidensis* MR-1 warrants further investigation.

REFERENCES:

Anjem, A., & Imlay, J. A. (2012). Mononuclear Iron Enzymes Are Primary Targets of Hydrogen Peroxide Stress. *Journal of Biological Chemistry, 287*(19), 15544-15556. Retrieved from http://www.jbc.org/content/287/19/15544.abstractN2 -

Aylmore, M. G., & Muir, D. M. (2001). Thiosulfate leaching of gold—A review. *Minerals Engineering, 14*(2), 135-174. doi:https://doi.org/10.1016/S0892-6875(00)00172-2

Carbonero, F., Benefiel, A., Alizadeh-Ghamsari, A., & Gaskins, H. R. (2012). Microbial pathways in colonic sulfur metabolism and links with health and disease. *Frontiers in Physiology, 3*(448). doi:10.3389/fphys.2012.00448

Chonoles Imlay, K. R., Korshunov, S., & Imlay, J. A. (2015). Physiological Roles and Adverse Effects of the Two Cystine Importers of Escherichia coli. *Journal of Bacteriology, 197*(23), 3629. doi:10.1128/JB.00277-15

Dominy, J. E., Simmons, C. R., Karplus, P. A., Gehring, A. M., & Stipanuk, M. H. (2006). Identification and Characterization of Bacterial Cysteine Dioxygenases: a New Route of Cysteine Degradation for Eubacteria. *Journal of Bacteriology, 188*(15), 5561-5569. Retrieved from http://jb.asm.org/content/188/15/5561.abstractN2

Doong, R.-a., & Schink, B. (2002). Cysteine-Mediated Reductive Dissolution of Poorly Crystalline Iron(III) Oxides by Geobacter sulfurreducens. *Environmental Science & Technology, 36*(13), 2939-2945. doi:10.1021/es0102235

Dott, W., & Trüper, H. G. (1976). Sulfite formation by wine yeasts. *Archives of Microbiology, 108*(1), 99-104. doi:10.1007/BF00425098

Dupont, C. L., & Ahner, B. A. (2005). Effects of copper, cadmium, and zinc on the production and exudation of thiols by Emiliania huxleyi. *Limnology and Oceanography, 50*(2), 508-515. doi:10.4319/lo.2005.50.2.0508

Eschenbruch, R. (1972). Sulphate uptake and sulphite formation related to the methionine and/or cysteine content of grape must during the fermentation by strains of Saccharomyces cerevisiae. *Vitis, 11*, 222-227.

Fahey, R. C., & Newton, G. L. (1988). Determination of low molecular weight thiols using monobromobimane fluorescent labeling and high-performance liquid chromatography - NASA-CR-182932. In.

Flynn, T. M., O'Loughlin, E. J., Mishra, B., DiChristina, T. J., & Kemner, K. M. (2014). Sulfur-mediated electron shuttling during bacterial iron reduction. *Science, 344*(6187), 1039-1042. doi:10.1126/science.1252066

Fortin, C., & Campbell, P. G. C. (2001). Thiosulfate Enhances Silver Uptake by a Green Alga: Role of Anion Transporters in Metal Uptake. *Environmental Science & Technology, 35*(11), 2214-2218. doi:10.1021/es0017965

Goff, J., Terry, L., Mal, J., Schilling, K., Pallud, C., & Yee, N. (2019). Role of extracellular reactive sulfur metabolites on microbial Se(0) dissolution. *Geobiology, 17*(3), 320-329. doi:10.1111/gbi.12328

Hoffmann, M. R. (1977). Kinetics and mechanism of oxidation of hydrogen sulfide by hydrogen peroxide in acidic solution. *Environmental Science & Technology, 11*(1), 61-66.

Jiang, Y., Dong, Y., Luo, Q., Li, N., Wu, G., & Gao, H. (2014). Protection from Oxidative Stress Relies Mainly on Derepression of OxyR-Dependent KatB

and Dps in Shewanella oneidensis. *Journal of Bacteriology, 196*(2), 445. doi:10.1128/JB.01077-13

Kleinzeller, A., Kotyk, A., & Kovac, L. (1959). Utilization of Inorganic Sulphate by Baker's Yeast. *Nature, 183*(4672), 1402-1403. doi:10.1038/1831402a0

Kramer, J. R., Bell, R. A., & Smith, D. S. (2007). Determination of sulfide ligands and association with natural organic matter. *Applied Geochemistry, 22*(8), 1606-1611. doi:https://doi.org/10.1016/j.apgeochem.2007.03.026

Lewis, A. E. (2010). Review of metal sulphide precipitation. *Hydrometallurgy, 104*(2), 222-234. doi:https://doi.org/10.1016/j.hydromet.2010.06.010

Liu, D., Dong, H., Zhao, L., & Wang, H. (2014). Smectite Reduction by Shewanella Species as Facilitated by Cystine and Cysteine. *Geomicrobiology Journal, 31*(1), 53-63. doi:10.1080/01490451.2013.806609

Lohmayer, R., Kappler, A., Lösekann-Behrens, T., & Planer-Friedrich, B. (2014). Sulfur species as redox partners and electron shuttles for ferrihydrite reduction by Sulfurospirillum deleyianum. *Applied and Environmental Microbiology, 80*(10), 3141-3149. doi:10.1128/AEM.04220-13

Martínez, C. E., Jacobson, A. R., & McBride, M. B. (2004). Lead Phosphate Minerals: Solubility and Dissolution by Model and Natural Ligands. *Environmental Science & Technology, 38*(21), 5584-5590. doi:10.1021/es049617x

Millero, F. J., Gonzalez-Davila, M., & Santana-Casiano, J. M. (1995). Reduction of Fe(III) with sulfite in natural waters. *Journal of Geophysical Research: Atmospheres, 100*(D4), 7235-7244. doi:10.1029/94JD03111

Myers, C. R., & Nealson, K. H. (1988). Bacterial Manganese Reduction and Growth with Manganese Oxide as the Sole Electron Acceptor. *Science, 240*(4857), 1319-1321. doi:10.1126/science.240.4857.1319

Owens, R. A., & Hartman, P. E. (1986a). Export of glutathione by some widely used Salmonella typhimurium and Escherichia coli strains. *Journal of Bacteriology, 168*(1), 109-114. doi:10.1128/jb.168.1.109-114.1986

Owens, R. A., & Hartman, P. E. (1986b). Glutathione: a protective agent in Salmonella typhimurium and Escherichia coli as measured by mutagenicity and by growth delay assays. *Environ Mutagen, 8*(5), 659-673. doi:10.1002/em.2860080503

Park, S., & Imlay, J. A. (2003). High Levels of Intracellular Cysteine Promote Oxidative DNA Damage by Driving the Fenton Reaction. *Journal of Bacteriology, 185*(6), 1942-1950. doi:10.1128/jb.185.6.1942-1950.2003

Sekowska, A., Kung, H. F., & Danchin, A. (2000). Sulfur metabolism in Escherichia coli and related bacteria: facts and fiction. *J Mol Microbiol Biotechnol, 2*(2), 145-177. Retrieved from https://www.ncbi.nlm.nih.gov/pubmed/10939241

Shatalin, K., Shatalina, E., Mironov, A., & Nudler, E. (2011). H_2S: A Universal Defense Against Antibiotics in Bacteria. *Science, 334*(6058), 986-990. doi:10.1126/science.1209855

Siu, T., & Jia, C. Q. (1999). Kinetic and Mechanistic Study of Reaction between Sulfide and Sulfite in Aqueous Solution. *Industrial & Engineering Chemistry Research, 38*(10), 3812-3816. doi:10.1021/ie990254x

Smirnova, G. V., Muzyka, N. G., Ushakov, V. Y., Tyulenev, A. V., & Oktyabrsky, O. N. (2015). Extracellular superoxide provokes glutathione efflux from Escherichia coli cells. *Research in Microbiology, 166*(8), 609-617. doi:https://doi.org/10.1016/j.resmic.2015.07.007

Smith, D. A., Sessions, A. L., Dawson, K. S., Dalleska, N., & Orphan, V. J. (2017). Rapid quantification and isotopic analysis of dissolved sulfur species. *Rapid Commun Mass Spectrom, 31*(9), 791-803. doi:10.1002/rcm.7846

Sobota, J. M., & Imlay, J. A. (2011). Iron enzyme ribulose-5-phosphate 3-epimerase in Escherichia coli is rapidly damaged by hydrogen peroxide but can be protected by manganese. *Proceedings of the National Academy of Sciences, 108*(13), 5402. doi:10.1073/pnas.1100410108

Tiedje, J. M. (2002). Shewanella—the environmentally versatile genome. *Nature Biotechnology, 20*(11), 1093-1094. doi:10.1038/nbt1102-1093

Van Loon, L. L., Mader, E. A., & Scott, S. L. (2001). Sulfite Stabilization and Reduction of the Aqueous Mercuric Ion: Kinetic Determination of Sequential Formation Constants. *The Journal of Physical Chemistry A, 105*(13), 3190-3195. doi:10.1021/jp003803h

Wu, G., Li, N., Mao, Y., Zhou, G., & Gao, H. (2015). Endogenous generation of hydrogen sulfide and its regulation in Shewanella oneidensis. *Frontiers in microbiology, 6*, 374-374. doi:10.3389/fmicb.2015.00374

Wu, G., Wan, F., Fu, H., Li, N., & Gao, H. (2015). A Matter of Timing: Contrasting Effects of Hydrogen Sulfide on Oxidative Stress Response in Shewanella oneidensis. *Journal of Bacteriology, 197*(22), 3563-3572. doi:10.1128/jb.00603-15

Xue, H., Goncalves, M. d. L. S., Reutlinger, M., Sigg, L., & Stumm, W. (1991). Copper(I) in fogwater: determination and interactions with sulfite.

Environmental Science & Technology, 25(10), 1716-1722. doi:10.1021/es00022a006

Zhang, J., Wang, F., House, J. D., & Page, B. (2004). Thiols in wetland interstitial waters and their role in mercury and methylmercury speciation. *Limnology and Oceanography, 49*(6), 2276-2286. doi:10.4319/lo.2004.49.6.2276

Zhang, J. Z., & Millero, F. J. (1993). The products from the oxidation of H2S in seawater. *Geochimica et Cosmochimica Acta, 57*(8), 1705-1718. doi:https://doi.org/10.1016/0016-7037(93)90108-9

FIGURES:

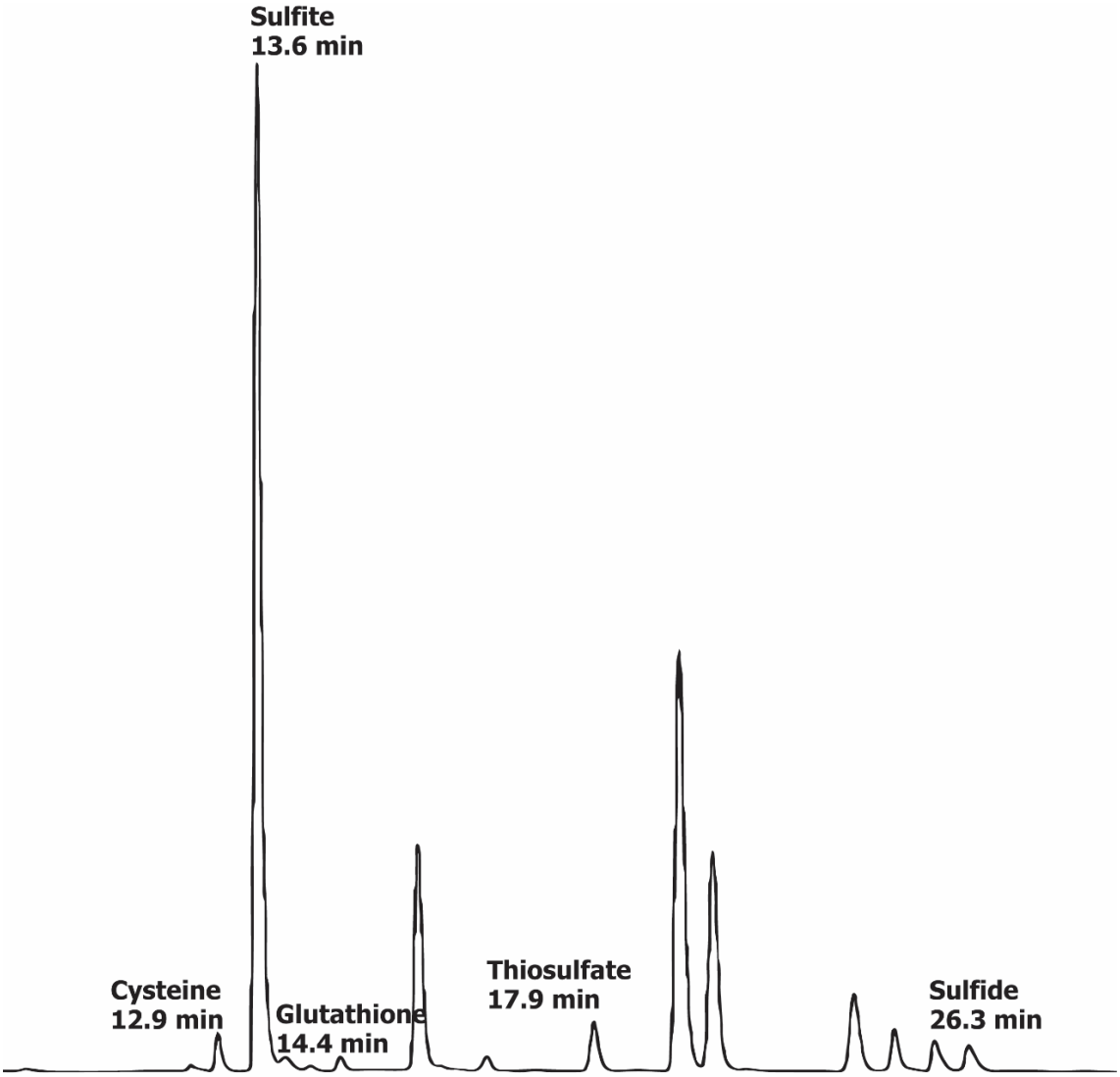

Figure 5.1. Sample chromatogram of mBBr-derivatized sulfur metabolites in the extracellular medium of *S. oneidensis* MR-1. The chromatogram is of a sample taken from a stationary phase culture grown under anaerobic conditions.

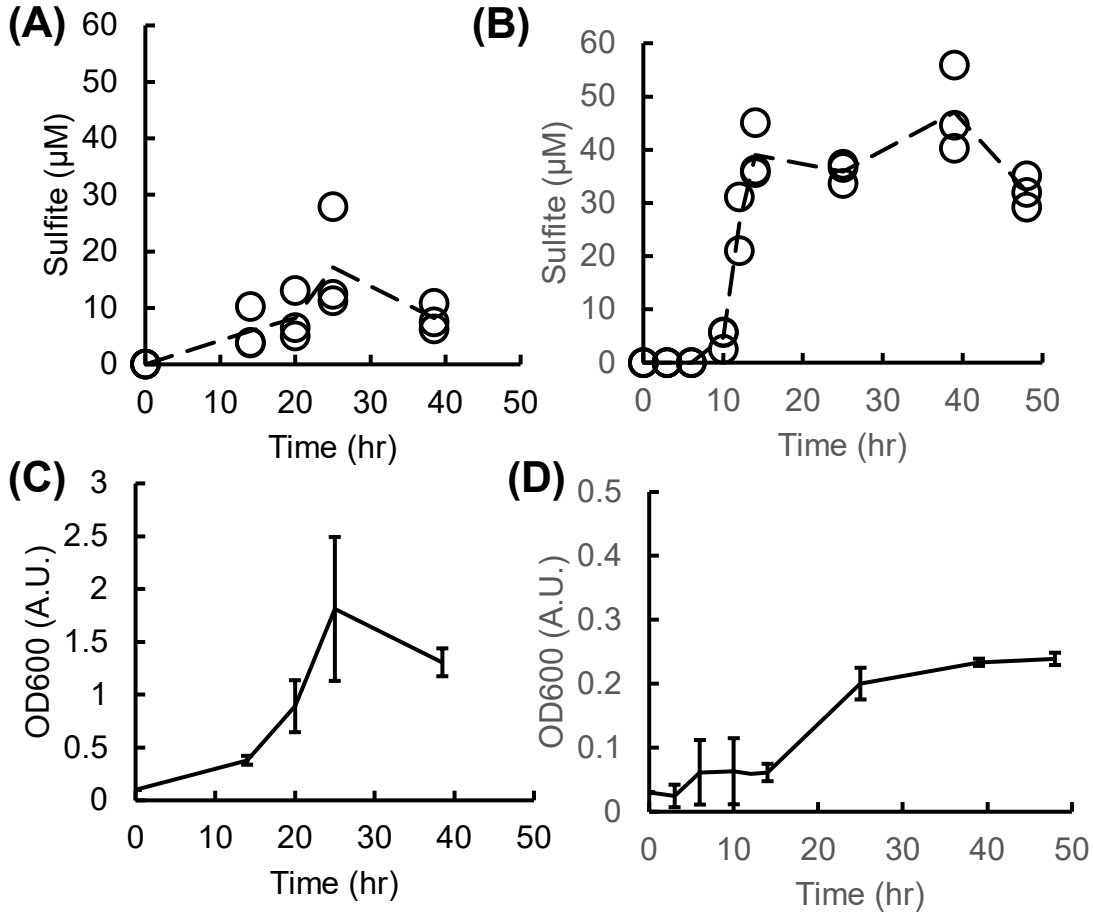

Figure 5.2. Extracellular sulfite in *S. oneidensis* MR-1 cultures. Cultures were grown in MR1 medium with lactate as a carbon source under aerobic conditions (A, C) or anaerobic conditions with fumarate as the electron acceptor (B,D). Sulfite concentrations in the cultures are shown in panels A and B. Individual replicates are shown as open circles with averages plotted as the dashed line. Optical density is shown in panels C and D as the average of three replicates with error bars (S.D.) shown. Note that the y-axes are different for panels C and D.

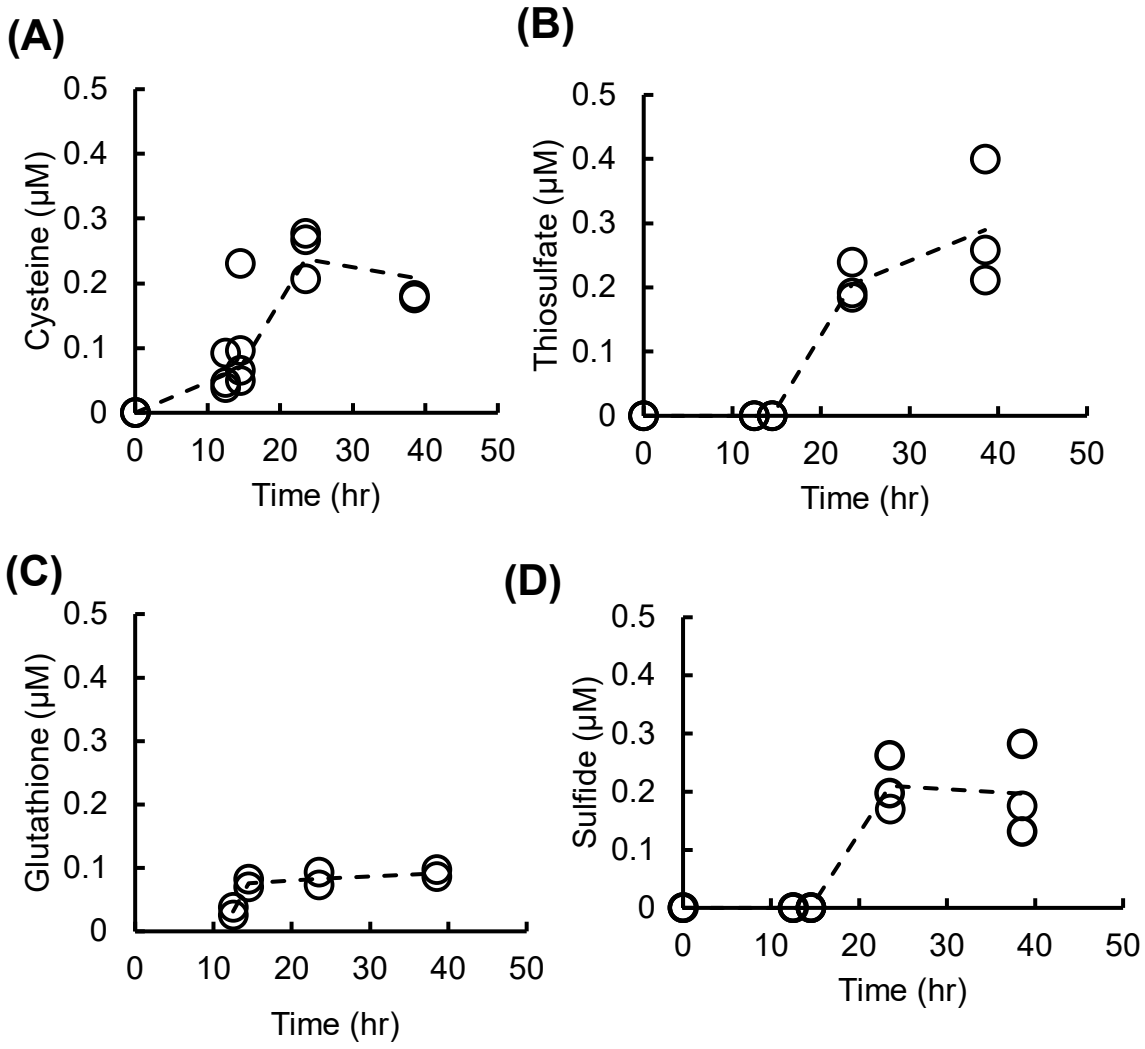

Figure 5.3. Cysteine (A),thiosulfate (B), glutathione (C), and (D) sulfide production by *S. oneidensis* MR-1 . Cells were grown under anaerobic conditions on MR1 media with lactate as a carbon source and fumarate as the terminal electron acceptor. Individual replicates (at least two per timepoint) are shown as open circles with averages plotted as the dashed line. Note that the scale of the y-axis is different from the scale of the y-axis in the sulfite plots in **Figure 5.2.**

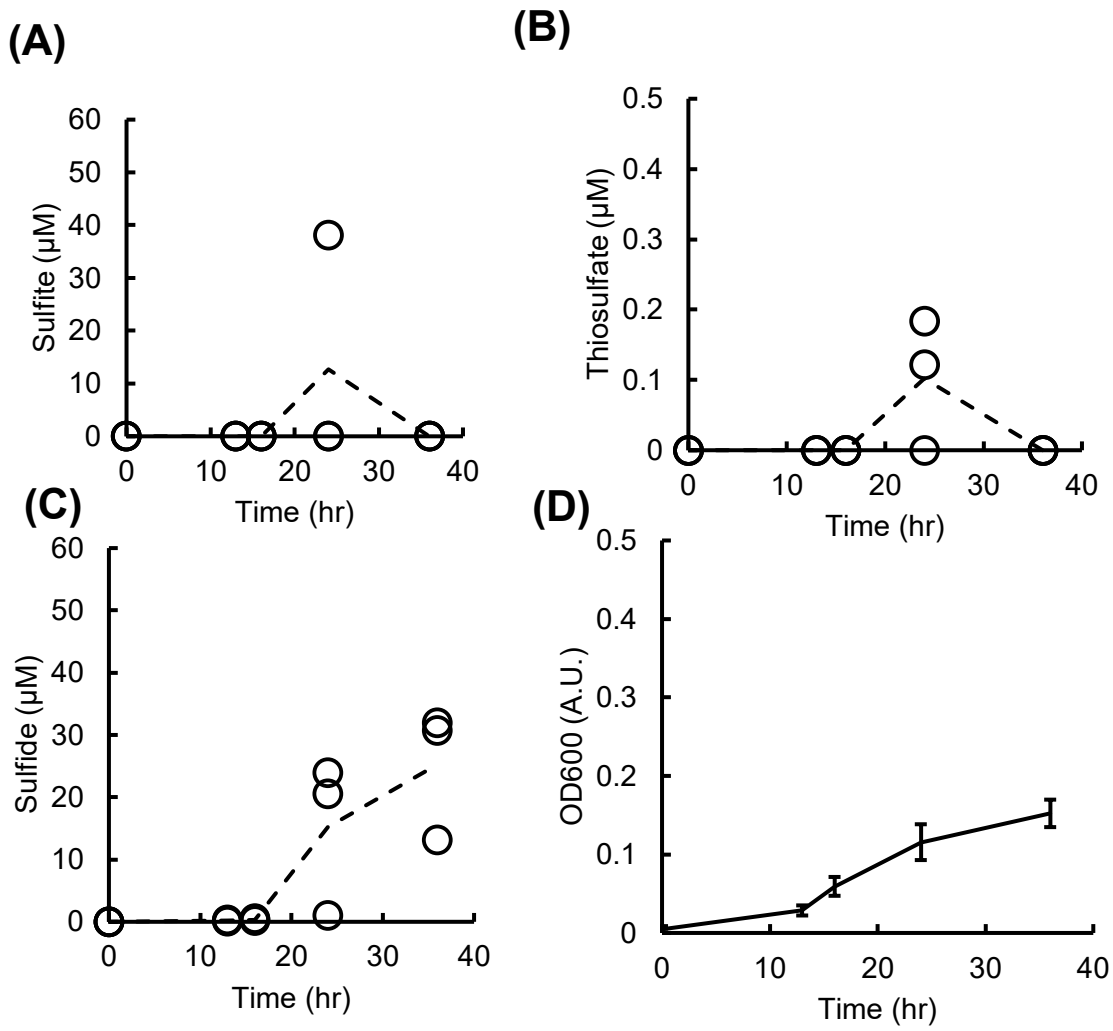

Figure 5.4. Sulfite (A), sulfide (C), and thiosulfate (B) production by *S. oneidensis* MR1 on sulfate-limited medium with cysteine added as a sulfur source. Cell density is shown in panel D. Cells were grown on MR1 lactate medium under anaerobic conditions with lactate as a carbon source and fumurate the electron acceptor. For panel D, the line represents the average of three replicates and error bars represent the standard deviation. For panels A-C, individual replicates are shown as open circles with averages plotted as the

dashed line. Note that the scale of the y-axis is different between panel B and panels A and C.

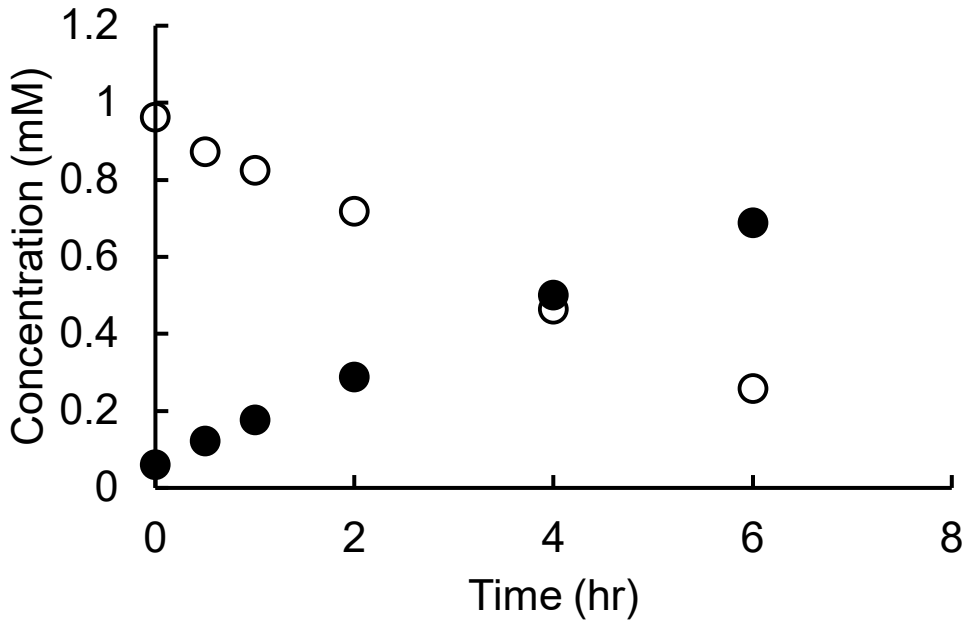

Figure 5.5. Oxidation of sulfite to sulfate in Milli-Q water under aerobic conditions. 1 mM sulfite was prepared in Milli-Q water. Samples were collected at regular intervals and immediately analyzed by ion chromatography. Black circles represent sulfate concentrations and unfilled circles represent sulfite concentrations.

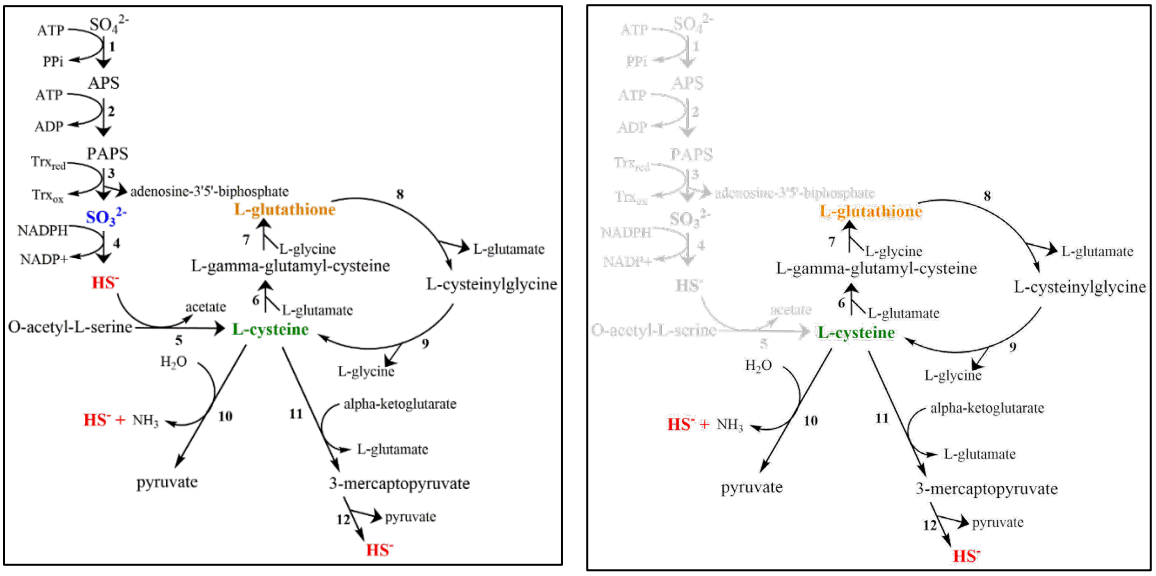

Figure 5.6. Identification of sulfur metabolic pathways of *S. oneidensis* MR-1 cells predicted to be active during growth on sulfate (A) or cysteine (B) as the sulfur source. Metabolites detected in this study are highlighted in color. KEGG was used to identify sulfur metabolic pathways. Abbreviations are: sulfate (SO_4^{2-}), adenosine-5'-phosphosulfate (APS), 3'-phosphoadenylyl-sulfate (PAPS), adenosine triphosphate (ATP), adenosine diphosphate (ADP), pyrophosphate (PPi), thioredoxin reduced/oxidized ($Trx_{red/ox}$), sulfite (SO_3^{2-}), sulfide (HS^-), nicotinamide adenine dinucleotide phosphate (NADP+/NADPH).

Enzymes for the pathways are numbered on the diagram and are as follows. **(1)** sulfate adenylyltransferase CysDN (SO_3726, SO_3727), **(2)** adenylyl sulfate kinase CysC (SO_3723), **(3)** thioredoxin-dependent phosphoadenylyl-sulfate reductase CysH (SO_3736), **(4)** sulfite reductase CysIJ (SO_3737, SO_3738), **(5)** cysteine synthase CysK (SO_2903), **(6)** glutamate-

cysteine ligase GshA (SO_3559), **(7)** glutathione synthase GshB (SO_0831), **(8)** gamma-glutamyltransferase GgtAB (SO_1952, SO_0741), **(9)** aminopeptidases PepA (SO_0959, SO_1117, SO_1368), PepB (SO_0876), PepD (SO_1115), PepN (SO_1059, SO_2600), **(10)** methionine gamma-lyase MdeA (SO_1812), O-acetylhomoserine-lyase MetY (SO_1095), **(11)** aspartate (cysteine) aminotransferase aspC (SO_2406), **(12)** mercaptopyruvate sulfurtransferase SseA (SO_1261).

CHAPTER 6
CONCLUSIONS AND FUTURE DIRECTIONS

This dissertation presents several illustrative examples of how microbial sulfur metabolism plays an important role in mediating the toxicity and biogeochemistry of metalloids. In **Chapters 2** and **3** of this thesis, I demonstrated that cellular sulfur metabolism is involved in the transport, reduction of, and toxicity of tellurate. I showed that in addition to selenate and selenite, the sulfate transporter CysPUWA also transports tellurate into the cytoplasm. In contrast, the high-specificity sulfate transporter of *E.* coli – CysZ— does not appear to play a role in tellurate transport and toxicity. When the CysPUWA transporter was inactivated, less tellurate was removed from the media compared to the wild-type strain. Additionally, I observed less darkening of the media—the classic indicator of elemental tellurium formation—in this mutant strain. This supports a model in which tellurate is transported into the cytoplasm for its final reduction to elemental tellurium. Tellurate transport into the cytoplasm appears to be a necessary step in mediating the toxic effects of the compound. Tellurate sensitivity was significantly decreased in the strain carrying a mutation in the CysPUWA transporter.

Future work should investigate if other transporters are involved in tellurate uptake. For tellurite, there is not a single dedicated transporter for its entry into the cells (Elías et al., 2012; Elías et al., 2015). It seems likely that they may also be the case for tellurate. I still observed tellurate uptake – albeit significantly diminished—by the strain carrying the CysPUWA mutation. Thus,

another transporter (or transporters) is likely playing a secondary role in tellurate transport into the cells. Targets for exploring this question would first be the known tellurite transporters: PitA and ActP. Another possibility is the molybdate transporter ModABC which will also non-specifically transport substrates other than molybdate such as sulfate and tungstate (Aguilar-Barajas, Díaz-Pérez, Ramírez-Díaz, Riveros-Rosas, & Cervantes, 2011)

Finally, the work done in **Chapter 2** with tellurate transport and by others with tellurite transport (Borsetti, Toninello, & Zannoni, 2003; Elías et al., 2012; Elías et al., 2015) demonstrates the important role that cellular uptake into the cytoplasm plays in the toxicity of tellurate and tellurite. It would be interesting to determine if differences in rates of uptake control differences in tellurate/tellurite sensitivity between organisms. Are cells that are naturally deficient in tellurate/tellurite also more resistant to these compounds? Extending this idea further, some organisms have been suggested to reduce tellurate and tellurite in the periplasm (Maltman, Donald, & Yurkov, 2017). Does this localization of the tellurate/tellurite reduction activity to the periplasm have an impact on their toxicity towards the cells?

What happens when tellurate enters the cytoplasm is described in **Chapter 3.** This question has only recently begun to be explored by researchers without any sort of definitive answer. A previous study by our lab showed that inactivation of genes involved in molybdopterin biosynthesis inhibit tellurate reduction. However, a specific tellurate reductase was never identified (Theisen, Zylstra, & Yee, 2013). Interestingly, the Δ*cysW* mutant first came to my attention

when I was screening the Keio Collection library for mutants that had lost the ability to reduce tellurate. However, I fortuitously stumbled upon the phenomenon that *E. coli* is significantly more resistant to tellurate when grown on minimal defined media compared to when it is grown on a rich media. The MICs of tellurate on these differing media types are two orders of magnitude apart (0.015 vs. 1 mM). I was curious to know the basis for this observation rather than brushing it off as merely "rich media effects". Understanding the mechanism underlying this phenomenon provides important insights into the cellular toxicity of tellurate.

What I found was that cystine played an important role the increased toxicity of tellurate when cells were grown on a rich media background. Cystine is the oxidized form of cysteine that is found in commercial media nutritional supplements (e.g., yeast extract, tryptone, peptone, etc.). I found that cystine must be transported into the cytoplasm for this potentiation of the toxicity of tellurate to be observed. Cystine will be reduced to cysteine once inside the cytoplasmic compartment of *E. coli* (Chonoles Imlay, Korshunov, & Imlay, 2015). I hypothesized that the tellurate and the cysteine may be reacting intracellularly and that that interaction is key in the toxicity of tellurate. Indeed, I found that when intracellular thiols are oxidized with the oxidizing-agent diamide, that the cells' resistance to tellurate increases. These diamide-exposed cultures were also observed to form less elemental tellurium, suggesting a role for intracellular thiols in tellurate reduction and toxicity. In a series of *in vitro* experiments, I observed that tellurate reduction to elemental tellurium occurs concurrent to

cysteine oxidation. Since tellurite may form as an intermediate of this reaction, I confirmed that cysteine will similarly reduce tellurite to elemental tellurium. Together, these results suggest that cysteine reduces tellurate intracellularly and that this reaction contributes to the cellular toxicity of tellurate. For many metals, their intracellular reduction by thiols or enzymes is often a mechanism of detoxification (Lloyd & Lovley, 2001). Tellurate is interesting in that it seemingly goes counter to this general trend. It is important for future work to clarify whether this is simply due to its reduction to the more toxic intermediate tellurite by cysteine or if the reaction itself is inherently detrimental, such as if reactive oxygen species (ROS) are being produced concurrent to the reaction. The latter has been observed during the *in vitro* reduction of tellurite by catalase and is a well-characterized phenomenon during selenite reduction by glutathione (Kessi & Hanselmann, 2004; Pérez et al., 2007)

Interestingly, when thiol oxidation is measured *in vivo* following tellurate exposure, I observed substantial depletion of the glutathione pool but only minor (but still significant) depletion of the cysteine pool. When tellurate was reacted with glutathione *in vitro* no reaction was observed. Thus, glutathione may be depleted secondary to cysteine depletion in order to maintain cysteine pools within the cell and/or glutathione may be depleted in reaction with the tellurite that may form from tellurate reduction. While it was already known that tellurite exposure depletes the glutathione pool of *E. coli*, the reaction between the two has never actually been characterized (Turner, Aharonowitz, Weiner, & Taylor, 2001). Since tellurite may form during tellurate reduction, I then reacted tellurite

with glutathione *in vitro*. What I observed was that no elemental tellurium forms from this reaction. However, unlike tellurate, I observed significant oxidation of glutathione in these reactors. This suggests that the two react forming a soluble tellurium intermediate. Since further glutathione oxidation is not observed when glutathione is added in excess of the 4:1 ratio of glutathione:tellurite, I propose that 4 mol glutathione will react with 1 mol tellurite to form 4 mol of tellurodiglutathione, comparable to the reduction of selenite with glutathione. However, this reaction differs from the reaction between selenite and glutathione because when glutathione is in excess, it will reduce the selenodiglutathione further to glutathioselenol which spontaneously dismutates to elemental selenium and glutathione (Turner, Weiner, & Taylor, 1998). However, I failed to observe elemental tellurium formation when glutathione is added in excess. To my knowledge, this is the first time anyone has characterized the reaction between tellurite and glutathione as most work has assumed that glutathione and other thiols will directly reduce tellurite to elemental tellurium (Chasteen, Fuentes, Tantaleán, & Vásquez, 2009).

Future work should focus on the chemical reactions between tellurite, tellurate, and intracellular thiols. These reactions have been characterized to a considerable depth in respect to selenite (Kessi & Hanselmann, 2004). However, we are unaware of any reports of interactions between tellurate and biological thiols. Additionally, even though tellurite has been well-studied, it is often assumed that it is directly reduced to elemental tellurium by cellular thiols, the exact reaction mechanism and stable intermediates have never been

characterized. We also show here that—at least in regards to tellurate and tellurite—that "cellular thiols" cannot be considered as the homogenous entity they are often portrayed as (Chasteen et al., 2009). While cysteine reduces both tellurite and tellurate to elemental tellurium without the formation of stable intermediates, glutathione is non-reactive with tellurate and reduces tellurite to another soluble form rather than to elemental tellurium. It would be interesting to try to identify the soluble intermediate(s) that form(s) in the reaction of glutathione with tellurite. This could potentially be important in understanding the toxicity of tellurate and tellurite. For example, selenite reacts with glutathione to form various soluble reduced intermediates including selenide. The selenide formed by this reaction appears to mediate selenite toxicity independent of ROS formation (Tarze et al., 2007). Selenodiglutathione is toxic to mammalian cell lines and triggers cell-death via ROS-independent patheays (Wallenberg et al., 2014; Wu, Lanfear, & Harrison, 1995). These soluble intermediates of tellurate/tellurite reduction could possibly explain the observation of others that tellurite remains toxic to cells under anaerobic conditions (albeit to a lesser extent than under aerobic conditions) (Presentato, Turner, Vasquez, Yurkov, & Zannoni, 2019). It also would be interesting to explore how tellurate and tellurite react with the other major intracellular thiols of *E. coli*—such as acetyl-CoA and homocysteine—as well as the intracellular thiols of other organisms not found in *E. coli* such as bacillithiol and mycothiol.

I then shifted my focus from intracellular tellurate reduction to extracellular interactions of sulfur metabolites with selenium. In **Chapter 4** I

isolated a *Bacillus* species (*Bacillus* sp. JG17) from seleniferous soils in the Punjab region of India. While much attention has been given to the reduction of the selenium oxyanions to elemental selenium, very little work has been done in the opposite direction: the mobilization of elemental selenium to its more soluble and toxic forms. The mechanism by which organisms solubilize elemental selenium remain unknown. After learning that the observed selenium-solubilization activity was localized to the extracellular compartment, I focused on characterizing the extracellular metabolites produced by *Bacillus* sp. JG17. I observed that this strain produces stable and detectable quantities of sulfide, sulfite, and thiosulfate under aerobic conditions. These concentrations of the sulfur metabolites are reactive with elemental selenium and solubilize it to the extents observed in our cultures. The results of this study demonstrated that biogenic inorganic sulfur metabolites have the potential to impact the solubility and speciation of selenium compounds in the environment.

In future studies, it would be interesting to directly measure the selenosulfur compounds formed in the reaction between biogenic sulfur compounds and elemental selenium. Determining their stability and if they are ultimately oxidized to selenite and/or selenate is also crucial. However, this work is challenging to pursue due to the lack of established methods for analytical detection of selenosulfur compounds, the lack of standard reference materials for selenosulfur compounds, and the question of how stable these compounds are in solution with regards to sample/standard preparation and storage. A recent study did use anion-exchange chromatography coupled to inductively coupled plasma

mass spectrometry (ICP-MS) to qualitatively detect selenosulfate in flue gas desulfurization waters so it is possible to at least detect (but perhaps more challenging to quantify) selenosulfur species in environmental samples.

Finally, in **Chapter 5** I was interested in exploring extracellular sulfur metabolite production by other organisms grown under non sulfur-respiring conditions. *Bacillus* sp. JG17 was a novel isolate and so no system for genetic manipulation exists that would allow for the ready use genetic tools to determine the mechanisms by which it produces and secretes sulfur metabolites. Instead I chose *Shewanella oneidensis* MR-1 to shift my focus on to. *S. oneidensis* MR-1 produces large quantities of sulfite during both aerobic growth and anaerobic growth with fumarate as an electron acceptor. While *S. oneidensis* MR-1 does respire elemental sulfur, thiosulfate, and sulfite, these experiments were performed under non-sulfur-respiring conditions. Higher production of sulfite was observed during anaerobic growth, likely due to the greater stability of the sulfite under anoxic conditions. Low quantities of thiosulfate, glutathione, cysteine, and sulfide were observed when the cells were grown with sulfate as the sulfur source. However, when the cells were switched to cysteine as a sulfur source, large quantities of sulfide were also detected.

Interestingly, when *S. oneidensis* MR-1 is switched from sulfate to cysteine as a sulfur source, sulfite production is repressed. This suggests that the sulfite may originate from the assimilatory sulfate reduction pathways, similar to sulfite production by eukaryotic yeasts (Hansen & Kielland-Brandt, 1996). It also seemingly rules out the possibility that sulfite is produced from cysteine

degradation (such as by a cysteine dioxygenase enzyme). I observed sulfide production rather than sulfite production when cysteine was provided as a sulfur source and did not identify any homologs to cysteine dioxygenases in the *S. oneidensis* MR-1 genome. However, it is also possible that cysteine may suppress sulfite export and that substantial quantities of sulfite may still be formed intracellularly under these conditions. Quantifying intracellular sulfite concentrations in cells grown on different sulfur sources could provide important insights into the dynamics of sulfur metabolism in *S. oneidensis* MR-1.

Future studies with *S. oneidensis* MR-1 should focus on identifying the transporter responsible for sulfite efflux. Sulfite efflux pumps are poorly characterized in bacteria. It has been suggested that the transmembrane protein TauE (CNE_RS30450) of the betaproteobacterium *Cupriavidus necator* may function as a sulfite efflux pump (Weinitschke, Denger, Cook, & Smits, 2007). Five possible homologs to this protein were identified in the genome of *S. ondeidensis* MR-1. These include four different 4-toluene sulfonate uptake permease family proteins (NP_717426.1, E=7e-19, Identity=12%, Similarity=27%; NP_716953.2, E=9e-11, Identity=9%, Similarity=28%; NP_717492.1, E=1e-8, Identity=8%, Similarity=24%; NP_719588.1, E=4e-7, Identity=16%, Similarity=35%) and the glycine uptake transporter YfcA (NP_718418.2, E=6e-18, Identity=11%, Similarity=28%). These proteins are all members of the TauE superfamily of proteins. In *Saccharomyces cerevisiae* and other fungi SSU1 is a well-characterized sulfite efflux pump (Park & Bakalinsky, 2000). A homolog to this transporter was found in the *S. oneidensis* MR-1 (E=4e-

14, Identity= 12%, Similarity= 24%). This protein is annotated as a tellurite resistance/dicarboxylate transporter (TDT) family protein (NP_718478.1).

Since all organisms—both prokaryotic and eukaryotic—have similar central sulfur metabolic pathways and produce intracellular thiols the findings described in this dissertation are likely transferrable to other organisms beyond *E. coli*, *Bacillus* sp. JG17, and *S. oneidensis* MR-1. Tellurium is an emerging environmental contaminant and as such it will become increasingly important to understand its biological processing. I showed that the inorganic metabolites of the central sulfur metabolic pathways are also important in controlling the speciation and solubility of selenium, and this process likely extends to tellurium. Biogenic sulfite, thiosulfate, and sulfide will solubilize elemental selenium, and possibly elemental tellurium, to its more mobile and—once the compounds are confirmed—likely more toxic forms. Other organisms will also produce these sulfur metabolites under non-sulfur respiring conditions—as we demonstrate with *S. oneidensis* MR-1. Thus, these organisms could potentially be a major source of biogenic sulfur metabolites in environments that are not sufficiently reducing to support sulfur respiratory metabolism. These biogenic sulfur metabolites then have the potential to not only impact the speciation and solubility of tellurium and selenium, but many other sulfur-reactive metals and metalloids as well.

REFERENCES:

Aguilar-Barajas, E., Díaz-Pérez, C., Ramírez-Díaz, M. I., Riveros-Rosas, H., & Cervantes, C. (2011). Bacterial transport of sulfate, molybdate, and related oxyanions. *BioMetals, 24*(4), 687-707. doi:10.1007/s10534-011-9421-x

Borsetti, F., Toninello, A., & Zannoni, D. (2003). Tellurite uptake by cells of the facultative phototroph Rhodobacter capsulatus is a ΔpH-dependent process. *FEBS Letters, 554*(3), 315-318. doi:https://doi.org/10.1016/S0014-5793(03)01180-3

Chasteen, T. G., Fuentes, D. E., Tantaleán, J. C., & Vásquez, C. C. (2009). Tellurite: history, oxidative stress, and molecular mechanisms of resistance. *FEMS Microbiology Reviews, 33*(4), 820-832. doi:10.1111/j.1574-6976.2009.00177.x

Chonoles Imlay, K. R., Korshunov, S., & Imlay, J. A. (2015). Physiological Roles and Adverse Effects of the Two Cystine Importers of Escherichia coli. *Journal of Bacteriology, 197*(23), 3629. doi:10.1128/JB.00277-15

Elías, A., Abarca, M. J., Montes, R. A., Chasteen, T. G., Pérez-Donoso, J. M., & Vásquez, C. C. (2012). Tellurite enters Escherichia coli mainly through the PitA phosphate transporter. *MicrobiologyOpen, 1*(3), 259-267. doi:10.1002/mbo3.26

Elías, A., Díaz-Vásquez, W., Abarca-Lagunas, M. J., Chasteen, T. G., Arenas, F., & Vásquez, C. C. (2015). The ActP acetate transporter acts prior to the PitA phosphate carrier in tellurite uptake by Escherichia coli. *Microbiological Research, 177*, 15-21. doi:http://dx.doi.org/10.1016/j.micres.2015.04.010

Hansen, J., & Kielland-Brandt, M. C. (1996). Inactivation of MET10 in brewer's yeast specifically increases SO2 formation during beer production. *Nat Biotech, 14*(11), 1587-1591. Retrieved from http://dx.doi.org/10.1038/nbt1196-1587

Kessi, J., & Hanselmann, K. W. (2004). Similarities between the Abiotic Reduction of Selenite with Glutathione and the Dissimilatory Reaction Mediated by Rhodospirillum rubrum and Escherichia coli. *Journal of Biological Chemistry, 279*(49), 50662-50669. doi:10.1074/jbc.M405887200

Lloyd, J. R., & Lovley, D. R. (2001). Microbial detoxification of metals and radionuclides. *Current opinion in biotechnology, 12*(3), 248-253. doi:https://doi.org/10.1016/S0958-1669(00)00207-X

Maltman, C., Donald, L. J., & Yurkov, V. (2017). Two distinct periplasmic enzymes are responsible for tellurite/tellurate and selenite reduction by strain ER-Te-48 associated with the deep sea hydrothermal vent tube

worms at the Juan de Fuca Ridge black smokers. *Archives of Microbiology, 199*(8), 1113-1120. doi:10.1007/s00203-017-1382-1

Park, H., & Bakalinsky, A. T. (2000). SSU1 mediates sulphite efflux in Saccharomyces cerevisiae. *Yeast, 16*(10), 881-888. doi:10.1002/1097-0061(200007)16:10<881::AID-YEA576>3.0.CO;2-3

Pérez, J. M., Calderón, I. L., Arenas, F. A., Fuentes, D. E., Pradenas, G. A., Fuentes, E. L., . . . Vásquez, C. C. (2007). Bacterial Toxicity of Potassium Tellurite: Unveiling an Ancient Enigma. *PLOS ONE, 2*(2), e211. doi:10.1371/journal.pone.0000211

Presentato, A., Turner, R. J., Vasquez, C. C., Yurkov, V., & Zannoni, D. (2019). Tellurite-dependent blackening of bacteria emerges from the dark ages. *Environmental Chemistry, 16*(4), 266-288. doi:10.1071/EN18238

Tarze, A., Dauplais, M., Grigoras, I., Lazard, M., Ha-Duong, N. T., Barbier, F., . . . Plateau, P. (2007). Extracellular production of hydrogen selenide accounts for thiol-assisted toxicity of selenite against Saccharomyces cerevisiae. *J Biol Chem, 282*(12), 8759-8767. doi:10.1074/jbc.M610078200

Theisen, J., Zylstra, G. J., & Yee, N. (2013). Genetic Evidence for a Molybdopterin-Containing Tellurate Reductase. *Applied and Environmental Microbiology, 79*(10), 3171-3175. doi:10.1128/aem.03996-12

Turner, R. J., Aharonowitz, Y., Weiner, J. H., & Taylor, D. E. (2001). Glutathione is a target in tellurite toxicity and is protected by tellurite resistance determinants in Escherichia coli. *Canadian Journal of Microbiology, 47*(1), 33-40.

Turner, R. J., Weiner, J. H., & Taylor, D. E. (1998). Selenium metabolism in Escherichia coli. *BioMetals, 11*(3), 223-227. doi:10.1023/A:1009290213301

Wallenberg, M., Misra, S., Wasik, A. M., Marzano, C., Björnstedt, M., Gandin, V., & Fernandes, A. P. (2014). Selenium induces a multi-targeted cell death process in addition to ROS formation. *Journal of cellular and molecular medicine, 18*(4), 671-684. doi:10.1111/jcmm.12214

Weinitschke, S., Denger, K., Cook, A. M., & Smits, T. H. M. (2007). The DUF81 protein TauE in Cupriavidus necator H16, a sulfite exporter in the metabolism of C2 sulfonates. *Microbiology, 153*(9), 3055-3060. doi:https://doi.org/10.1099/mic.0.2007/009845-0

Wu, L., Lanfear, J., & Harrison, P. R. (1995). The selenium metabolite selenodiglutathione induces cell death by a mechanism distinct from

H2O2 toxicity. *Carcinogenesis, 16*(7), 1579-1584. doi:10.1093/carcin/16.7.1579

APPENDIX 1

ISOLATION AND DRAFT GENOME OF A TELLURATE-RESISTANT ENTEROBACTER SPECIES FROM THE HUDSON RIVER,

OR

WHAT IS "HIGHLY TELLURATE-RESISTANT" ANYWAYS?

INTRODUCTION

While tellurate reduction and resistance has been given relatively little attention in general, what little attention it has received has mainly focused on enriching for "highly-resistant" tellurate-reducing organisms from environments that have high levels of tellurium present (Baesman et al., 2007; Csotonyi, Stackebrandt, & Yurkov, 2006; Maltman, Piercey-Normore, & Yurkov, 2015). Indeed, in Maltman et. al., the *Pseudomonas* strain isolated from gold mine tailings is purported to have "…very high levels of aerobic and anaerobic resistance to metal(loid) oxides…" (Maltman et al., 2015). Gold mine tailings are often cited as examples of environments where high concentrations of tellurium compounds are present due to the association of tellurides with gold (Wray, 1998). However, the concept of "highly tellurate resistant" appears poorly constrained. In this study, we isolated a microorganism from river sediments that do not have historical Te

contamination that had levels of tellurate resistance comparable to some of the "highly-resistant" strains reported in the literature (**Table A1.3**). It was our goal to demonstrate that the ability to reduce tellurate and to be resistant to "higher" levels of tellurate are not exclusive to organisms isolated from deep sea vents, gold mine tailings, and other contaminated environments. Additionally, we conducted a review of the literature to try to determine the reported extremes of tellurate resistance. We also consider comparability of these results in regards to methodology used.

MATERIALS AND METHODS

Isolation and identification

Sediment samples were collected in Hoboken New Jersey along the lower Hudson River in December of 2014. A small amount of the sediment was inoculated in artificial seawater medium and shaken at 30 °C for 5 days. After that point, the culture was spread on M9 plates with 0.4% glucose and 100 μM tellurate and incubated at room temperature until darkening of colonies growing on plates was observed ("M9," 2006). The darkening of the colonies was indicative of tellurate reduction to elemental tellurium. Several colonies were selected and streaked out on the same medium for further isolation and identification.

Genome sequencing and analysis

DNA was extracted using a PowerSoil DNA Isolation Kit (MOBIO). The draft genome for HRSW was generated at MicrobesNG (Birmingham, UK). The procedure to genome sequencing is as follows. Genomic DNA was purified using an equal volume of SPRI beads and then resuspended in EB buffer. DNA was quantified in triplicates with the Quantit dsDNA HS assay in an Ependorff AF2200 plate reader. Genomic DNA libraries were prepared using Nextera XT Library Prep Kit (Illumina, San Diego, USA) following the manufacturer's protocol with the following modifications: 2 ng of DNA were used as input, and PCR elongation time was 1 minute. DNA quantification and library preparation were carried out on a Hamilton Microlab STAR automated liquid handling system. Pooled libraries were quantified using the Kapa Biosystems Library Quantification Kit for Illumina on a Roche light cycler 96 qPCR machine. Libraries were sequenced on the Illumina HiSeq using a 250bp paired end protocol. Reads were adapter trimmed using Trimmomatic 0.30 with a sliding window quality cutoff of Q15 (Bolger, Lohse, & Usadel, 2014). De novo assembly was performed on samples using SPAdes version 3.7 (Bankevich et al., 2012), and contigs were annotated using Prokka 1.11 (Seemann, 2014). PATRIC was used to obtain genome statistics and for genome analysis (Gillespie et al., 2011).

BLAST was used to search for annotated sequences with high sequence homology to the 16S sequence to determine phylogeny (Altschul, Gish, Miller, Myers, & Lipman, 1990). 16S rRNA gene sequences of isolates and representative *Enterobacteriacae* species were aligned with MUSCLE. Alignments were

trimmed to aligned regions and a phylogenetic tree was constructed with MEGA 7 using the Maximum Likelihood Method with 100 bootstraps.

Growth characteristics on tellurate

To confirm reduction of tellurate to Te(0), the loss of soluble tellurium in the medium was measured using ICP-OES. Triplicate cultures and triplicate autoclaved controls were prepared by diluting overnight cultures into M9 medium. Cells were growth in a shaking incubator at 200rpm and 30 °C. After 24 hours of growth, cultures were spiked with 0.1 mM tellurate. Samples were collected immediately after the tellurate spike and again after 48 hours of incubation with tellurate.

Samples for tellurium analysis were filtered (0.2 μm filters), acidified (2% nitric acid), and then analyzed using an iCAP 7400 ICP-OES analyzer (Thermo Fisher) at a wavelength of 214.282 nm. The loss dissolved tellurium from the aqueous medium was attributed to cellular accumulation and reduction to Te(0).

The minimum inhibitory concentration (MIC) of tellurate for HRSW in different medium was determined. An overnight culture of cells was washed in phosphate-buffered saline solution and diluted back to a starting cell density of 5 x 10^5 cells/mL in 96-well plates containing the indicated medium. Tellurate was added to individual wells at concentrations ranging from 0 to 3 mM. MIC experiments were performed in M9 medium (see recipe above), LB medium ("LB (Luria-Bertani) liquid medium," 2006), and M9 medium supplemented with tryptone (10 g/L), yeast extract (5 g/L), casamino acids (3 g/L), and cystine (0.04

g/L). The concentrations for tryptone, yeast extract, and casamino acids were determined either based on their concentrations in LB medium (tryptone and yeast extract) or based on the estimated concentration of cystine in the supplement (casamino acids) so as to match the approximate concentration of cystine present in LB medium. Estimates of cystine concentrations in the medium components were obtained from the manufacturer (BD). The concentration of cystine supplement added was intended to be similar to the concentration of cystine estimated to be present in LB medium (0.04 g/L).

RESULTS AND DISCUSSION

Isolation and characterization

HRSW was isolated from the lower Hudson river in Hoboken, NJ. The organism was one of several that formed dark-colored colonies on M9 medium plates containing 100 μM tellurate (**Figure A1.1A**). The strain was found to be capable of growth at high concentrations of tellurate with an MIC on M9 medium of 3 mM (**Table A1.1**). Visible reduction of tellurate to Te(0) was observed in live cultures of HRSW through the formation of a black/brown precipitate within the culture (**Figure A1.1B**). No visible formation of of Te(0) was observed in the autoclaved control (**Figure A1.1B**). Total soluble tellurium was measured using ICP-OES. The loss of soluble tellurium over time in the live cultures confirmed that HRSW was reducing tellurate to Te(0) (**Figure A1.3**). Tellurate reduction occurred at a rate of 230 ± 30 nM/hr in the live cultures and 42 ± 33 nM/hr in the autoclaved controls.

MIC on different media

In **Chapter 3** it was demonstrated that the toxicity of tellurate (as well as selenite, selenite, and tellurite) towards *Escherichia coli* was heavily dependent on the presence of cystine in the growth medium. Cystine can be added as a separate chemical or it exists as a component of nutrient supplements such as yeast extract, peptone, beef extract, etc. A similar cystine-dependence was observed in HRSW (**Table A1.1)**. As both HRSW and *E. coli* are members of the same family, *Enterobacteriaceae*, it is difficult to say if this observation represents a ubiquitous phenomenon. However, it does suggest that this observation is more than just a quirk of the K-12 laboratory strains of *E. coli*. Similar experiments should be performed in organisms taken from a broader taxonomic range.

Genome and Phylogeny

The draft genome of HRSW consists of 110 contigs with the longest at 320,521 bp. The entire draft genome is 4,855,081 bp long. The overall GC content of the genome is 54.89%. The 16S rRNA gene sequence was retrieved and a BLAST search was used to determine the phylogeny of HRSW. The 16S rRNA gene of HRSW has 99% similarity to that of *Enterobacter asburiae* (**Figure A1.2**). Strain HRSW therefore will be called *Enterobacter* sp. HRSW.

Literature Review and Discussion

HRSW was isolated from an environment (the Hudson river) where tellurium is not expected to be present in significant quantities, but nonetheless exhibited tellurate resistance comparable to *Pseudomonas* strains found in tellurium-contaminated gold mine tailing. The MICs for tellurate for *Pseudomonas* sp. CM3 are 3.9 and 3.2 for aerobic and anaerobic conditions, respectively (**Table A1.3)**. These are relatively similar values to what we observe here (3 mM) for HRSW. Further review of the literature revealed many organisms with MICs for tellurate reported in the range of 1-4 mM (**Table A1.3**). In fact, *E. coli* is one of the few organisms reported to have a relatively low MIC for tellurate, three orders of magnitude below many of the others (Araya et al., 2004). However, we observed in **Chapter 3** that when *E. coli* is grown on M9 medium with no additional nutrient enrichment the MIC of tellurate is 1 mM (compared 0.015 mM on LB medium). Thus, it seems that these >1 mM values that are reported in some sources as "high" may just be the norm for many organisms. Additionally, an organism's innate level of resistance to tellurate appears to be independent of the location it was isolated from. Organisms isolated from clinical environments show similar levels of resistance as those isolated from deep sea vents and mine tailings (Csotonyi et al., 2006; Harrison, Ceri, Stremick, & Turner, 2004; Maltman et al., 2015).

A review of the literature also makes apparent that there is no standardization in methodology in how the MIC of tellurate is determined for different organisms, making it impossible for researchers to label their particular

strain “highly resistant”. This is unsurprising given that tellurate has not been heavily-studied. But even the more commonly-studied tellurite, selenite, and selenate suffer from similar issues. The most glaring problem in regards to methodology is that the MIC of each organism reported in **Table A1.3** was determined on different types of medium. **Chapter 3** of this work outlines the medium-dependence of tellurate resistance in *E. coli* (a similar medium dependence was also observed for tellurite, selenite, and selenite). A similar pattern is observed here for HRSW (**Table A1.2**), suggesting that this phenomenon may exist in organisms beyond *E. coli*. Therefore, it is challenging to draw meaningful comparisons between the MIC values reported in the literature. The range of MICs identified in the literature search is similar to the range we observe in the MICs for *E. coli* and HRSW merely through changing the composition of the medium that the test is performed in. **Table A1.3** highlights the variability in medium composition (when available) among the different publications.

HRSW was initially isolated and of interest to us because it showed high innate levels of tellurate resistance, comparable to organisms previously isolated from more tellurium-rich environments. However, a review of the literature suggests that the level of resistance seen in HRSW and these other organisms may not be unusually high. However, any comparisons to the literature must be undertaken with caution due to the lack of standardization of medium between labs performing MIC measurements. HRSW itself has an MIC of 0.3 on LB medium while also having an MIC of 3 on M9 minimal medium with no

additional supplementation. This range more than spans the range of MIC we identified in the literature in **Table A1.3.** Nonetheless HRSW remains interesting, in part, because we have obtained its draft genome. Given that HRSW is closely related to *E. coli*, genetic tools developed for *E. coli* may be adaptable to HRSW. Additionally, it is interesting that—despite being closely related to E. coli—HRSW does show a higher level of resistance to tellurate on both M9 (3 vs. 1 mM MICs) and LB (0.3 vs. 0.015 mM MICs) **(Table 2, Table 1 in Chapter 3)**. It would be interesting to explore the question of why the two have such difference in their levels of tellurate resistance.

As a closing remark, the motivation for researching mechanisms of resistance to tellurium and selenium oxyanions is often given as something along the lines of: we're searching for organisms with high levels of resistance to these compounds that can also transform the compounds to their less toxic forms so that we can apply them towards bioremediation purposes. And so we see organisms being isolated from places like deep sea vents (Csotonyi et al., 2006; Maltman, Walter, & Yurkov, 2016), gold mine tailings (Maltman et al., 2015), selenium-contaminated sites, and others (Stolz et al., 1999). In fact, we do the same thing here in **Chapter 4** of this work when we described a Se(0)-solubilizing *Bacillus* species isolated from selenium-contaminated soils in India. However, what this small study and literature review here shows us is that you do not have to go across the world or to the bottom of the ocean to find organisms that are interesting and useful to study. As our example here shows, tellurate-

reducing organisms with higher levels of resistance can be cultivated from soils, sediments, and waters in our immediate surroundings.

FIGURES

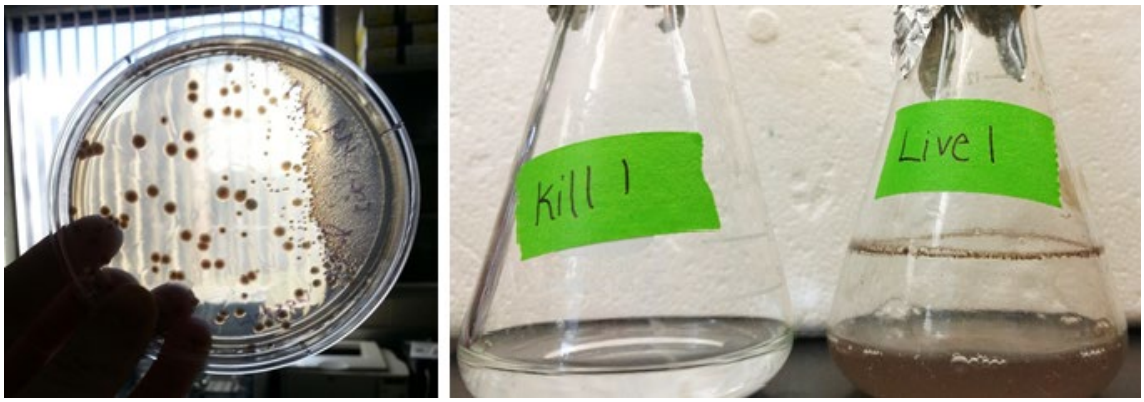

Figure A1.1. Growth of *Enterobacter* sp. HRSW on tellurate-containing medium. (Left) Initial isolation of HRSW from Hudson River sediment. Culture was streaked on M9 minimal medium plates containing 100 uM tellurate. Formation of a dark precipitate was due to the formation of Te(0). Darkened colonies were selected for further analysis. (Right) HRSW grown in liquid M9 medium containing 100 μM tellurate. The flask on the left is an autoclaved control. The flask on the right are live cells. The darkening of the medium is due to the reduction of tellurate to Te(0). Loss of soluble tellurate over time was confirmed using ICP-OES (**Figure A1.3**).

Table A1.1. Tellurate MICs for HRSW on different media

Media	MIC (mM)
LB	0.3
M9	3
M9 + yeast extract (5 g/L)	1.5
M9 + tryptone (10 g/L)	1
M9 + casamino acids (3 g/L)	0.4
M9 + cystine (0.04 g/L)	0.6

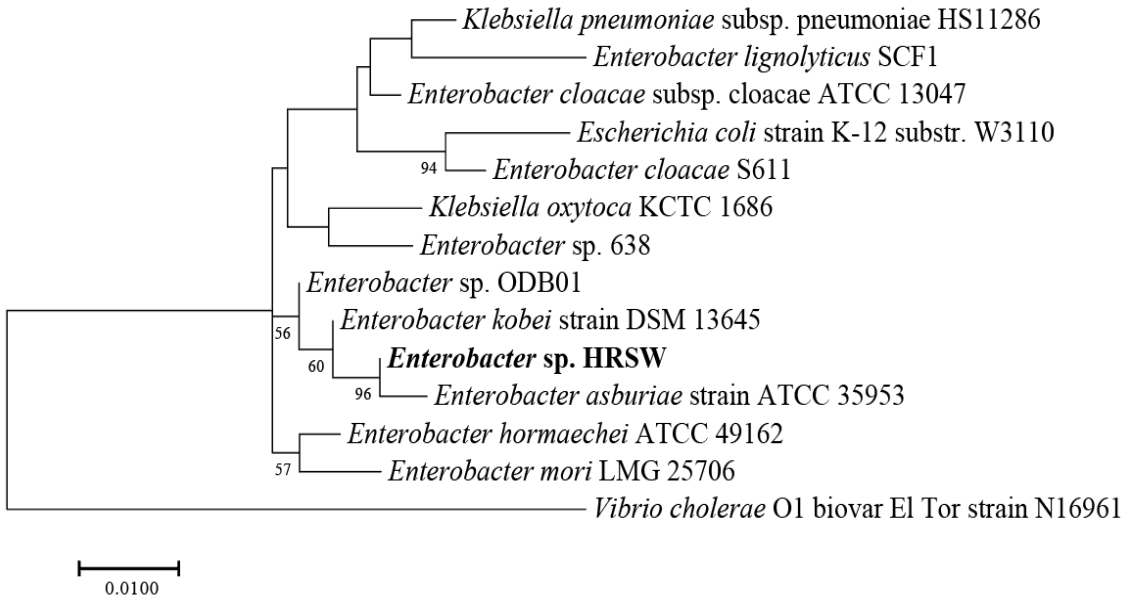

Figure A1.2. Maximum-likelihood phylogenetic tree of the 16S rRNA gene sequences showing the relationship of strain HRSW and closely related species. The tree is drawn to scale with branch lengths measured in the number of nucleotide substitutions per site.

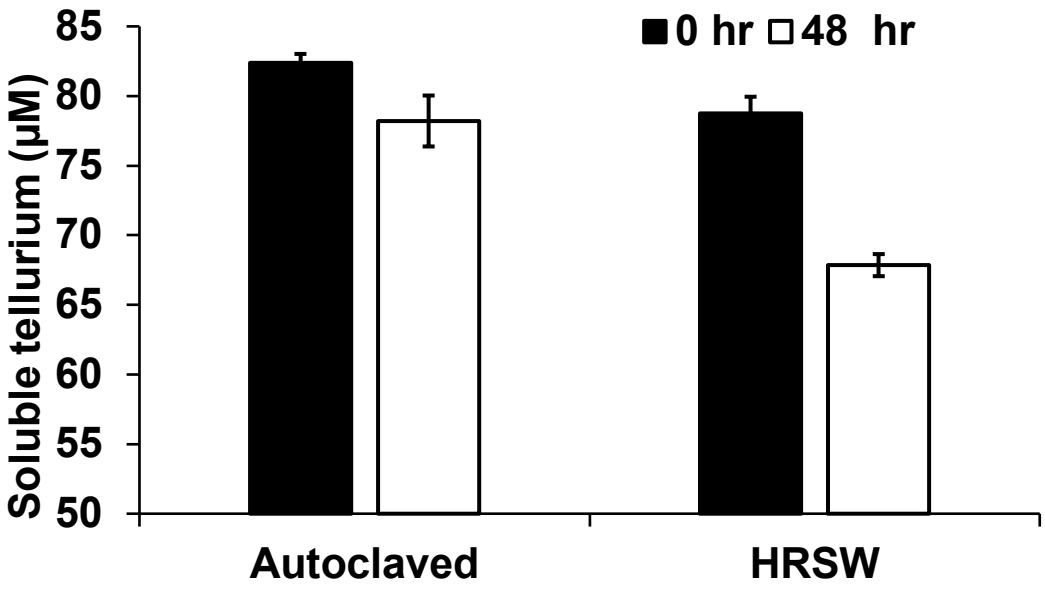

Figure A1.3. Measurement of tellurate reduction to Te(0) by HRSW.

The loss of soluble tellurium (tellurate) due to its reduction to the insoluble Te(0) was measured using ICP-OES. Bars represent the average of three replicates.

Table A1.2. Genome characteristics of HRSW

Feature	
Size	4,855,081 bp
Contigs	110
G+C %	54.89%
CDS	4858
Proteins with functional assignments	4224
Hypothetical proteins	634
rRNA genes	11
tRNA genes	78

Figure A1.4 HRSW 16S rRNA gene sequence

>fig|547.98.rna.86| SSU rRNA ## 16S rRNA, small subunit ribosomal RNA [Enterobacter HRSW | 547.98]
cttaaattgaagagtttgatcatggctcagattgaacgctggcggcaggcctaacacatgcaagtcgaacggtag
cacagagagcttgctctcgggtgacgagtggcggacgggtgagtaatgtctgggaaactgcctgatggagggg
gataactactggaaacggtagctaataccgcataacgtcgcaagaccaaagaggggaccttcgggcctcttgc
catcagatgtgcccagatgggattagctagtaggtggggtaacggctcacctaggcgacgatccctagctggtct
gagaggatgaccagccacactggaactgagacacggtccagactcctacgggaggcagcagtggggaatatt
gcacaatgggcgcaagcctgatgcagccatgccgcgtgtatgaagaaggccttcgggttgtaaagtactttcagc
ggggaggaaggcgataaggttaataaccttgtcgattgacgttacccgcagaagaagcaccggctaactccgtg
ccagcagccgcggtaatacggagggtgcaagcgttaatcggaattactgggcgtaaagcgcacgcaggcggtc
tgtcaagtcggatgtgaaatccccgggctcaacctgggaactgcattcgaaactggcaggctagagtcttgtaga
gggggtagaattccaggtgtagcggtgaaatgcgtagagatctggaggaataccggtggcgaaggcggccc
cctggacaaagactgacgctcaggtgcgaaagcgtggggagcaaacaggattagataccctggtagtccacgc
cgtaaacgatgtcgacttggaggttgtgcccttgaggcgtggcttccggagctaacgcgttaagtcgaccgcctgg
ggagtacggccgcaaggttaaaactcaaatgaattgacgggggcccgcacaagcggtggagcatgtggtttaat
tcgatgcaacgcgaagaaccttacctactcttgacatccagagaactttccagagatggattggtgccttcgggaa
ctctgagacaggtgctgcatggctgtcgtcagctcgtgttgtgaaatgttgggttaagtcccgcaacgagcgcaac
ccttatcctttgttgccagcggttaggccgggaactcaaaggagactgccagtgataaactggaggaaggtggg
gatgacgtcaagtcatcatggcccttacgagtagggctacacacgtgctacaatggcgcatacaaagagaagcg
acctcgcgagagcaagcggacctcataaagtgcgtcgtagtccggattggagtctgcaactcgactccatgaagt
cggaatcgctagtaatcgtagatcagaatgctacggtgaatacgttcccgggccttgtacacaccgcccgtcacac
catgggagtgggttgcaaaagaagtaggtagcttaaccttcgggagggcgcttaccactttgtgattcatgactgg
ggtgaagtcgtaacaaggtaaccgtaggggaacctgcggttggatcacctccttac

Organism	Source	Location of Origin	MIC (mmol/L)	Reduces Te(VI) to Te(0)?	Method for determining MIC
Enterobacter sp. HRSW	This work	Hudson River, NJ, USA	M9: 3 LB: 0.3 For others see **Table 1**	Yes	M9 minimal medium. Dilute overnight culture and grow in different concentrations of tellurate ~18 hr LB medium. Same as above.
Shewanella sp. *ER*-Te-48	(Csotonyi et al., 2006)	Deep sea hydrothermal vent, eastern Pacific Ocean	>1.11	Yes	Injected into 120-ml crimp-sealed bottles containing 80 ml of PG medium amended with tellurate (0 and 300 µg/ml) Medium: PG medium is a minimal medium with 0.2 g/L yeast extract supplemented (Lyalkova & Yurkova, 1992)
Pseudomonas aeruginosa ATCC 27853,	(Harrison et al., 2004)	Clinical isolate (Medeiros, O'Brien, Wacker, & Yulug, 1971)	>1.3	Yes	Minimum inhibitory concentrations were determined by reading the turbidity of the challenge plate at 650 nm on a 96-well microtiter plate reader. Medium: LB medium enriched with vitamin B1
Staphylococcus aureus ATCC 29213	(Harrison et al., 2004)	Clinical isolate (Soni, Chakrapani,	1.0	Yes	Minimum inhibitory concentrations

		& Chopra, 2015)			were determined by reading the turbidity of the challenge plate at 650 nm on a 96-well microtiter plate reader. Medium: LB medium enriched with vitamin B1
Sulfurospirillum barnesii	(Baesman et al., 2007)	Selenium-contaminated freshwater marsh (Stolz et al., 1999)	2	Yes	Mineral salts medium with no reducing agents or yeast extract added
E. coli JM109	(Araya et al., 2004)	K-12 derivative (Yanisch-Perron, Vieira, & Messing, 1985)	0.00926	Yes	Minimal inhibitory concentrations (MICs) of potassium tellurite and of potassium tellurate were determined in liquid medium after 24 h of growth Medium: ATCC medium supplemented with 6 g/L tryptone, 4 g/L yeast extract (Chiong, Barra, González, & Vásquez, 1988)
Pseudomonas sp. CM-3	(Maltman et al., 2015)	Gold mine tailings, Manitoba, Canada	Aerobic: 3.9 Anaerobic: 3.2	Yes	Aerobic: Bacteria were inoculated and grown in RO medium in the dark with different concentrations of Tellurate. RO medium is a mineral salts medium supplemented with 1 g/L

					Bacto-Peptone and 1 g/L yeast extract (Yurkov, Krieger, Stackebrandt, & Beatty, 1999) Anaerobic: same way, but using AMR medium which is a mineral salts medium supplemented with 1 g/L yeast extract
Acenitobacter sp.VS3	(Burton, Giddings, DeBrine, & Fall, 1987)	Volta Reservoir, California, USA	4	Not indicated	Caseine-peptone-starch agar (composition unknown) supplemented with tellurate and incubated for >48 hours.
Aeromonas hydrophila VS6	(Burton et al., 1987)	Volta Reservoir, California, USA	2	Not indicated	See above
Arthrobacter sp. VW8	(Burton et al., 1987)	Volta Reservoir, California, USA	1	Not indicated	See above
Bacillus sp. KW3	(Burton et al., 1987)	Kesterson Reservoir, California, USA	4	Not indicated	See above
Citrobacter freundii KS8	(Burton et al., 1987)	Kesterson Reservoir, California, USA	>4	Not indicated	See above
Corynebacterium sp. KS6	(Burton et al., 1987)	Kesterson Reservoir, California, USA	0.125	Not indicated	See above
Corynebacterium sp. VS1	(Burton et al., 1987)	Volta Reservoir, California, USA	1	Not indicated	See above
Corynebacterium sp. VS5	(Burton et al., 1987)	Volta Reservoir, California, USA	4	Not indicated	See above

Flavobacterium sp. KS4	(Burton et al., 1987)	Kesterson Reservoir, California, USA	0.25	Not indicated	See above
Flavobacterium sp. VW5	(Burton et al., 1987)	Volta Reservoir, California, USA	0.25	Not indicated	See above
Pseudomonas aeruginosa VS7	(Burton et al., 1987)	Volta Reservoir, California, USA	1	Not indicated	See above
Pseudomonas cepacia KS5	(Burton et al., 1987)	Kesterson Reservoir, California, USA	0.03	Not indicated	See above
Pseudomonas sp. VW7	(Burton et al., 1987)	Volta Reservoir, California, USA	4	Not indicated	See above
Aeromonas sp. KA33	(Burton et al., 1987)	Kesterson Reservoir, California, USA	0.5	Not indicated	See above
Corynebacterium sp. VS13	(Burton et al., 1987)	Volta Reservoir, California, USA	0.25	Not indicated	See above
Pseudomonas aeruginosa VS10	(Burton et al., 1987)	Volta Reservoir, California, USA	4	Not indicated	See above

Table A1.3. Tellurate-reducing organisms reported in the literature and the MIC of tellurate for each.

APPENDIX 2
CATALASE DOES NOT REDUCE TELLURATE TO TE(0)

The enzyme catalase has previously been shown to act as an NAD(P)H-dependent tellurite reductase (Calderón et al., 2006). We were interested in determining if catalase will also reduce tellurate to Te(0) in an NADH-dependent manner. A reactor was set up containing tellurate (0.5 mM), catalase (0.35 mg/mL), NADH (10 mM), and Tris HCl (50 mM). To validate our method and replicate the results of Calderón et. al. we set up a second reactor containing 0.5 mM tellurite in place of tellurate. The reactors were incubated at 37°C. We observed darkening of the medium over the course of 24 hours in the reactor containing tellurite, indicating that it was being reduced to Te(0). However, this result was not observed for tellurate. While tellurate may be reduced to tellurite with no further reduction to Te(0), this seems unlikely as catalase does reduce tellurite to Te(0) and NADH is added in excess (**Figure A2.1)**.

We confirm here the prior observations that tellurite is reduced to Te(0) by catalase but that catalase is unable to reduce tellurate to Te(0).

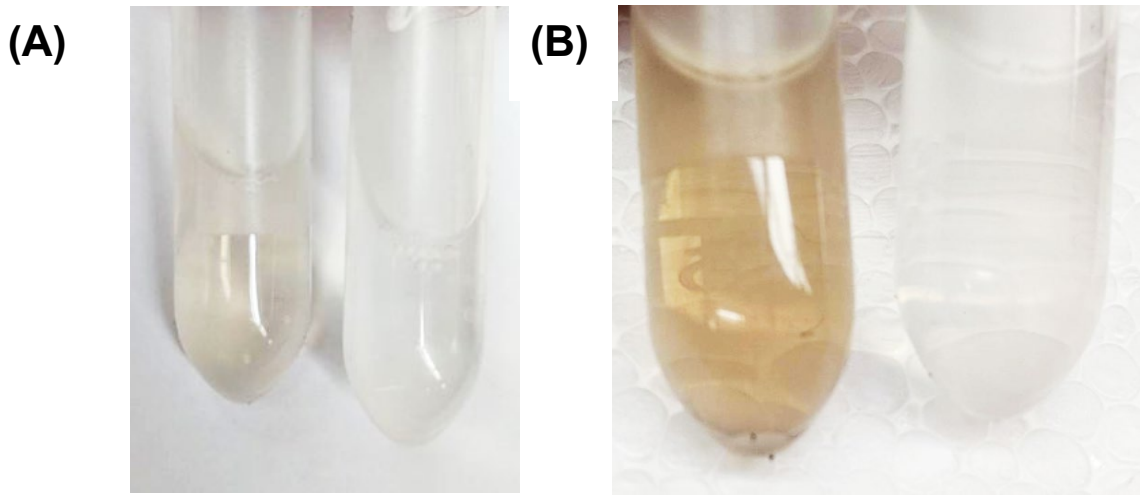

Figure A2.1. Reactions of catalase with tellurate and tellurite. Reactor set-ups are described above. (A) Te(0) formation is observed in the reactor containing tellurite (left) but not tellurate (right) after 2 hours of incubation. (B) After an additional 24 hours of incubation, the tellurite reactor showed further darkening (left) but the tellurate reactor remained clear (right).

APPENDIX 3

SUPPLEMENTARY MATERIAL FOR CHAPTER 3

Table A3.1. Calculated concentrations of amino acids in LB medium

Component	Yeast Extract (Supplier: BD) Concentration	Tryptone (Supplier: BD) Concentration	Concentration in LB (g/L)*
Aspartate	1.6%	0.40%	0.12
Glutamate	6.6%	1.4%	0.47
Cystine	0.20%	0.30%	0.040
Methionine	0.60%	1.0%	0.13
Arginine	1.4%	2.2%	0.29
Leucine	3.0%	4.8%	0.63
Isoleucine	1.8%	1.3%	0.22
Valine	0.50%	1.7%	0.20
Histidine	0.40%	0.50%	0.070
Tryptophan	2.2%	0.80%	0.19
Threonine	1.1%	0.70%	0.13
Alanine	5.6%	1.0%	0.38
Glutamine	0.20%	0.1%	0.020
Glycine	1.0%	0.2%	0.070
Lycine	1.9%	5.5%	0.65
Asparagine	1.0%	0.60%	0.11
Phenylalanine	2.0%	3.0%	0.40
Proline	0.80%	0.20%	0.06
Serine	1.3%	0.70%	0.14
Tyrosine	0.80%	0.50%	0.090

***Calculated using a standard LB recipe of 10 g/L tryptone and 5 g/L yeast extract**

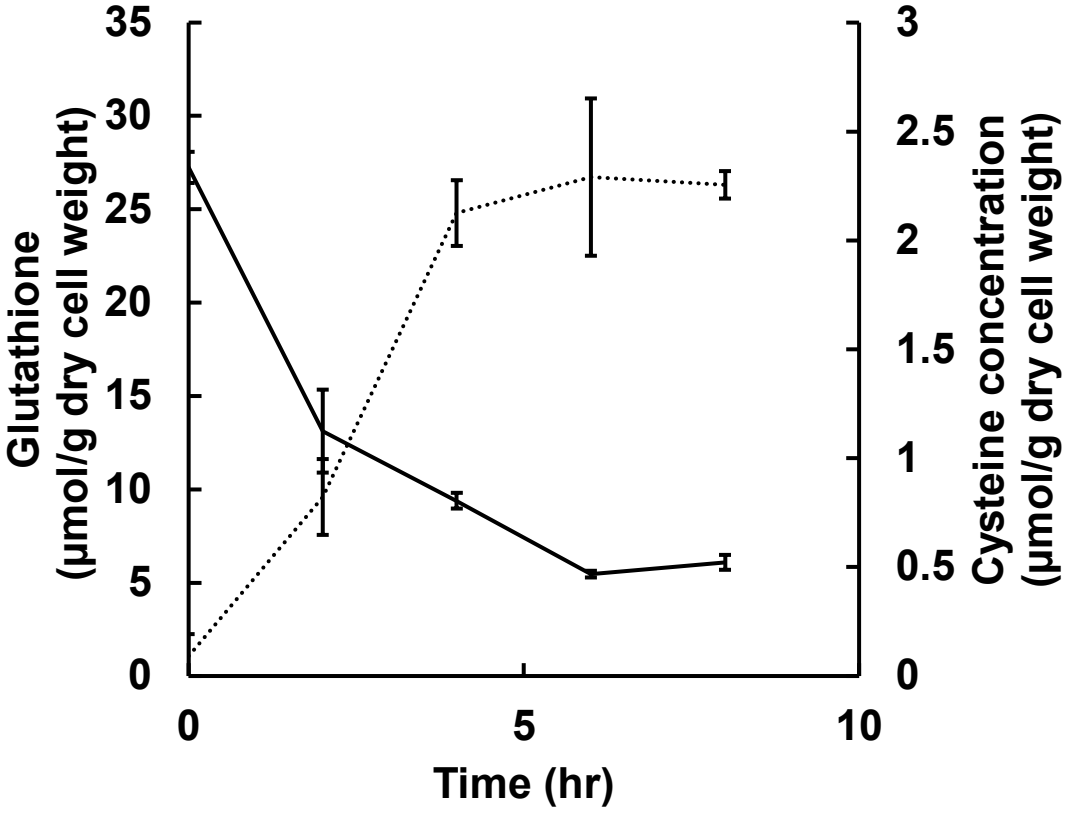

Figure A3.1. Intracellular concentration of glutathione (dotted line) and cysteine (solid line) in *E. coli*. Cells were grown on LB medium.

APPENDIX 4

SUPPLEMENTARY MATERIAL FOR CHAPTER 4

	JG-17	*Bacillus aryabhattai* B8W22	*Bacillus megaterium* ATCC 14581
Source	This study	(Shivaji et al., 2009)	(Lawrence & Ford, 1916)
Colony morphology	Round, entire, raised	Entire, round flat	Entire, round, flat
Colony diameter (mm)	3-5	5-8	6-8
Colony color	cream	peach	white/cream
Carbon utilization (0.5% w/v)			
Glucose	+	+	+
Sucrose	+	+	+
Lactate	+	+	-
Acetate	+	+	+
Succinate	+	-	-
Citrate	-	-	-
Formate	-	+	-
Pyruvate	+	-	+
Glutamate	+	+	-
Propionate	-	+	+
Glycerol	+	+	+

Table A4.1. Strain characteristics of *Bacillus* sp. JG17 and two of its close relatives: *B. aryabhatti* B8W22 (100% identity) and *B. megaterium* ATCC 14581(99% identity). Physiological information for JG17 was determined on the mineral salts medium described in Chapter 4. Physiologcal information for the other two strains was obtained from the literature (Shivaji et al., 2009).

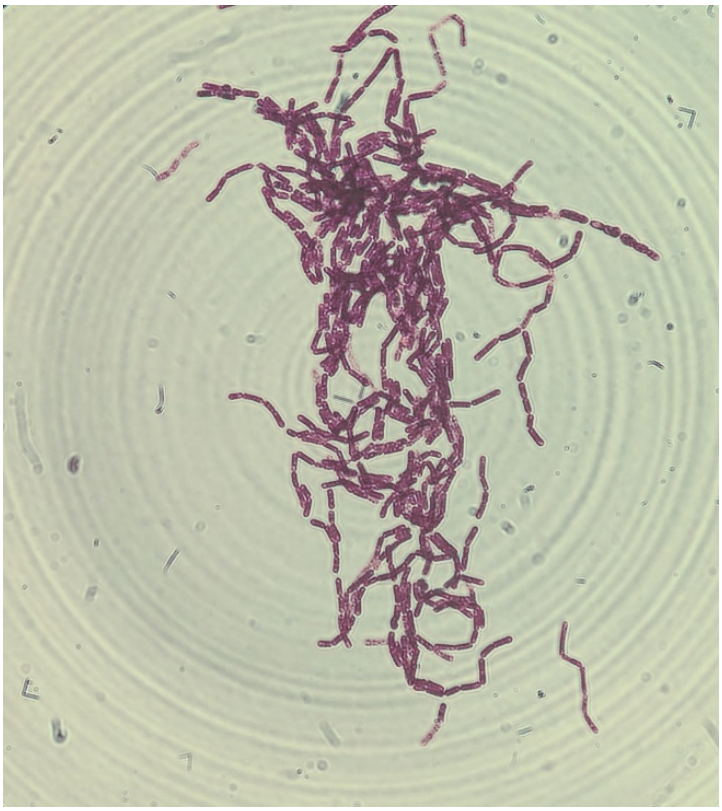

Figure A4.1. Gram stain of *Bacillus* sp. JG17

APPENDIX 5
SUPPLEMENTARY MATERIAL FOR CHAPTER 5

H_2O_2-exposure survival experiment

To investigate the biological function of extracellular sulfite production, oxidative stress experiments were conducted. Overnight cultures of *Shewanella oneidensis* MR-1 were diluted into fresh MR1 lactate medium (described in **Chapter 5**) and grown in a shaking incubator at 30 °C until they reached an optical density of 0.8. Cells were then washed in phosphate-buffered saline solution and diluted into fresh MR1 lactate medium at a starting OD of 0.1. Cells were then allowed to grow for 15 minutes at 30°C in a shaking incubator. After this initial period of growth, samples were taken and diluted for spot-plating to obtain cell counts. Then, 100 μM sulfite and 100 μM of H_2O_2 were added to triplicate cultures. Triplicate control cultures only had 100 μM H_2O_2 added. Cultures were grown for an hour with the H_2O_2 and then a second sample was taken and diluted for spot-plating to obtain cell counts. Cell counts at one hour were normalized against the counts for the sample culture prior to the exposure.

The results showed that exogenous sulfite protects against H_2O_2 oxidative stress. Following an hour exposure, none of the H_2O_2-exposed cells remained alive. In contrast, the cells co-treated with sulfite remained viable (**Figure A5.1**). These data indicate there is a functional role for the large quantities of sulfite produced by *S. ondeidensis* MR1. Sulfite is likely playing a similar role as exogenous sulfide and nitric oxide, which are known to protect cells against

H_2O_2-mediated oxidative stress, (Shatalin et al., 2008; Shatalin, Shatalina, Mironov, & Nudler, 2011).

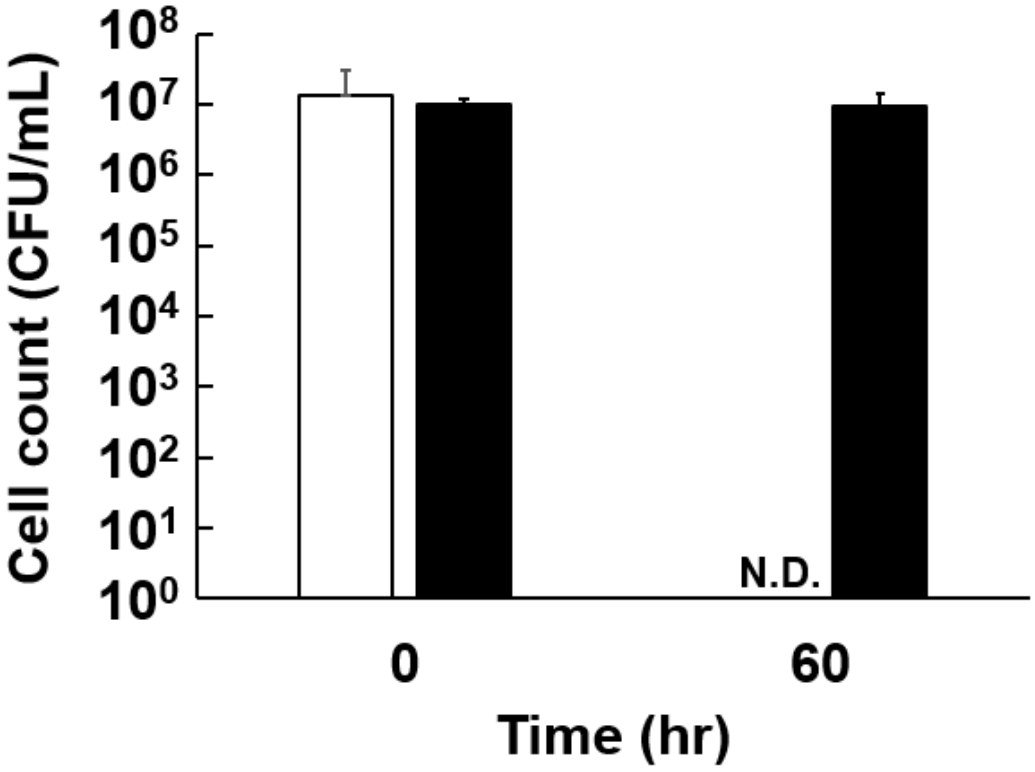

Figure A5.1. Effect of sulfite on cell survival following H_2O_2 exposure. Cells grown on MR1 lactate medium under aerobic conditions were exposed to 100 μM H_2O_2 (unfilled bars) and half the cultures were also exposed to 100 μM sulfite at the same time (black bars).

REFERENCES

Altschul, S. F., Gish, W., Miller, W., Myers, E. W., & Lipman, D. J. (1990). Basic local alignment search tool. *Journal of Molecular Biology, 215*(3), 403-410. doi:https://doi.org/10.1016/S0022-2836(05)80360-2

Araya, M. A., Swearingen, J. W., Plishker, M. F., Saavedra, C. P., Chasteen, T. G., & Vásquez, C. C. (2004). Geobacillus stearothermophilus V ubiE gene product is involved in the evolution of dimethyl telluride in Escherichia coli K-12 cultures amended with potassium tellurate but not with potassium tellurite. *JBIC Journal of Biological Inorganic Chemistry, 9*(5), 609-615. doi:10.1007/s00775-004-0554-z

Baesman, S. M., Bullen, T. D., Dewald, J., Zhang, D., Curran, S., Islam, F. S., . . . Oremland, R. S. (2007). Formation of Tellurium Nanocrystals during Anaerobic Growth of Bacteria That Use Te Oxyanions as Respiratory Electron Acceptors. *Applied and Environmental Microbiology, 73*(7), 2135-2143. doi:10.1128/aem.02558-06

Bankevich, A., Nurk, S., Antipov, D., Gurevich, A. A., Dvorkin, M., Kulikov, A. S., . . . Pevzner, P. A. (2012). SPAdes: a new genome assembly algorithm and its applications to single-cell sequencing. *Journal of computational biology : a journal of computational molecular cell biology, 19*(5), 455-477. doi:10.1089/cmb.2012.0021

Bolger, A. M., Lohse, M., & Usadel, B. (2014). Trimmomatic: a flexible trimmer for Illumina sequence data. *Bioinformatics (Oxford, England), 30*(15), 2114-2120. doi:10.1093/bioinformatics/btu170

Burton, G. A., Giddings, T. H., DeBrine, P., & Fall, R. (1987). High incidence of selenite-resistant bacteria from a site polluted with selenium. *Applied and Environmental Microbiology, 53*(1), 185-188. Retrieved from https://aem.asm.org/content/aem/53/1/185.full.pdf

Calderón, I. L., Arenas, F. A., Pérez, J. M., Fuentes, D. E., Araya, M. A., Saavedra, C. P., . . . Vásquez, C. C. (2006). Catalases are NAD(P)H-dependent tellurite reductases. *PLOS ONE, 1*(1), e70-e70. doi:10.1371/journal.pone.0000070

Chiong, M., Barra, R., González, E., & Vásquez, C. (1988). Resistance of Thermus spp. to Potassium Tellurite. *Applied and Environmental Microbiology, 54*(2), 610-612. Retrieved from https://aem.asm.org/content/aem/54/2/610.full.pdf

Csotonyi, J. T., Stackebrandt, E., & Yurkov, V. (2006). Anaerobic respiration on tellurate and other metalloids in bacteria from hydrothermal vent fields in

the eastern Pacific Ocean. *Appl Environ Microbiol, 72*(7), 4950-4956. doi:10.1128/AEM.00223-06

Gillespie, J. J., Wattam, A. R., Cammer, S. A., Gabbard, J. L., Shukla, M. P., Dalay, O., . . . Sobral, B. W. (2011). PATRIC: the comprehensive bacterial bioinformatics resource with a focus on human pathogenic species. *Infection and immunity, 79*(11), 4286-4298. doi:10.1128/IAI.00207-11

Harrison, J. J., Ceri, H., Stremick, C., & Turner, R. J. (2004). Differences in biofilm and planktonic cell mediated reduction of metalloid oxyanions. *FEMS Microbiology Letters, 235*(2), 357-362. doi:10.1111/j.1574-6968.2004.tb09610.x

Lawrence, J. S., & Ford, W. W. (1916). Spore-bearing Bacteria in Milk. *Journal of Bacteriology, 1*(3), 277-320.251. Retrieved from https://www.ncbi.nlm.nih.gov/pubmed/16558697

LB (Luria-Bertani) liquid medium. (2006). *Cold Spring Harbor Protocols, 2006*(1), pdb.rec8141. Retrieved from http://cshprotocols.cshlp.org/content/2006/1/pdb.rec8141.short

Lyalkova, N. N., & Yurkova, N. A. (1992). Role of microorganisms in vanadium concentration and dispersion. *Geomicrobiology Journal, 10*(1), 15-26. doi:10.1080/01490459209377901

M9. (2006). *Cold Spring Harbor Protocols, 2006*(1), pdb.rec8146. Retrieved from http://cshprotocols.cshlp.org/content/2006/1/pdb.rec8146.short

Maltman, C., Piercey-Normore, M. D., & Yurkov, V. (2015). Tellurite-, tellurate-, and selenite-based anaerobic respiration by strain CM-3 isolated from gold mine tailings. *Extremophiles, 19*(5), 1013-1019. doi:10.1007/s00792-015-0776-8

Maltman, C., Walter, G., & Yurkov, V. (2016). A Diverse Community of Metal(loid) Oxide Respiring Bacteria Is Associated with Tube Worms in the Vicinity of the Juan de Fuca Ridge Black Smoker Field. *PLOS ONE, 11*(2), e0149812. doi:10.1371/journal.pone.0149812

Medeiros, A. A., O'Brien, T. F., Wacker, W. E. C., & Yulug, N. F. (1971). Effect of Salt Concentration on the Apparent In-Vitro Susceptibility of Pseudomonas and Other Gram-Negative Bacilli to Gentamicin. *The Journal of Infectious Diseases, 124*(Supplement_1), S59-S64. doi:10.1093/infdis/124.Supplement_1.S59

Seemann, T. (2014). Prokka: rapid prokaryotic genome annotation. *Bioinformatics (Oxford, England), 30*(14), 2068-2069. doi:10.1093/bioinformatics/btu153

Shatalin, K., Gusarov, I., Avetissova, E., Shatalina, Y., McQuade, L. E., Lippard, S. J., & Nudler, E. (2008). Bacillus anthracis derived nitric oxide is essential for pathogen virulence and survival in macrophages. *Proceedings of the National Academy of Sciences, 105*(3), 1009. doi:10.1073/pnas.0710950105

Shatalin, K., Shatalina, E., Mironov, A., & Nudler, E. (2011). H_2S: A Universal Defense Against Antibiotics in Bacteria. *Science, 334*(6058), 986-990. doi:10.1126/science.1209855

Shivaji, S., Chaturvedi, P., Begum, Z., Pindi, P. K., Manorama, R., Padmanaban, D. A., . . . Narlikar, J. V. (2009). Janibacter hoylei sp. nov., Bacillus isronensis sp. nov. and Bacillus aryabhattai sp. nov., isolated from cryotubes used for collecting air from the upper atmosphere. *International Journal of Systematic and Evolutionary Microbiology, 59*(12), 2977-2986. doi:https://doi.org/10.1099/ijs.0.002527-0

Soni, I., Chakrapani, H., & Chopra, S. (2015). Draft Genome Sequence of Methicillin-Sensitive Staphylococcus aureus ATCC 29213. *Genome announcements, 3*(5), e01095-01015. doi:10.1128/genomeA.01095-15

Stolz, J. F., Ellis, D. J., Blum, J. S., Ahmann, D., Lovley, D. R., & Oremland, R. S. (1999). Sulfurospirillum barnesii sp. nov. and Sulfurospirillum arsenophilum sp. nov., new members of the Sulfurospirillum clade of the epsilon Proteobacteria. *Int J Syst Bacteriol, 49 Pt 3*, 1177-1180. doi:10.1099/00207713-49-3-1177

Wray, D. S. (1998). The impact of unconfined mine tailings and anthropogenic pollution on a semi-arid environment – an initial study of the Rodalquilar mining district, south east Spain. *Environmental Geochemistry and Health, 20*(1), 29-38. doi:10.1023/A:1006575127212

Yanisch-Perron, C., Vieira, J., & Messing, J. (1985). Improved M13 phage cloning vectors and host strains: nucleotide sequences of the M13mpl8 and pUC19 vectors. *Gene, 33*(1), 103-119. doi:https://doi.org/10.1016/0378-1119(85)90120-9

Yurkov, V. V., Krieger, S., Stackebrandt, E., & Beatty, J. T. (1999). Citromicrobium bathyomarinum, a Novel Aerobic Bacterium Isolated from Deep-Sea Hydrothermal Vent Plume Waters That Contains Photosynthetic Pigment-Protein Complexes. *Journal of Bacteriology, 181*(15), 4517. Retrieved from http://jb.asm.org/content/181/15/4517.abstract